NUREG/CR-6877
LA-UR-04-3970

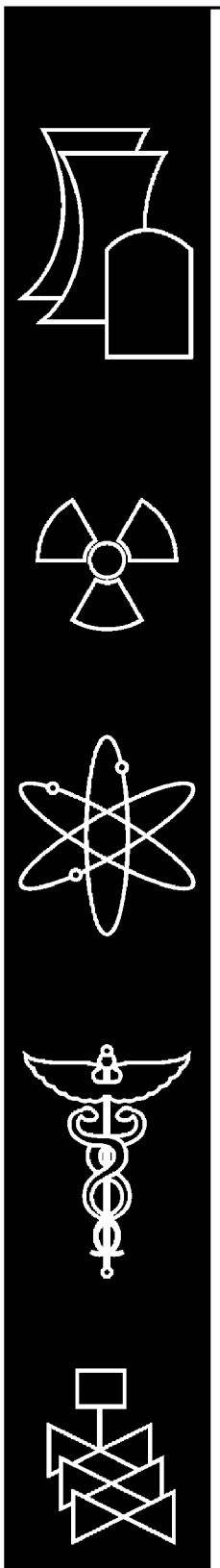

Characterization and Head-Loss Testing of Latent Debris from Pressurized-Water-Reactor Containment Buildings

Los Alamos National Laboratory

U.S. Nuclear Regulatory Commission
Office of Nuclear Regulatory Research
Washington, DC 20555-0001

NUREG/CR-6877
LA-UR-04-3970

Characterization and Head-Loss Testing of Latent Debris from Pressurized-Water-Reactor Containment Buildings

Manuscript Completed: August 2004
Date Published: July 2005

Principal Investigator: B.C. Letellier

Prepared by
M. Ding[1], A. Abdel-Fattah[1], S. Fisher[1] , B.C. Letellier[1]
K. Howe [2], J. Garcia [2]
C.J. Shaffer[3]

Principal Contractor:
[1]Los Alamos National Laboratory
Los Alamos, NM 87545

Subcontractor:
[2]University of New Mexico
Department of Civil Engineering
Albuquerque, NM 87110

Subcontractor:
[3] ARES Corporation
Albuquerque, NM 87106

T. Y. Chang, NRC Project Manager

Prepared for
Division of Engineering Technology
Office of Nuclear Regulatory Research
U.S. Nuclear Regulatory Commission
Washington, DC 20555-0001
NRC Job Code Y6041

ABSTRACT

To properly evaluate the performance of a pressurized water reactor (PWR) emergency core cooling system (ECCS) containment recirculation capability, it is necessary to estimate the total amount of debris that may be present in the containment pool during the recirculation phase. To be as accurate as possible, it is important to include a reasonable estimate of the latent dirt and foreign material that can be found in containment, in addition to the debris generated by a high-pressure pipe rupture. Past and recent testing has shown that even small volumes of fibrous debris present on an ECCS sump screen can filter particulates present in the sump pool very effectively, leading to the formation of composite debris beds that can produce significant pressure losses. Debris present during routine operations that is subjected to containment spray and pool transport may be a significant contribution to the particulates and/or fiber material that compose the sump screen debris bed.

To investigate the significance of this issue, the United States (U.S.) Nuclear Regulatory Commission (NRC) directed Los Alamos National Laboratory (LANL) to characterize the material composition and the hydraulic flow properties of actual plant debris samples.

This study was performed from August 2003 to June 2004. The purpose of the study was to quantify parameters critical to the proper application of the NUREG/CR-6224 head-loss correlation, such as specific surface area. Microfiltering, optical microscopy, and organic dissolution chemistry tests were performed to fractionate the fibrous and particulate components. Most tests were performed at the geochemistry laboratory of the Isotope and Nuclear Chemistry Facility at LANL, which has the necessary analytic equipment to make direct measurements of the hydraulic flow properties and to handle potential low-level radioactive waste streams. Hydraulic parameters representative of latent particulates were measured by testing larger quantities of surrogate debris in a vertical-flow test loop at the University of New Mexico. In addition to our attempt to provide the first quantitative characterization of PWR latent debris properties, this study provides a model of participation and cooperation between the US PWR industry and the NRC. Five volunteer plants contributed samples collected during their recent condition assessment surveys. Descriptions of test procedures and quantitative results are provided in the applicable sections of this report.

FOREWORD

Dirt, fiber, and other foreign materials that are normally found in nuclear power plant containment buildings are referred to as "latent debris." Latent debris, along with debris generated by a loss-of-coolant accident (LOCA), may be present in a pressurized-water reactor (PWR) containment pool during operation of the emergency core cooling system (ECCS) following a LOCA. Some of this debris could be transported to the sump screen, where it could cause a pressure drop (head loss) that could degrade ECCS performance following a LOCA in a PWR plant. This study was undertaken to characterize and assess the potential head loss contributions of latent debris.

This report documents the results of research that was sponsored by the U.S. Nuclear Regulatory Commission (NRC) and performed by Los Alamos National Laboratory and University of New Mexico. Latent debris samples were obtained from five volunteer PWR plants. A variety of experimental techniques were used to separate fibers and particles, measure the relative fiber and particle masses, and determine the relative quantity of each particle size contained in the latent debris samples. All latent debris samples contained measurable amounts of fiber and a wide range of particle sizes. The relative quantities of each particle size appear to be a function of the sample collection method, the locations within the plant that were sampled, and plant-specific debris differences. Therefore, the results obtained from the five volunteer plants may not fully capture the total variability associated with all the nuclear power plants, and plant-specific debris characterization may be preferable.

The head loss contribution of latent debris was determined separately for fiber and particle components. Based on a comparison of physical characteristics, the study concluded that the head loss associated with latent debris fibers can be conservatively assessed using fiberglass insulation properties. Head loss associated with particles was determined experimentally using surrogate debris. Surrogate debris was prepared from soil and sand to match the relevant physical characteristics measured for the latent debris samples. It was necessary to utilize surrogate debris because of the limited quantity and radioactive nature of the latent debris samples obtained from the volunteer plants.

The head loss data were used to estimate conservative hydraulic parameters for latent debris particles over a range of sump flow velocities and particle-to-fiber mass ratios based on a correlation documented in NUREG/CR-6224, "Parametric Study of the Potential for BWR ECCS Strainer Blockage Due to LOCA-Generated Debris," dated October 1995. However, both the NRC Office of Nuclear Regulatory Research (RES) and the Advisory Committee on Reactor Safeguards (ACRS) have identified several limitations in the head loss testing apparatus, testing procedures, and the applicability of the NUREG/CR-6224 head loss correlation for latent debris. These limitations cloud the interpretation of the head loss data and the validity of the estimated hydraulic parameters. Therefore, the RES staff is pursuing additional research to substantiate both the head loss measurements and the hydraulic parameters that this report recommends for use in the evaluation of head loss attributed to latent debris particles.

Carl J. Paperiello, Director
Office of Nuclear Regulatory Research
U.S. Nuclear Regulatory Commission

CONTENTS

Page

FIGURES

Page

TABLES

Page

EXECUTIVE SUMMARY

The study documented in this report does not represent a new issue; rather, the subject of latent debris has been discussed in several public meetings before, and the preliminary test results of this study were presented by Los Alamos National Laboratory (LANL) in the Nuclear Energy Agency/Nuclear Regulatory Commission (NEA/NRC) international workshop on "Debris Impact on Emergency Coolant Recirculation" in February 2004. In addition, this subject was discussed during the Advisory Committee, Reactor Safeguards (ACRS) Thermal-Hydraulics Subcommittee meeting on June 23, 2004, and is also being addressed in the Nuclear Energy Institute (NEI) industry guidance document "PWR Containment Sump Evaluation Methodology." [1]

When accounting for the total amount of debris that may be present in a pressurized-water-reactor (PWR) containment pool during operation of the Emergency Core-Cooling System (ECCS), it is important to include a reasonable estimate of the amount of dirt, fiber, and foreign material that can be found in containment, in addition to the debris generated by a loss-of-coolant accident (LOCA). Dirt and fiber that normally reside in containment are referred to herein as latent debris. Past and recent testing has shown that even small quantities of fibrous debris that are present on an ECCS sump screen can filter particulates that are present in the containment pool, thereby leading to increased pressure losses across the composite debris bed. Latent debris that is subjected to containment spray and pool transport may contribute an additional source of particulate and fiber material, or in some cases, it may represent the only significant source of fiber that is available to form and retain a debris bed on the sump screen.

Both the physical characteristics and the total inventory of latent debris must be understood to assess the potential contribution of this material to recirculation-flow head loss. This report does not provide estimates of total containment inventory, which can vary depending on plant geometry and plant cleanliness practices. However, LANL, under the direction of the United States Nuclear Regulatory Commission, has worked to characterize the material composition and hydraulic flow properties of actual plant debris samples. Beginning in August 2003 and ending in June 2004, this study has attempted to quantify latent-debris parameters—such as the fiber-to-particulate mass ratio, particulate size distributions, and the hydraulic properties of specific surface area (SSA) and porosity—that are needed for the proper application of the NUREG/CR-6224 [2] head-loss correlation. Sieving, optical microscopy, scanning electron microscopy, energy-dispersive spectroscopy, and nitrogen adsorption tests were used to fractionate and characterize the fibrous and particulate components. These tests were performed in the geochemistry laboratory of the Isotope and Nuclear Chemistry Facility at LANL, which has the necessary analytic equipment and safety procedures to handle and dispose of small quantities of low-level radioactive debris. Five volunteer PWR plants contributed latent-debris samples, which were collected during their recent condition assessment surveys.

Hydraulic parameters representative of latent particulates were measured by testing larger quantities of surrogate debris in a vertical-flow test loop at the University of New Mexico (UNM). This apparatus permits measurement of pressure drop (head loss) across a debris bed of known composition under a range of water velocities. Hydraulic parameters can be inferred from differential pressure data by iteratively applying predictive correlations until the model results envelop a variety of observed behavior. Surrogate particulate debris was generated by dry-sieving soil and sand into a range of particle diameters using different sieve sizes and by

recombining mass fractions to match the size distribution measured in the plant samples. The microflow characteristics of the surrogate also were compared to those of the plant debris by measuring packed-bed flow conductivity.

The hydraulic parameters of latent fiber are assumed to be the same as those for fiberglass insulation. Fiber surrogates were not investigated in detail because the head-loss contribution of latent fiber either will be dominated by particulates in thin-bed configuration or will represent a small increase to a fiberglass-dominated debris composition. Further, the characterization of latent fiber samples led LANL to conclude that it is conservative to assume that the latent fiber component has similar hydraulic properties to those of fiberglass. For these reasons, fiberglass is used as surrogate for latent fibers and the latent fiber fraction was not isolated for hydraulic testing in this study.

Foreign material (or the "other" debris category) was deemed unnecessary to be part of the surrogate debris. This foreign material consists of larger material, such as bolts, nuts, cable ties, and rags, and is not expected to be transported to the cooling system screen under recirculation flow velocities or to contribute to the formation of a uniform debris bed on the screen. The full range of sizes of latent debris, including this foreign material, should be considered if it is subject to high-velocity water transport toward the ECCS screen.

The principal findings of this study are based on analyses of samples from the volunteer PWRs. Samples were collected during refueling outages, sometimes before restart cleanliness procedures and sometimes after. All analyses are based on the assumption that proportional debris compositions are approximately constant even if the total inventory varies during an outage or during a plant lifetime. These samples represent the best information to date regarding latent containment debris but may not capture the full range of variability present in the population of nuclear power plants. Furthermore, the quality of the debris samples varied widely because of differences in collection methods and sample locations. Recommendations made in Section 5, "Conclusions and Recommendations," are intended to provide general guidance for plant-specific assessment of latent-debris contributions to sump-screen head loss. However, because of the limitation of data collected for this study, these recommendations may not be applicable to some of the operating PWR plants. In these cases, plant-specific debris characterization may be preferable to the default properties recommended.

ACKNOWLEDGMENTS

This project could not have been accomplished without the coordination efforts of the Nuclear Energy Institute and the cooperation of the five member utilities that submitted samples and freely discussed their individual debris-collection strategies. Their participation has improved the knowledge base relevant to potential sump-screen blockage and has provided insights that will benefit the entire nuclear utility community. Lab assistants William Roesch and James Madrid of LANL's Nuclear Design and Risk Analysis Group (D-5) and Doug Ware of LANL's Isotope and Nuclear Chemistry Group (C-INC) are recognized for their dedicated attention to detail during the hydraulic test procedures. Paul Reimus, also of LANL's C-INC Group, is appreciated for providing access to the radionuclide geochemistry lab for this rather unusual project. The authors would also like to express their gratitude for the contributions of Tsun-Yung Chang, Tony Hsia, Thomas Hafera, Robert Tregoning and other NRC staff members who reviewed the final report to improve its clarity, and quality.

The authors would like to acknowledge Nancy Butner of D-5 for her contributions to integrating and reviewing this document and Lisa Rothrock and Tamara Hallman of IM-1, Los Alamos National Laboratory, for their editing support.

ABBREVIATIONS

BET	Brunauer-Emmett-Teller (Method)
BJH	Barrett/Joyner/Halenda (Method)
BWR	Boiling-Water Reactor
CFR	Code of Federal Regulations
DG	Design Guide
ECC	Emergency Core-Cooling
ECCS	Emergency Core-Cooling System
EDS	Energy-Dispersive Spectroscopy
HEPA	High-Efficiency Particulate Air
HK	Horvath/Kawazoc (Method)
LANL	Los Alamos National Laboratory
LOCA	Loss-of-Coolant Accident
NTU	Nephelometric Turbidity Unit
NUREG	Nuclear Regulatory Commission publication; formerly referred to as Guides
NUREG/CR	NUREG published by another agency or company under contract with the Nuclear Regulatory Commission (Contractor Report)
PVC	Polyvinyl Chloride
PWR	Pressurized-Water Reactor
SEM	Scanning Electron Microscope
SSA	Specific Surface Area
UNM	University of New Mexico
USNRC	United States Nuclear Regulatory Commission

CHARACTERIZATION AND HEAD-LOSS TESTING OF LATENT DEBRIS FROM PRESSURIZED-WATER-REACTOR CONTAINMENT BUILDINGS

by

Mei Ding, Amr Abdel-Fattah, Stewart Fischer, Bruce Letellier,
Kerry Howe,* Janet Garcia,* and Clint Shaffer†

1 INTRODUCTION

This report presents the results of a United States Nuclear Regulatory Commission (USNRC)-sponsored project focused on characterizing debris that is resident in pressurized-water-reactor (PWR) containment buildings. Information is provided to establish the background and purpose for the work, and to document the details of the experimental protocols employed at Los Alamos National Laboratory (LANL) and the University of New Mexico (UNM) to collect the desired characterization data. In situ debris samples were provided to LANL by five individual volunteer plants for use in the project. This report also presents experimental results and recommendations regarding the hydraulic properties of latent debris that are important to sump-screen head-loss analyses. The term "latent" refers to debris that is already present and that resides inside the containment structure before a postulated loss-of-coolant accident (LOCA) occurs (as opposed to debris that is generated by the LOCA).

Section 2 provides a discussion of the background and purpose for this effort. Section 3 describes experimental procedures that are employed for physical characterization tests and summarizes the observations. Recommendations also are provided in this section for designing a suitable surrogate for latent particulate that can be used for large-scale head-loss testing. Section 4 describes the methods used to measure the hydraulic properties of both latent-debris and surrogate samples, summarizes experimental data, and provides recommendations for appropriate hydraulic parameters to use in the NUREG/CR-6224 [2] head-loss correlation for sump-screen vulnerability assessments. Section 5 addresses the limitations of the current effort, summarizes findings and recommendations, and suggests potential areas for future improvement.

2 BACKGROUND AND PURPOSE

The USNRC is interested in evaluating accident scenarios at commercial PWR nuclear power plants in which latent debris is washed into reactor containment sumps during LOCAs. Latent or "pre-LOCA" debris could contribute to clogging of screens that are upstream of pumps that supply cooling water to a reactor core. Examples of latent debris include ordinary dust and dirt, insulation fibers, clothing fibers, paper fibers, pieces of plastic, metal filings, paint chips, human hair, and anything else that may reside on a floor or other surface inside an industrial building.

The total inventory of latent debris will vary depending on the geometry of a plant, rigor of the plant's cleanliness program, age of the plant, and time during normal operations, including outages. This report does not attempt to assess the quantity of latent debris in containment but rather focuses on characteristics such as fiber-to-particulate mass ratios, particulate size distribution, and hydraulic properties of the various constituents. It is assumed that the proportional composition of latent debris provided by the volunteer plants is reasonably constant regardless of the collection time during an outage.

A primary safety concern related to long-term recirculation cooling following a LOCA is LOCA-generated and pre-LOCA debris material that is transported to debris interceptors (i.e., sump strainers or screens) that results in strainer blockage and degraded emergency core-cooling (ECC) pump performance. Regulatory Guide 1.82, "Water Sources for Long-Term Recirculation Cooling Following a Loss-of-Coolant Accident," [3] suggests that the cleanliness of the reactor containment during plant operation (i.e., pre-LOCA or latent debris) be considered when the amount and type of debris available to block the ECC sump screens is being estimated. The potential for this material to impact the head loss across the ECC sump screens should be considered. This study focuses on characterizing latent-debris material and assessing its potential to contribute to sump-screen blockage.

Past and recent testing has shown that even small quantities of fibrous debris that are present on an ECC sump screen can effectively filter particulates that are present in the containment pool, leading to significant pressure losses across the composite debris bed. Latent debris that is present during routine operations (pre-LOCA or resident debris) and that is subjected to containment spray (or wash-down from a coolant-pipe rupture) and pool transport may contribute a source of particulate and fibrous material. The USNRC and its contractors have studied pressure drop across "filter beds" as a function of the physical properties of the filter bed and the linear flow velocity through the bed. [2] Semiempirical equations have been developed using a combination of fluid-flow theory and experimental results to predict pressure drop across filter beds. Some of the most important parameters in these correlations are the density of the filter bed and the surface area per unit volume within the bed. The relative volume of "fibers" and "particles" in the bed is also important because the compressibility of the bed depends on this ratio. A recent article in *Nuclear News* presents a good summary of the sump-clogging issue and a status of the regulatory analysis of the problem. [4]

This study, which is funded by the USNRC, focuses on characterizing the pre-LOCA or latent debris that is resident in a PWR containment building. Specifically, the focus of this effort is to collect representative pre-LOCA debris from PWR containments and to characterize the dust, dirt, and fiber that are present in the samples with respect to their physical attributes and their

hydraulic properties within mixed-debris filter beds. The PWR industry, through the coordination of the Nuclear Energy Institute, agreed to provide samples of resident debris that were needed to complete this characterization effort. Five PWR licensees participated in this study. A total of five sets of samples were received at LANL for analysis, four of which were totally characterized. The fifth sample was not characterized fully because it was dominated by paint chips generated from pressure washing and was therefore deemed to be unrepresentative of PWR containment debris. Material property data collected for the latent-debris samples establish the basis for preparation of a particulate-debris surrogate that is suitable for large-scale head-loss testing at UNM. The objective of head-loss testing is to quantify the hydraulic properties of latent debris that are needed for the proper application of the NUREG/CR-6224 [2] debris-bed head-loss correlation.

Previous work has focused on filter-bed materials that would be generated during a LOCA, not on debris that is already present in the containment structure. For this project, latent debris was collected from within PWR containment buildings and shipped to LANL for physical characterization. This characterization included qualitative separation of "fiber" and "particle" fractions from the remainder of the latent debris; determination of particle-size distributions; microphotographic classification of fibers; determination of fiber diameter, density, and morphology; determination of average particle density of the debris; and measurement of the surface area per unit weight of the debris particles. LANL's Geochemistry Laboratory was enlisted for this work because the latent debris was found to contain very low levels of radioactivity (primarily gamma-emitting activation products) and therefore had to be handled in a radiological facility.

3 PHYSICAL CHARACTERIZATION OF LATENT-DEBRIS SAMPLES

This chapter follows the format of a self-contained laboratory report and first describes the experimental methods used for each phase of debris physical characterization (Section 3.1) before presenting and discussing the observations (Section 3.2). The final section of this chapter (Section 3.3) offers guidance to direct the formulation of a suitable surrogate debris.

3.1 Experimental Protocol

Shipment of radioactive debris samples from candidate PWRs and the associated receipt and inspection at LANL required that a simple protocol be established before work could begin in the Geochemistry Laboratory. After the debris was collected at the plant site, its radionuclide content was determined by gamma spectroscopy to satisfy shipping requirements. A complete gamma spectrum of the bulk debris was provided to LANL by each participant so that a radioactive material receipt request could be filed through established LANL Geochemistry Laboratory procedures. The results indicate that the debris contains radionuclide quantities lower than the acceptable limit for the total radionuclide inventory in the Geochemistry Laboratory. The quantities of latent debris received from these five PWRs vary from grams to kilograms. The total activity of debris samples from all five PWRs did not exceed the Radiological Category B facility limit. In this study, the five debris samples are simply referred to as Plants A, B, C, D, and E. The debris received from Plant E was not characterized fully because it was dominated by paint chips and judged by comparison to be atypical of latent plant debris.

When the material was received at the Geochemistry Laboratory, it was taken first to the laboratory count room for unpackaging, followed by gamma counting, and spectral analysis. The gamma spectroscopic report from the nuclear plant also was included in the shipping package for verification and material identification. The count-room personnel determined if they could detect any radionuclides present in the debris that would preclude laboratory work in the facility because of conflicts with other sensitive experimental programs. For the five debris samples received, the count-room personnel concluded that the samples did not contain significant nuclides from fuel elements (the radioactivity is generally attributable to activation products). Alpha and beta counting was not conducted on the samples because the radioactivity in the samples is very heterogeneous (contained in only a few particles) and because it is not possible to prepare the samples for alpha or beta counting without incurring greater risk of contamination.

Once gamma counting was completed, the debris material was transferred into the Geochemistry Laboratory and experimental work began. The experimental scope was as follows.

1. The debris was removed from its shipping container and transferred to Laboratory containers.

2. The “fiber” and “particle” fractions were separated from the remaining (or “other”) debris items.

3. The weight of fine particles attached to swiping (masolin) cloth or filter paper was determined.

4. The fiber thickness/diameter was determined.

5. The bulk density of fibers was estimated.

6. Particle surface area and density measurements were taken.

7. Microphotographic classification of fibers was performed.

8. Scanning electron microscope (SEM)/energy-dispersive spectroscopy (EDS) methods were used to characterize representative particulate and fiber.

The following subsections describe the procedures and analytic techniques used for each of the above steps, respectively. Data are tabulated and observations are summarized in Section 3.2.

3.1.1 Removal of Debris from Shipping Containers

The latent debris was collected by the PWR licensees (according to site-specific procedures that varied among the volunteer plants) and packaged for shipment. At LANL, the shipping containers were unpacked in the Geochemistry Laboratory and the debris packages were removed. The debris was packaged in plastic bags and plastic containers, as shown in Fig. 1. Some sets of samples consisted of small quantities (a few grams) of debris in double-contained baggies (e.g., Ziploc® bags). The debris was either loose in the bags or adhered to masolin cloth, paper "swipes," or vacuum filters. Debris was removed from each bag and placed into small plastic trays. Filter/swipe papers were shaken gently to remove any loose debris. Clean, wet filter papers were used to wash the debris adhered to the bags. Next, the swipes were agitated gently in a water bath to remove the debris. One sample consisted of six high-efficiency particulate air (HEPA) filters, with the quantity of debris ranging from 160 to 750 g in each filter. Because of its greater quantity, transfer of this debris to the Laboratory sample containers was performed in a glove bag to prevent potential spilling and inhalation of the debris particles and fibers.

Initially, sample segregation was preserved exactly as the material was shipped. For later tests, it was necessary to aggregate the subsamples provided by a single plant. For example, Plant A provided many bags representing the debris collected from many different locations in containment, but each bag contained less than a gram of material. Sample labels provided by the plants were not preserved. Instead, sequential sample numbers were assigned, by volunteer plant, as each batch was processed through the characterization procedure. The sequential numbers are used to reference individual samples throughout this report.

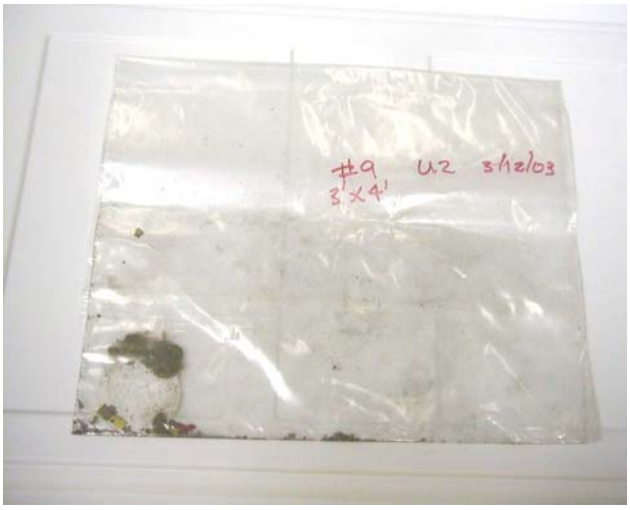

Plant A

Plant B

Plant C

Plant D

Fig. 1. Representative latent plant debris as shipped.

3.1.2 Separation of "Fiber" and "Particle" with Sieving

For debris samples from Plants A, B, and D (Samples 4 and 15), wet sieving was employed to separate "fiber" and "particle" fractions from the remainder of the debris by using a 0.132-in.-

mesh-size sieve. Dry sieving was employed for Plants C and D (Samples 1, 2, 3, 6, 8, and 10).* This initial gross separation of debris resulted in bins of fiber, particulate, and "other" material, as shown in Fig. 2 (Plant A debris). Examples of "other" material include chips of plastic and paint, foam ear plugs, wire clippings, and metal foil. In most cases, significant manual manipulation was required to separate fibers from the imbedded particulate, and this separation was never perfectly complete. Visible particulates remained trapped in fiber clumps and on cloth swipes. Microphotos presented in Fig. 25 illustrate the trapping of much smaller (<10-μm diameter) particulates as well. Some residual fiber also can be noted in some of the larger particulate-size categories.

Fig. 2. Composition of debris (Plant A).

The particles having a size fraction <0.132 in. were separated further by wet sieving into four fractions: >2 mm, 500 μm to 2 mm, 75 μm to 500 μm, and <75 μm. Once acceptable separation was achieved, the water was allowed to evaporate in a hood until the samples were sufficiently dry. Fig. 3 through Fig. 22 present representative photographs of the initial separation of debris from each of the four PWR plants A, B, C, and D into fiber and particulate bins with size gradations.

* Characteristics of the samples, including sample quantity and radioactivity level, determined whether dry or wet sieving was employed to separate the "fiber" and "particle" fractions from the remainder of the debris. Sample quantities greater than 20 g were separated using wet sieving to minimize dust entrapment of contaminated material. Wet sieving was necessary for the Plant A samples because of the small sample quantities that adhered to filter papers. The filter paper was "washed" to remove the material for analysis. In general, wet sieving was found to be more effective at collecting and managing samples of all size categories.

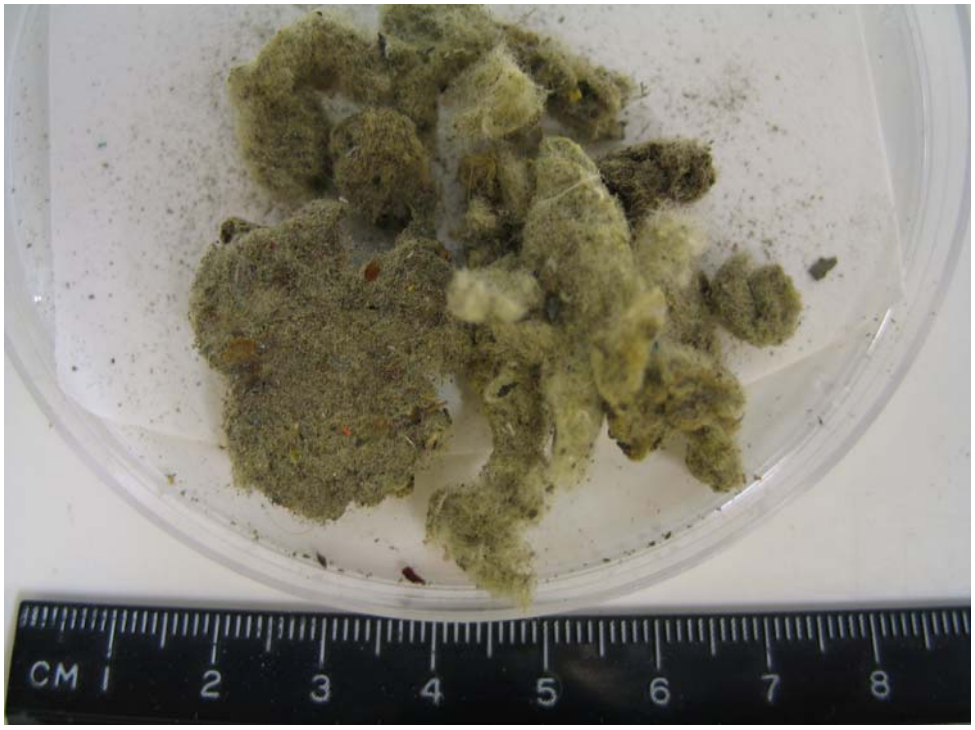

Fig. 3. Fiber (Plant A).

Fig. 4. Fiber (Plant B).

Fig. 5. Particulate >2 mm (Plant A).

Fig. 6. Particulate 500 µm to 2 mm (Plant A).

Fig. 7. Particulate 75 µm to 500 µm (Plant A).

Fig. 8. Particulate <75 µm (Plant A).

Fig. 9. Particulate >2 mm (Plant B).

Fig. 10. Particulate 500 µm to 2 mm (Plant B).

Fig. 11. Particulate 75 µm to 500 µm (Plant B).

Fig. 12. Particulate <75 µm (Plant B).

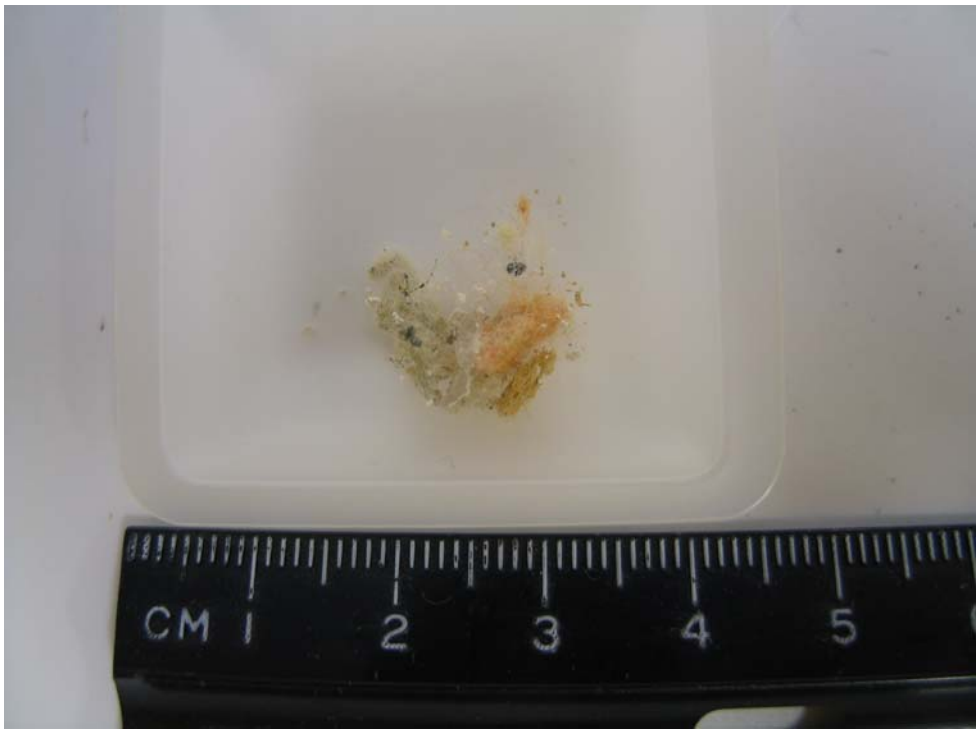

Fig. 13. Fiber (Plant C).

Fig. 14. Fiber (Plant D).

Fig. 15. Particulate >2 mm (Plant C).

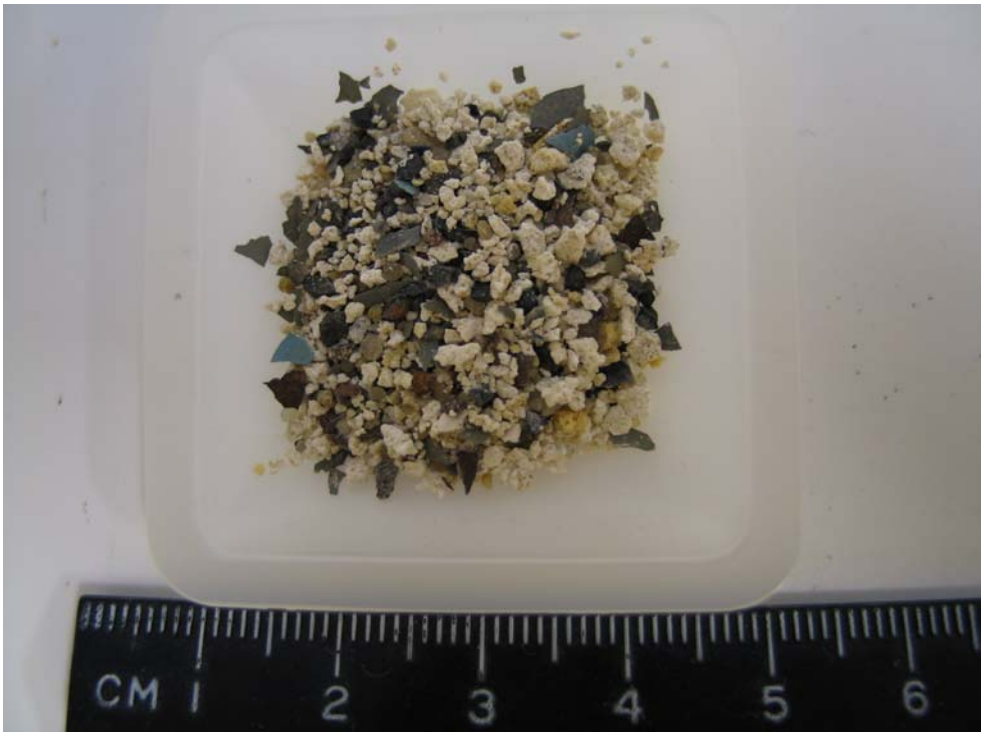

Fig. 16. Particulate 500 µm to 2 mm (Plant C).

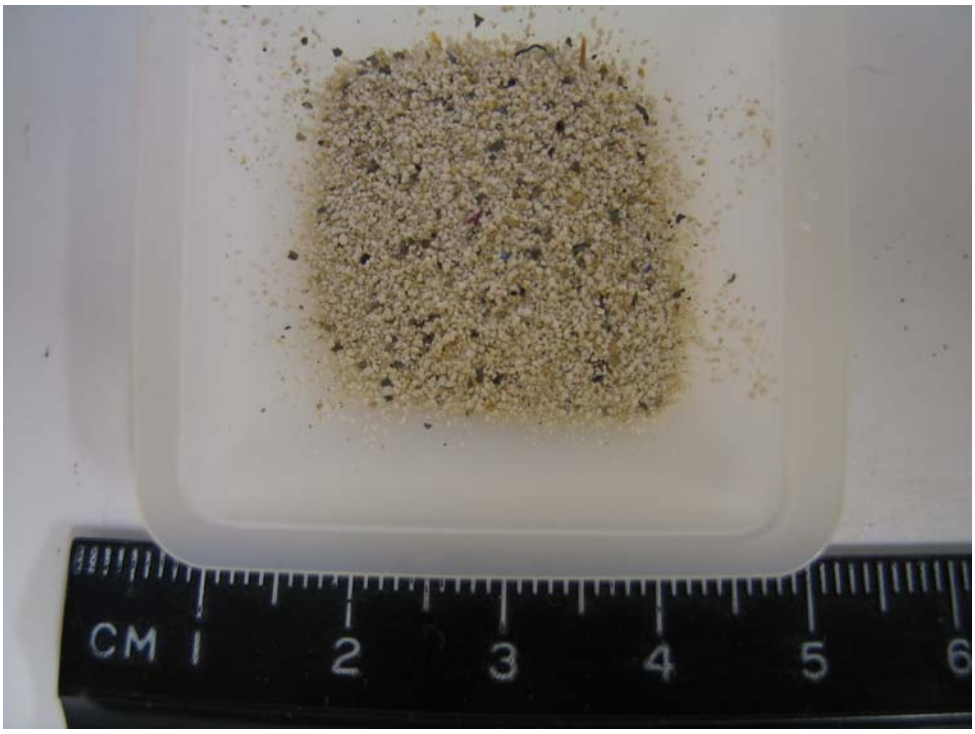

Fig. 17. Particulate 75 µm to 500 µm (Plant C).

Fig. 18. Particulate <75 µm (Plant C).

Fig. 19. Particulate >2 mm (Plant D).

Fig. 20. Particulate 500 µm to 2 mm (Plant D).

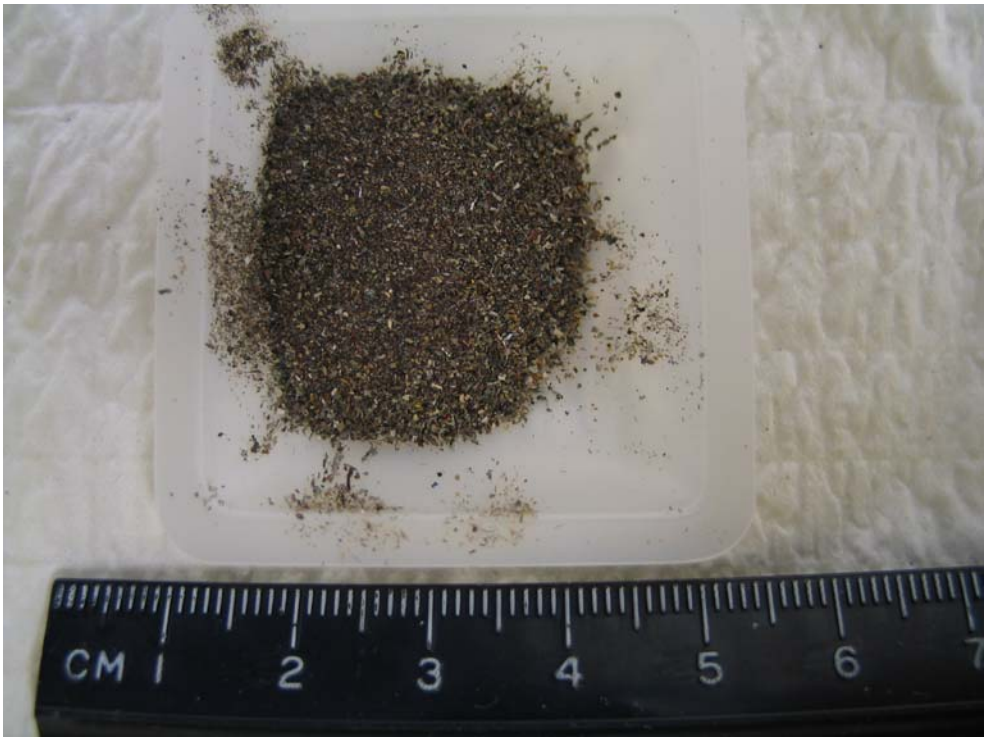

Fig. 21. Particulate 75 µm to 500 µm (Plant D).

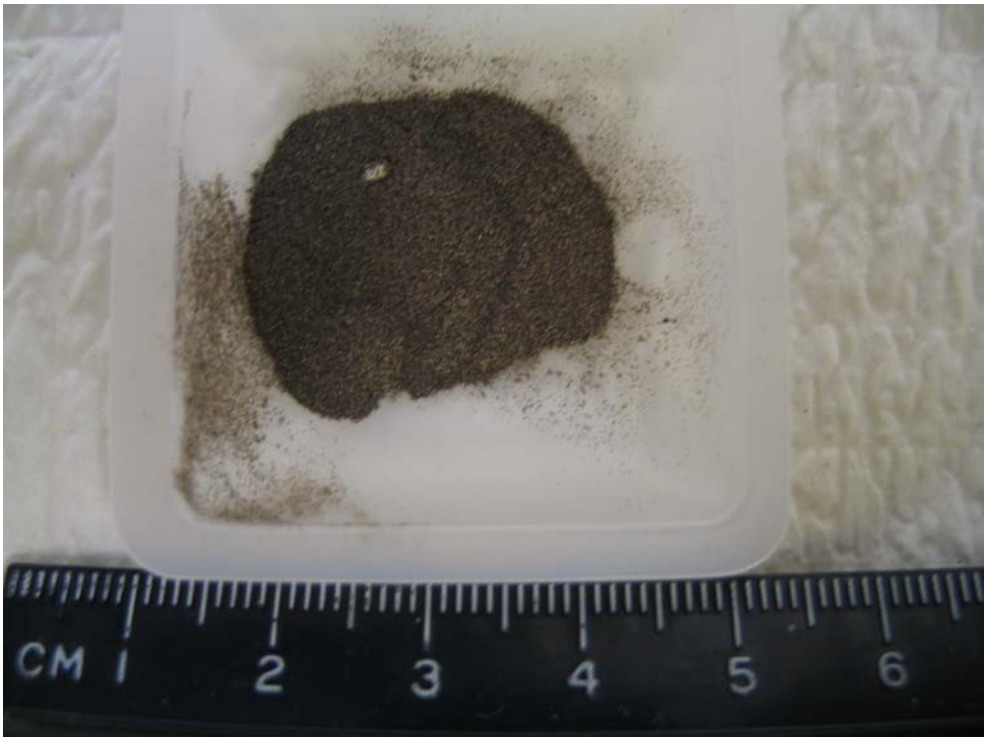

Fig. 22. Particulate <75 µm (Plant D).

The particulate matter for Plant C (Fig. 15 through Fig. 18) is lighter in color than the particulate from Plants A, B, and D. This light-colored particulate material consists of iron, silicon, manganese, and titanium compounds, based on SEM/EDS. These measurements are discussed in Section 3.1.8. Fig. 23 demonstrates the separation scheme employed to segregate the latent debris. Small or very fine particulate information (i.e., <10 μm) was obtained through analysis of debris-collection media, as discussed in Section 3.1.3.

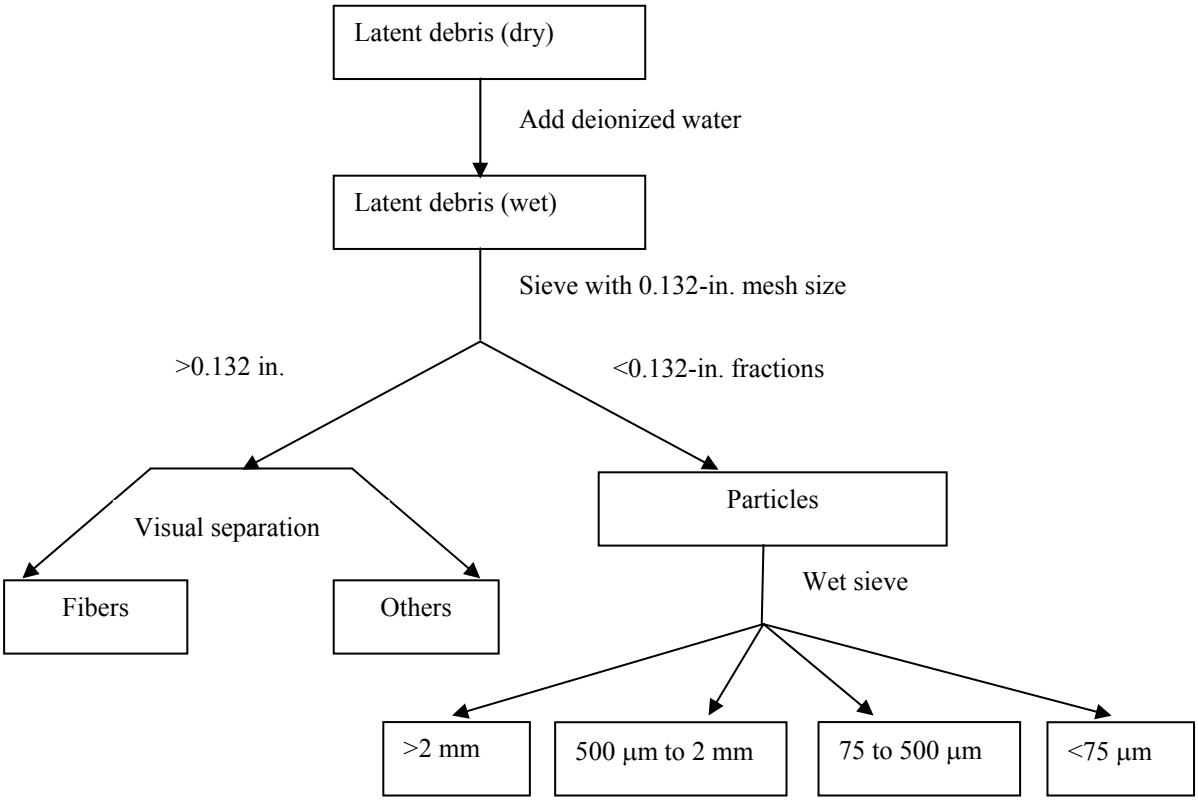

Fig. 23. Qualitative flow schematic for separation of latent debris.

3.1.3 Weight of Fine Particles Attached to Cloth and Filter Paper

At Plant D, masolin cloth was used to sweep up large debris and coarse particles. During this sweeping process, smaller or fine particles (mostly <10 μm, based on photomicrographs and SEM photographs) attached themselves to the masolin. Fig. 24 and Fig. 25 present SEM images of "clean" and "dirty" portions of the masolin, respectively. The SEM image of the "dirty" cloth in Fig. 25 clearly shows attachment of the very small particles (mostly <10 μm). Similarly, at Plants A and B, vacuums with filters were employed to collect debris. In these instances, fine particles also are observed to be trapped in the filter, similar to the debris shown in Fig. 25. On the filters from Plant A, very little fibrous debris remained on the filter paper. However, for Plant B, the HEPA filters retained some fraction of fiber that could not be removed easily. Thus, for Plant B, the estimated weight of fine particles was reduced by a small fraction to compensate for these trapped fibers.

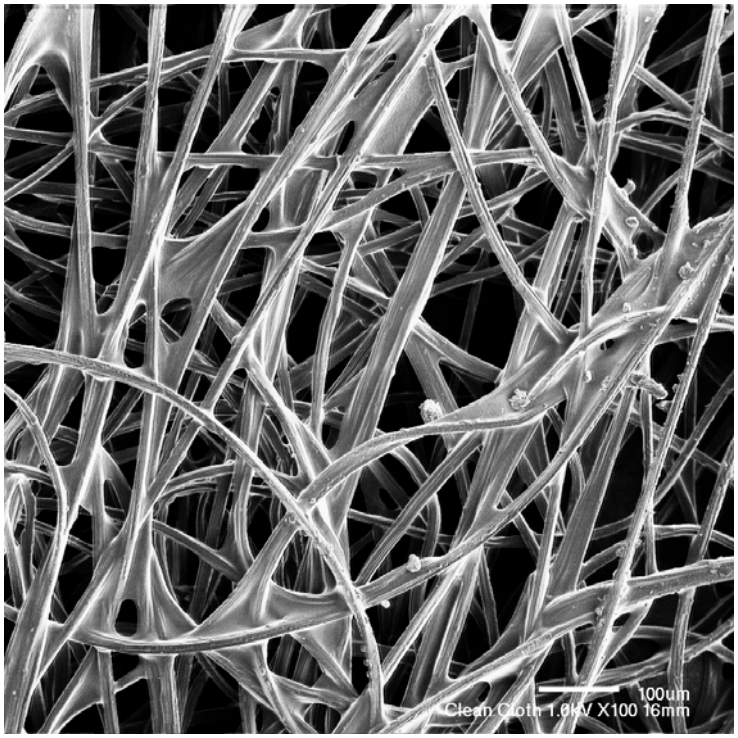

Fig. 24. Clean masolin cloth (Plant D).

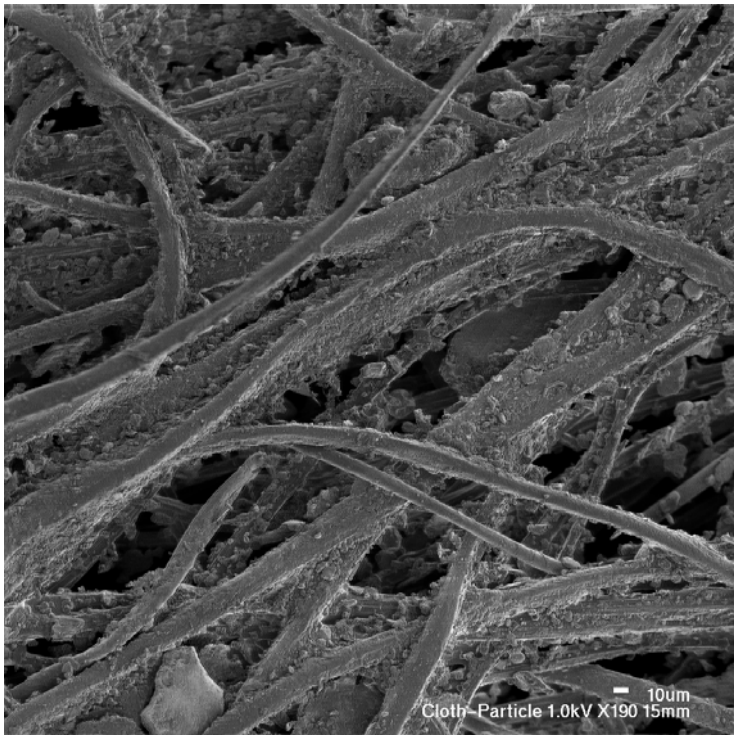

Fig. 25. Dirty masolin cloth (Plant D).

The following method was employed to determine the fractions of fine particles in the debris for Plants A and D. Because of the difficulty in removing fine particles from the cloth or filter paper, the weight of fine particles attached to the cloth or paper was determined by experimentally measuring the difference between clean and dirty cloth/paper weights. A portion of the clean cloth/paper was weighed, and the weight of cloth/paper per unit area was assumed constant. Thus, the fine-particle weight (g) in the cloth or filter paper is equal to the weight of the dirty cloth/paper minus the weight of the same cloth/paper when it is clean. Equations (1) and (2) were used to calculate the amount of fine particles attached to the masolin cloth or filter paper as

$$W_{(fine,\ p)} = W_d - W_c \tag{1}$$

and

$$W_c = A_{d/c} \times K_c \quad , \tag{2}$$

where

$A_{d/c}$ = the area of dirty cloth/paper (cm^2),
K_c = the weight of cloth/paper per unit area (g/cm^2) when the cloth/paper is clean,
W_d = the weight of dirty cloth/paper (g), and
$W_{(fine,\ p)}$ = the weight of fine particles attached on cloth/paper.

An assumption inherent in the above analysis is that the bulk of the fine particles trapped in the cloth/filter paper is <10 μm. Fig. 25 qualitatively supports this assumption. To apply Eqs. (1) and (2) to determine $W_{(fine,\ p)}$, the total area of dirty cloth/paper, the weight per unit area of clean cloth/paper, and the weight of the dirty cloth/paper were measured.

3.1.4 Determination of Fiber Thickness/Diameter

To assist with the determination of fiber thickness or diameter, several high-resolution optical microscopic images were captured from randomly selected samples of fiber debris obtained from different plants. Examples of these images are shown in Fig. 26, Fig. 27, and Fig. 28. Each image encompassed a varied number of the fibers, ranging from one to seven. A spatial calibration of the images was performed and verified against a 10-μm-stage micrometer. An image-processing routine was used to determine the edges of the fibers in each image. The routine employs a median filter to smooth the image and then detects fiber boundaries using a compass filter. A watershed procedure then is used to reconstruct the fiber boundaries. The thickness of each fiber was determined as the shortest distance between two opposite edges. Each in-focus fiber was measured once and only in-focus fibers were measured. The total number of fibers measured was 630 (Plant A: 116, Plant B: 231, and Plant C: 283). For irregular or flat fibers, the thickness was chosen as the largest identified dimension.

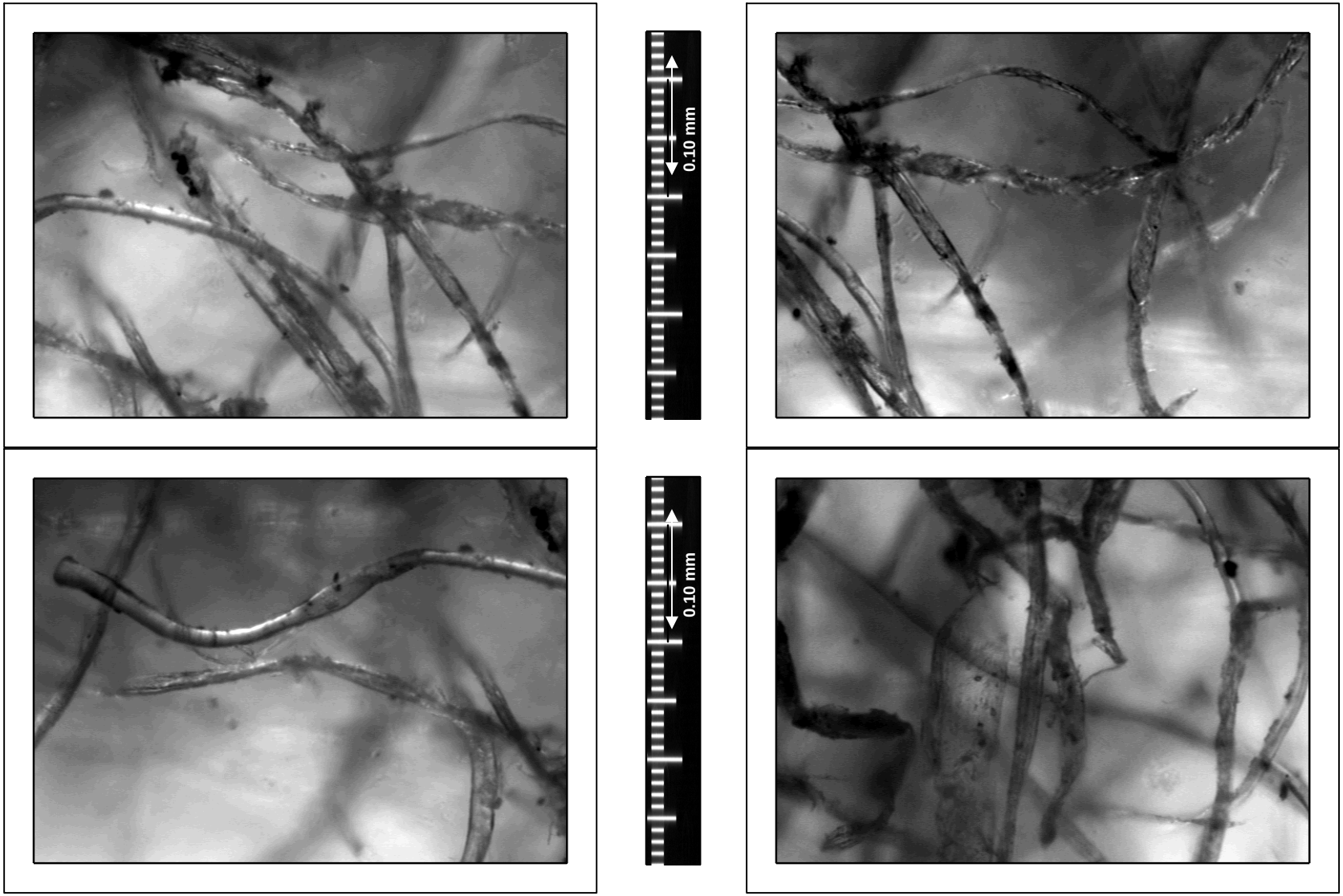

Fig. 26. Photo images of fiber (Plant A).

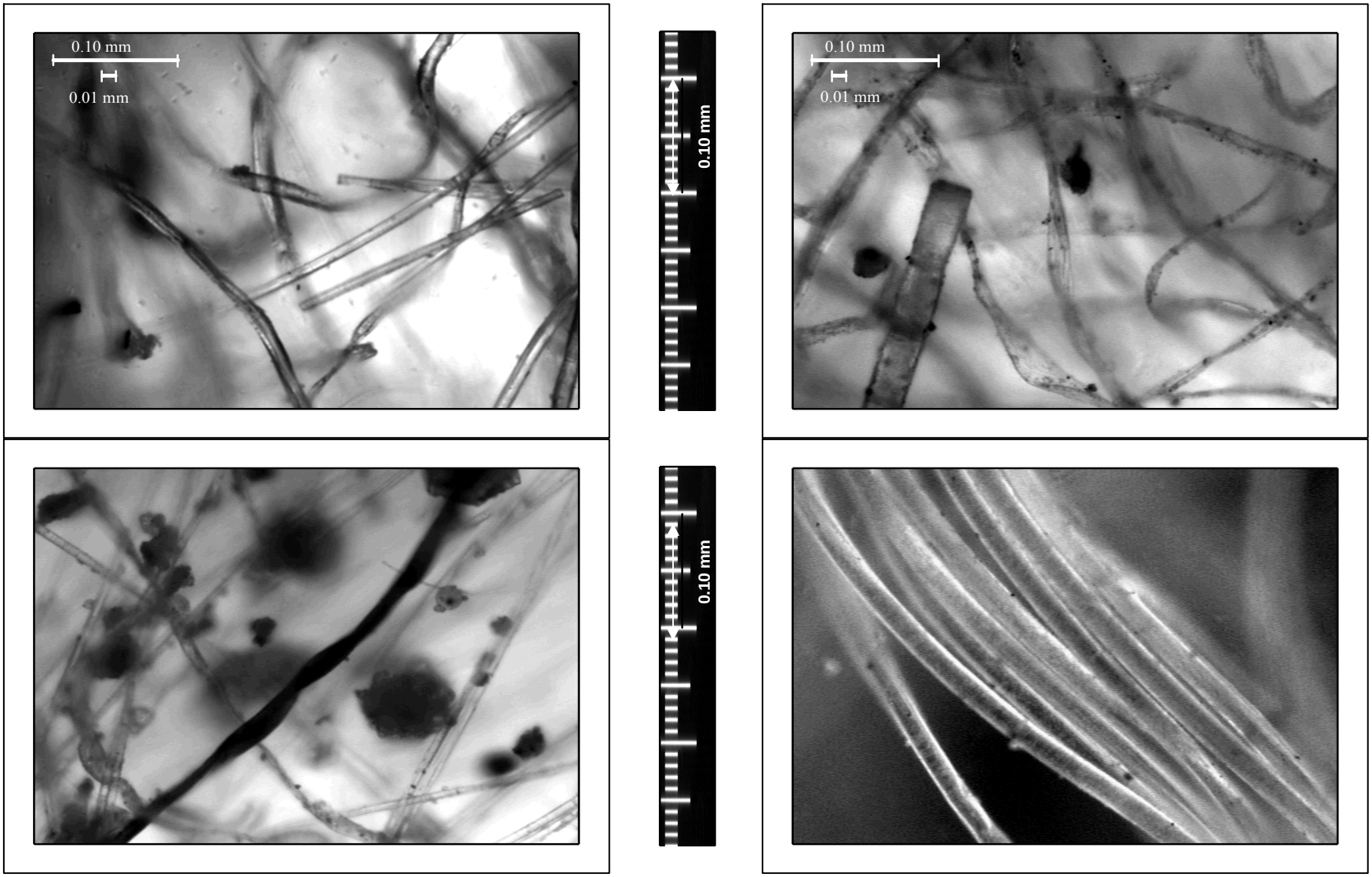

Fig. 27. Photo images of fiber (Plant B).

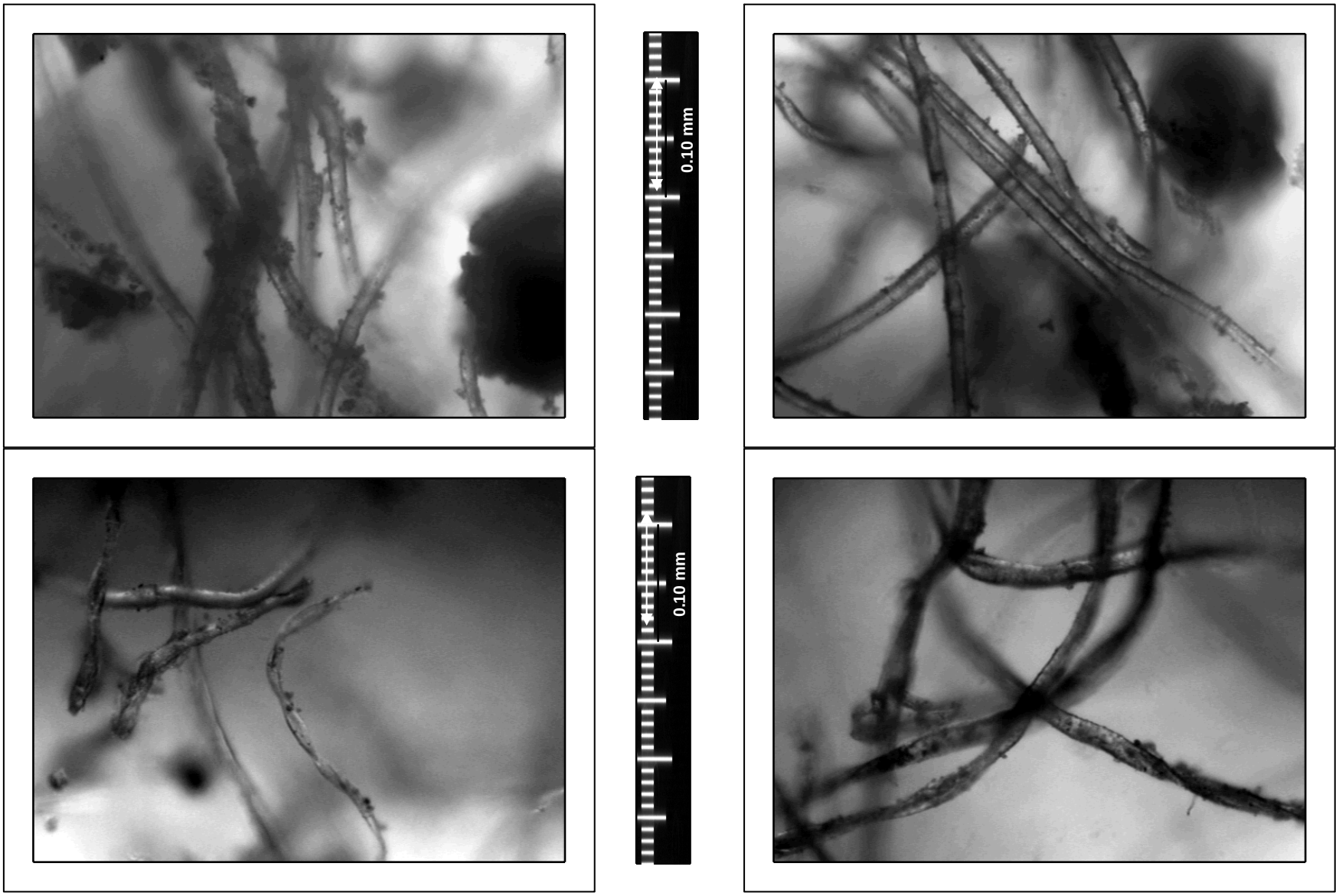

Fig. 28. Photo images of fiber (Plant C).

3.1.5 Estimation of Material and Filter-Bed Fiber Density

The material density of a clump of fibers (henceforth termed "fiber mass") can be expressed as

$$D\ (g/cm^3) = W(g)/V(cm^3)\ , \qquad (3)$$

where

D = the bulk density of a fiber mass,
W = the weight of the fiber mass, and
V = the volume of the fiber mass.

The material density of a fiber mass can be computed by measuring the weight of the fiber and its associated volume by water displacement. The weight of a fiber mass was measured directly using a balance. The volume of fiber mass was determined as follows.

1. Deionized water was added to a scaled cylinder and the volume of water in the cylinder was recorded.

2. A weighed fiber mass was transferred into the cylinder, making sure that the fiber mass was completely submerged.

3. The cylinder containing fiber mass and water was allowed to set for at least 48 hours to ensure that the fiber mass was submerged completely and was in contact with the water and to allow any air trapped in the fiber mass to escape. During this standing period, the cylinder was covered with a cap of plastic film to minimize or prevent evaporation.

4. The combined volume of water and fiber mass in the scaled cylinder was recorded. The difference of the water volume in the cylinder before and after the addition of the fiber mass represents the volume of the fiber mass.

Representative fibrous debris samples from Plant B were tested to determine the dry and wet fiber-bed densities. Both samples were weighed dry and then placed individually into a 500-ml graduated cylinder. The initial dispersed volume of each sample was recorded. The sample then was compressed by applying an axial force to a plug that just fit the inside diameter of the graduated cylinder. The dry compressed volume of the fiber sample was recorded.

The samples then were tested to determine the wet compressed density of the fiber when subjected to a steady flow of water. An 8-in.-long cylinder with a 0.5-in.-diameter was loaded with the dry fiber debris. The mass of fiber required to fill the tube was recorded. Distilled water was pumped slowly through the tube as the fiber debris material slowly compressed. The approach velocity of the water was 0.43 ft/s. The water flow continued for about 5 min until no additional compression of the fiber bed could be observed visually. The compressed length of the debris then was measured.

3.1.6 BET Surface Area and Density Measurement of Particles

The surface areas of representative samples of the debris particle size fractions were measured by nitrogen adsorption methods. The nitrogen adsorption Brunauer-Emmett-Teller (BET) instrumentation is shown in Fig. 29. The particle samples were dried, weighed, and then loaded into a glass sample cell for measuring. The samples were loaded inside a hood to prevent spilling and inhalation. The nitrogen adsorption BET surface area was measured using a Quantachrone Nova 1200 instrument. This technique also provided estimates of volume and, thus, estimates of the particulate-sample densities. Nitrogen adsorption is sensitive to submicron-sized pores within a soil sample. It is not clear that water flow in a composite debris bed is affected by such small-scale features of the particulate; therefore, the surface areas determined by this method are not identical to the specific surface area (SSA) needed for application of the NUREG/CR-6224 [2] head-loss correlation. To avoid confusion, internal surface area determined by nitrogen adsorption will be referred to as BET surface area in units of m^2/g, and the parameter needed directly for head-loss applications will be referred to as the hydraulic SSA, S_v, in units of ft^2/ft^3.

Fig. 29. Nitrogen adsorption BET instrumentation.

3.1.7 Microphotographic Classification of Fibers

Fibrous debris varied in size and quantity for each sample. A metallurgical microscope, shown in Fig. 30, with a 20X objective lens was used to identify the size/shape of the fibrous debris separated from the above procedures. Each sample was loaded onto a microscope slide using glue.

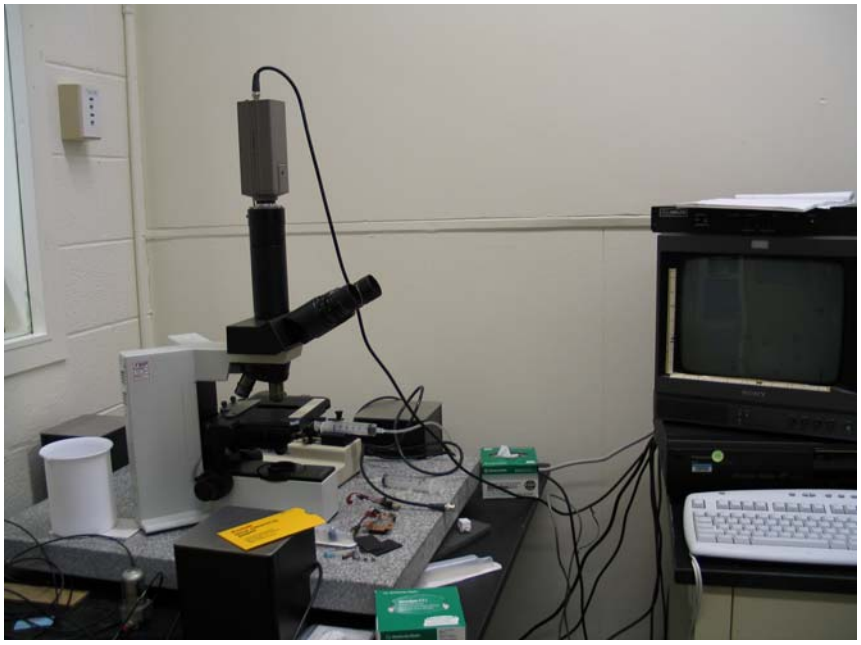

Fig. 30. Metallurgical microscope.

3.1.8 Scanning Electron Microscope/Energy-Dispersive Spectroscopy

Fiber and particle subsamples that either appeared to be very representative or were of special interest because of an unusual characteristic (e.g., shape and color) were selected for SEM/EDS characterization to show the surface topography and to qualitatively determine elemental composition. This equipment is shown in Fig. 31.

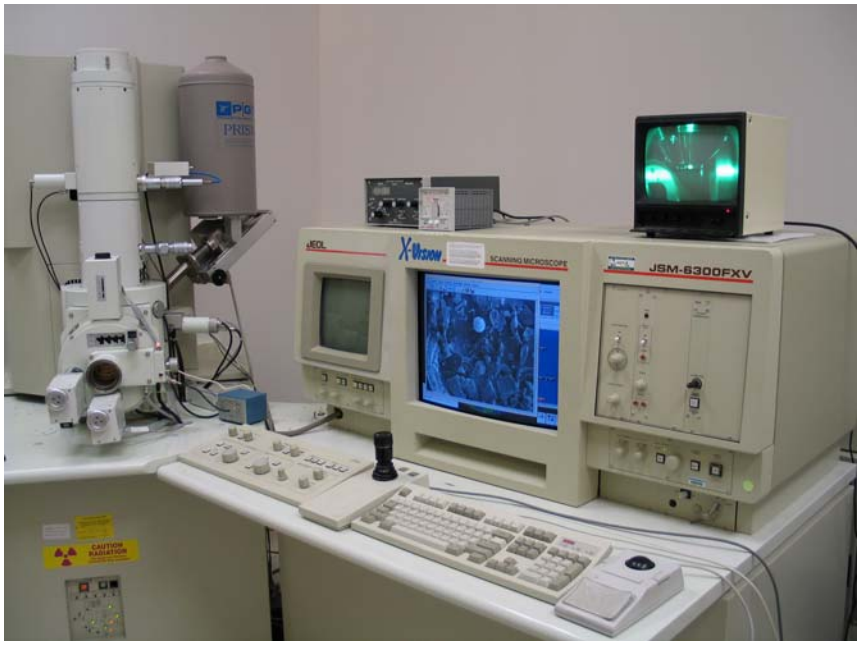

Fig. 31. SEM/EDS instrumentation.

3.2 Characterization Results and Discussion

As presented in the previous section, a variety of analytic techniques was used to characterize the physical attributes of latent debris. The principal results of these methods are now discussed in several subsections, including composition of debris (Section 3.2.1), classification of fibers (Section 3.2.2), fiber density and diameter measurements (Section 3.2.3), BET surface area and particulate density measurements (Section 3.2.4), and characteristics of pores in latent-debris particulates (Section 3.2.5). Note that these sections do not correspond identically with the eight previous subsections that presented the analytic methods because the results from several methods have been combined.

3.2.1 Composition of Debris

Debris samples from four PWRs, namely Plants A, B, C, and D, were fully characterized through all processes described above. The quantities of debris received from each of these four plants were significantly different, varying from <10 g to several thousand grams. In general, the debris consisted of three major fractions, as illustrated in Fig. 2 (i.e., fiber, particulate, and other flakes, pieces, and objects that may be less transportable).

Table 1 summarizes the debris-collection method employed at each plant, the typical locations at which debris was collected, and the time during the plant operational cycle that the debris was collected. The debris-collection method has a large influence on the overall quantity of particulate collected, as well as on the size of the particles collected. The masolin sweep and vacuuming collection process employed at Plants A, B, and D yielded much larger fractions of fine particulate compared with the scraping technique used at Plant C.

Table 1. Latent-Debris Collection Process at Plants A, B, C, and D

Plant	Collection Method	Collection Locations	Collection Time
A	5-gal. vacuum with a 2-in., in-line filter (unspecified commercial filter)	Cable trays, floor, top of electrical panels, top of duct	After plant was cleaned before returning to operation
B	Vacuum with HEPA filter	Refueling floor	As part of the containment cleanup at end of outage
C	Gentle scraping with a metal scraper	Floor, top of junction box, under stairs, on snubber support, cable tray	After plant was cleaned before returning to operation
D	Masolin sweep of floor areas	Top of duct, stairwell, floor, steam line, pipe restraint	After plant was cleaned before returning to operation

Determining the composition of debris started with the initial separation of debris into fibers, particles, and remaining debris (i.e., “other”). As discussed in Section 3.1.2, initial separation of debris employed either wet or dry sieves. The weight percentage of each size fraction of every

sample is different, depending on where and how the sample was collected. Table 2 lists the initial separation results of debris from the four plants. Note that masses of individual samples from Plant A and Plant C were combined into respective totals to estimate the bulk mass fraction of each debris category. Subsamples from Plants B and D were individually large enough to be considered as replicate estimates of mass fraction for each debris category.

At times, separation was difficult because very small particles adhered to clumps of fiber and were nearly impossible to separate completely. The trapping of small particulate on the fibrous debris can be seen clearly in the SEM photograph of fibers from Plant A (Fig. 32 and Fig. 33). Similarly, some shorter fibers are retained in the particulate fraction and cannot be removed. This observation is confirmed by the SEM photograph of particulate fines (<75 μm) from Plant A (Fig. 37).

The quantity of debris in the individual debris samples from Plant A was determined to be insufficient to conduct further characterization tests. However, for each of the samples from Plant A, a small vacuum filter was included that enabled an estimate to be made of the quantity of fine particulate (i.e., <10 μm). To enable further characterization testing, all of the individual debris samples were combined to represent Plant A.

In contrast to Plant A, the quantities of debris in each sample from Plant B were large enough to allow further characterization on an individual basis. Analysis of the HEPA filters included with the Plant-B debris, according to Section 3.1.3 protocol, enabled a rough estimate of the quantity of fine particulate to be made.

Similar to Plant A, the quantity of debris in the individual debris samples from Plant C was insufficient to conduct further characterization tests for all samples. However, the character of each sample from Plant C seemed quite different when compared with Plants A and B. As noted previously, the particulate in the Plant-C debris was light colored, suggesting a significant presence of titanium and manganese oxides. The collection technique of scraping employed at Plant C precluded an estimate of the fine particulate (i.e., that are <75 μm).

The debris received for Plant D was sufficient to allow characterization individually for each of the eight samples provided. For samples D6, D8, D10, and D15, the masolin cloth used to sweep floor debris was included with the sample. Analysis of the masolin cloth (see Section 3.1.3, Fig. 24 and Fig. 25) allowed a better estimate of the amount of fine particulate in the debris sample.

Table 2. Weight Fraction of Latent Debris from Plants A, B, C, and D

Plant A				**Plant B**				**Plant C**				**Plant D[e]**			
	Weight (g)				***Weight (g)***				***Weight (g)***				***Weight (g)***		
ID	P[a]	F[b]	O[b]	ID	P	F	O	ID	P	F	O	ID	P	F	O
A1	0.32	0.02	0.02	B1	214	20	41	C1	4.42	0.05	0.66	D1	2.51	0.47	0.13
A2	0.45	0.06	0.12	B2	369	64	59	C2	NA[d]	0.30	NA	D2	0.29	NA	NA
A3	0.06	0.07	NA	B3	390	37	82	C3	0.77	<0.01	1.90	D3	12.45	0.28	1.00
A4	1.18	0.41	0.04	B4	592	47	53	C4	0.23	NA	0.13	D4	34.34	2.20	32.73
A5	0.15	NA	0.24	B5	792	34	255	C5	1.23	0.02	1.90	D6	5.56	0.10	4.85
A6	0.54	0.02	0.18	B6	122	50	121	C6	0.16	0.04	0.37	D8	9.15	0.09	3.47
A7	0.24	NA	0.06		***Weight (wt %)***			C7	4.20	0.35	7.59	D10	11.98	0.74	2.85
A8	0.05	0.01	NA	B1	78	7	15	C8	3.76	NA	0.19	D15	74.92	7.00	66.90
A9	0.76	0.21	0.12	B2	75	13	12						***Weight (wt %)***		
A10	0.38	0.11	0.07	B3	77	7	16					D1	80.58	15.17	4.25
A11	0.23	0.01	0.39	B4	85	7	8					D2	100.00	0.00	0.00
A12	0.2	NA	NA	B5	73	3	24					D3	90.64	2.06	7.30
A13	0.1	0.08	NA	B6	42	17	41					D4	49.57	3.18	47.25
A14	0.4	0.04	0.01									D6	52.87	0.98	46.16
Total	**5.42**	**1.04**	**1.25**					**Total**	**13.77**	**0.76**	**12.74**	D8	71.96	0.73	27.32
	Weight (wt %)								***Weight (wt %)***			D10	76.91	4.77	18.32
A	**70**	**13**	**16**					**C**	**50.50**	**2.79**	**46.72**	D15	50.34	4.70	44.95

[a] P = particles.
[b] F = fibers.
[c] O = others.
[d] NA = insufficient material to weigh or not present in sample.
[e] Nonsequential sample numbers provided by Plant D were preserved for convenient cross reference. Sample numbers D5, D7, D9, and D11–D14 were not provided.

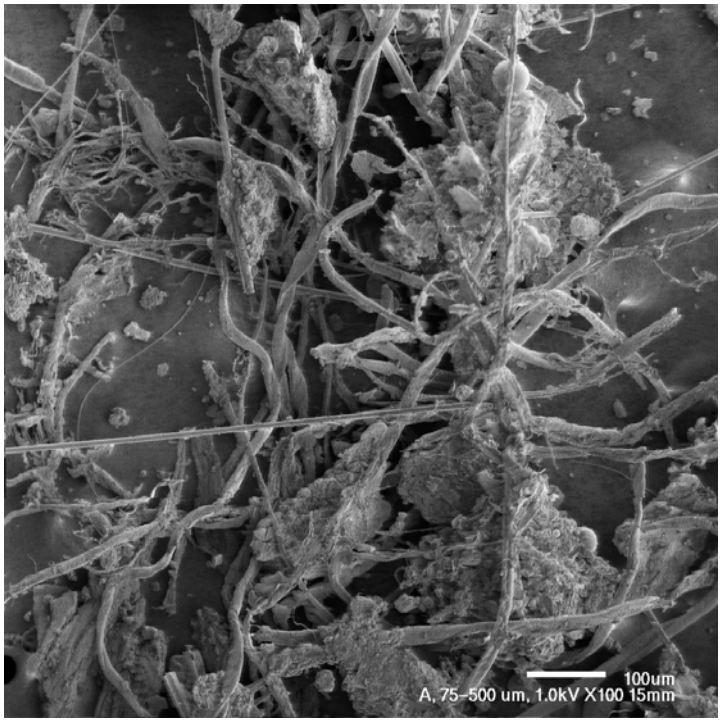

Fig. 32. SEM image of Plant-A fibers at 100 µm.

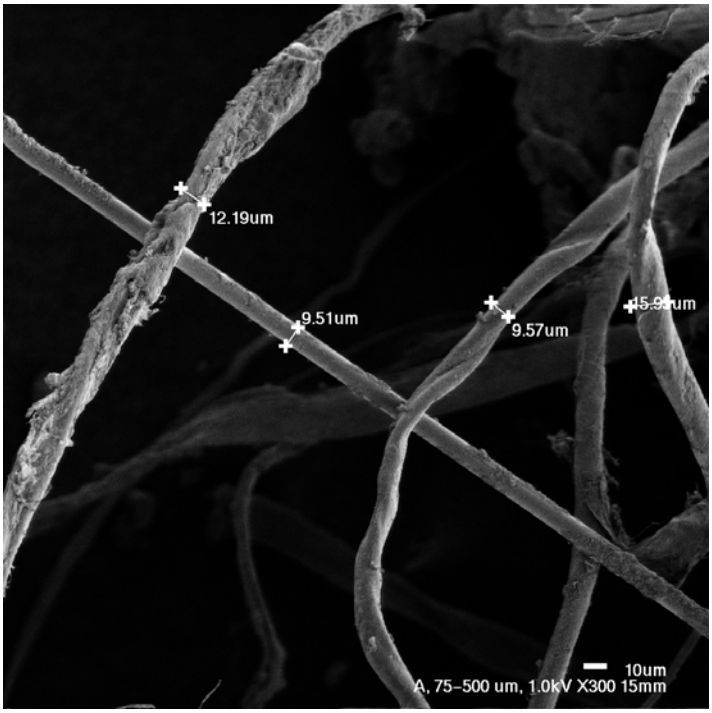

Fig. 33. SEM image of Plant-A fibers at 10 µm.

Fig. 34 summarizes the results of the initial separation of debris for Plants A, B, C, and D. In Fig. 34, the six individual samples from Plant B and eight individual samples from Plant D are shown, whereas the combined results for Plants A and C are presented. The results are shown by weight percent; not surprisingly, particulate fractions significantly exceed fiber or "other" fractions for most samples.

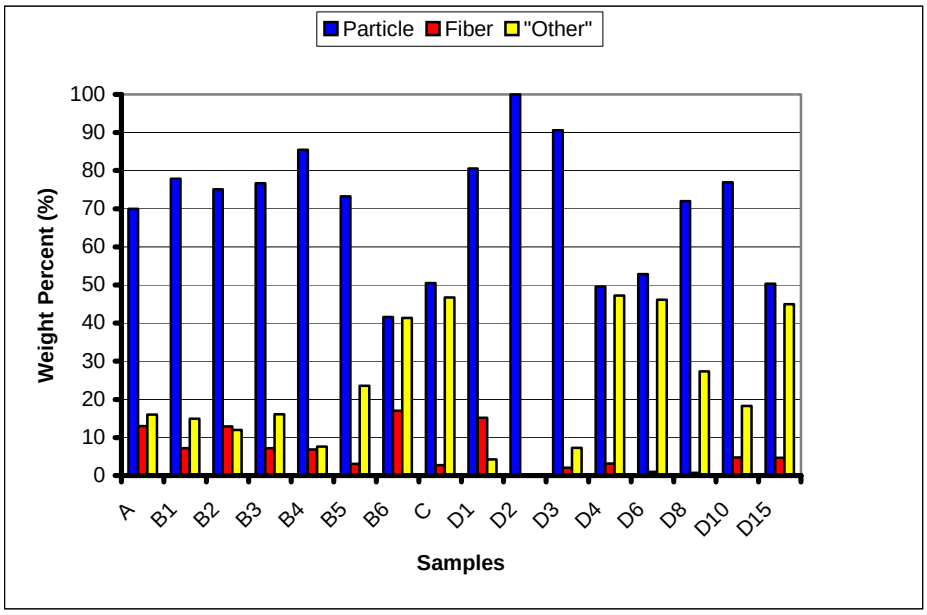

Fig. 34. Composition of latent debris from Plants A, B, and C.

To assist with development of a surrogate debris formula for head-loss testing, the "other" debris category was deemed not applicable. The "other" debris consists of larger material, such as bolts, nuts, cable ties, rags, and other large material, that is not expected to transport to the cooling system screen under recirculation flow velocities or to contribute to the formation of a uniform debris bed on the screen. Because of the lack of transport expected based on previous testing, this "other" material should not be considered in the surrogate debris preparation. However, during containment pool fill, this material may impact the sump screen and pose a concern for screen penetration. If significant quantities of this material were present, such as large amounts of degraded containment coatings, and the sump-screen geometry was unfavorable, such as a horizontal screen at floor level with no curbing, material in this category may pose a potential to block significant portions of the screen area.

Table 3 excludes the "other" category of debris and summarizes the particle and fiber fraction for each of the debris samples from the four plants. Table 3 also provides an overall summary of the weight fraction of particulate and fiber by plant. Fig. 35 graphically displays the information in Table 3, and thus, presents the weight percent of particulate and fibers for each of the test samples. Because debris remaining on the plant HEPA filters could not be thoroughly separated and analyzed, Plant-B particulate percentages are most likely to be low. Overall particulate percentages range on a sample basis from a low of 71% to nearly 100%. On a plant-average basis, the particulate fractions ranged from 84% to 95%.

Table 3. Particulate and Fiber Weight Fractions from Plants A, B, C, and D

Plant	Particle Weight	Fiber Weight	% Particle	% Fiber
A	5.42	1.04	84	16
B1	214	20	91	9
B2	369	64	85	15
B3	390	37	91	9
B4	592	47	93	7
B5	792	34	96	4
B6	122	50	71	29
B Total	2479	252	91	9
C	13.77	0.76	95	5
D1	2.51	0.47	84	16
D2	0.29	0	100	0
D3	12.45	0.28	97	3
D4	34.34	2.20	94	6
D6	5.56	0.1	98	2
D8	9.15	0.09	99	1
D10	11.98	0.74	94	6
D15	74.92	7.0	91	9
D Total	151.2	10.88	93	7
	Sample Range	Total Particulate	71%–100%	
		Total Fiber	0%–29%	
	Plant Range	Particulate	84%–95%	
		Fiber	5%–16%	

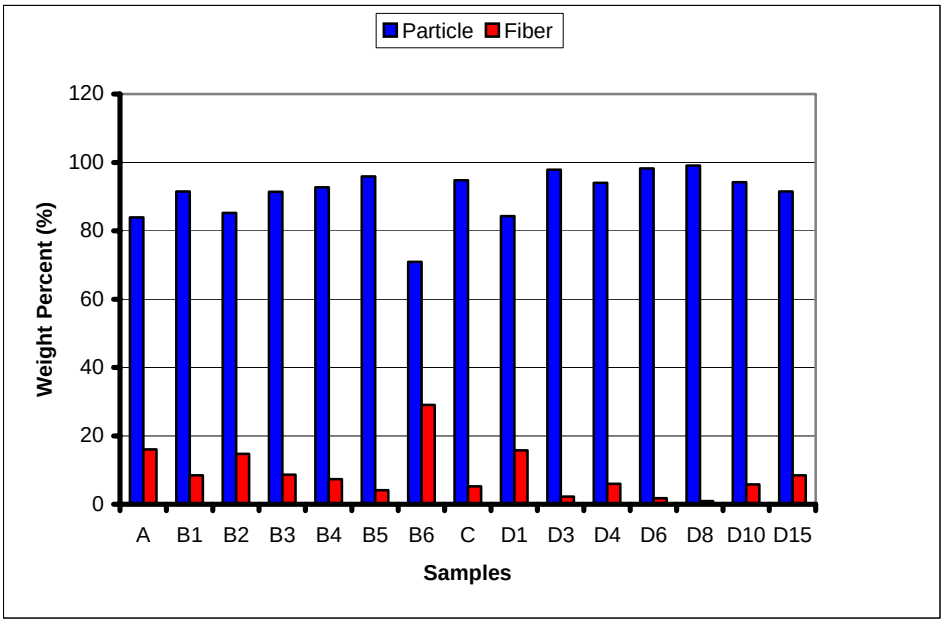

Fig. 35. Weight fraction of particles and fibers for Plants A, B, C, and D.

To characterize the particulate in more detail, the debris-sample particle fraction was further separated into four particle-size categories using sieves with mesh sizes >2 mm, 500 µm, and 75 µm. Table 4 presents the particle-size-distribution results for Plants A, B, C, and D, respectively. The data in the "<75 µm" column of Table 4 include an estimate of the mass of <10-µm particles, as determined using Section 3.1.3 protocol. As discussed previously, this estimate was based on the visual observations of the SEM photographs of masolin cloth and vacuum filters that showed large quantities of fine particles (i.e., <10 µm trapped in the cloth/paper). Fig. 36 and Fig. 37 present SEM photos of representative portions of the 75- to 500-µm particulate from Plant A and the <75-µm particulate from Plant B, respectively. It is interesting to note that, as shown in Fig. 37, small, short fiber sections are present in the <75-µm particulates. Fig. 38 presents an x-ray analysis of several particles shown. Silicon and iron were detected, which suggests the presence of sand and metal. The metal may have originated from welding sputter and fumes (note the spherical particles in Figs. 36 and 37). Because of the wet-sieving process employed for particle separation, some particles are lost and the particle weights may not agree exactly among Tables 2, 3, and 4.

Table 4. Particle-Size Distributions of Plants A, B, C, and D Debris

Sample ID	*>2 mm*		*500 µm–2 mm*		*75–500 µm*		*<75 µm*	
	g	**wt%**	**g**	**wt%**	**g**	**wt%**	**g**	**wt%**
A	1.50	39.54	0.32	8.31	1.24	32.56	0.74	19.60
B1	26.03	15.54	48.04	28.69	9.97	5.95	43.42	49.81
B2	53.25	17.65	79.48	26.34	41.15	13.64	127.90	42.38
B3	77.76	23.84	121.03	37.10	40.15	12.42	86.89	26.63
B4	54.73	11.48	65.13	13.66	51.55	10.81	305.53	64.06
B5	134.51	20.65	130.44	20.03	92.23	14.16	294.19	45.17
B6	10.21	20.22	6.72	13.31	7.74	15.33	25.82	51.14
Btotal	356.49	18.43	450.84	23.31	242.79	12.55	883.75	45.70
C1	0.69	20.18	2.01	58.77	0.69	20.18	0.03	0.88
C2	NM	NM	NM	NM	NM	NM	NM	NM
C3	0.51	66.23	0.24	31.17	0.02	2.6	NM	NM
C4	0.06	26.09	0.10	43.48	0.07	30.43	NM	NM
C5	0.49	39.84	0.62	50.41	0.12	9.77	NM	NM
C6	NM	NM	0.13	81.25	0.03	18.75	NM	NM
C7	0.47	11.19	2.33	55.48	1.37	32.62	0.03	0.71
C8	0.45	11.97	2.84	75.53	0.47	12.50	NM	NM
Ctotal	2.67	19.4	8.27	60.0	2.77	20.1	0.06	0.50
D1	0.24	9.66	0.68	27.19	1.36	54.28	0.22	8.86
D2	NM	NM	NM	NM	0.11	39.47	0.17	60.53
D3	1.02	8.21	3.44	27.65	6.50	52.23	1.48	11.91
D4	2.06	6.01	12.92	37.63	17.74	51.67	1.61	4.70
D6	0.56	10.12	1.25	22.54	0.37	6.70	3.37	60.64
D8	1.21	13.25	2.24	24.51	0.65	7.13	5.04	55.10
D10	2.34	19.56	3.33	27.82	1.51	12.63	4.79	39.99
D15	4.89	6.53	26.28	35.08	27.84	37.16	15.91	21.24
Dtotal	12.32	8.20	50.14	33.20	56.08	37.10	32.59	21.50

NM = Not Measurable: Debris sample did not contain a measurable amount of particulate in this bin.

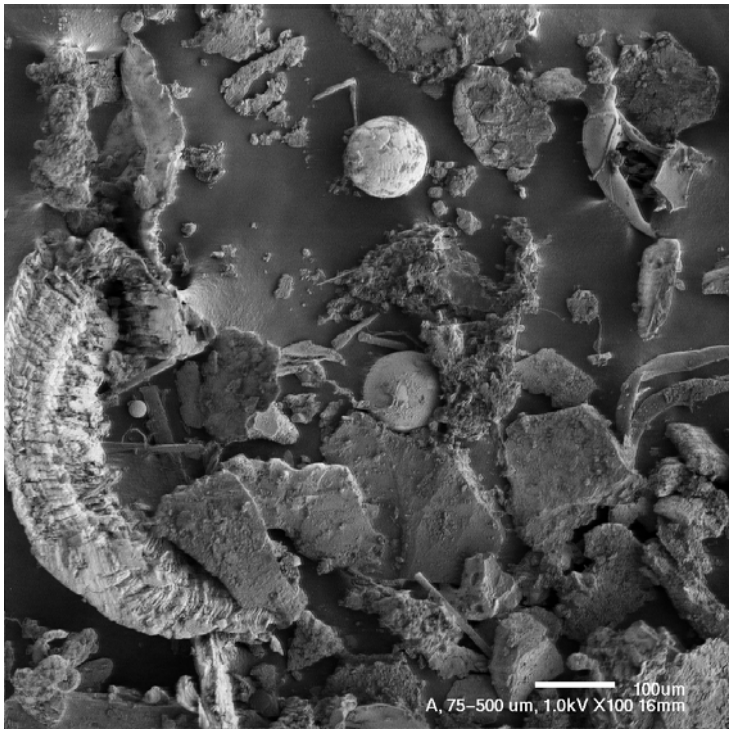

Fig. 36. SEM photo of 75- to 500-µm particles from Plant A.

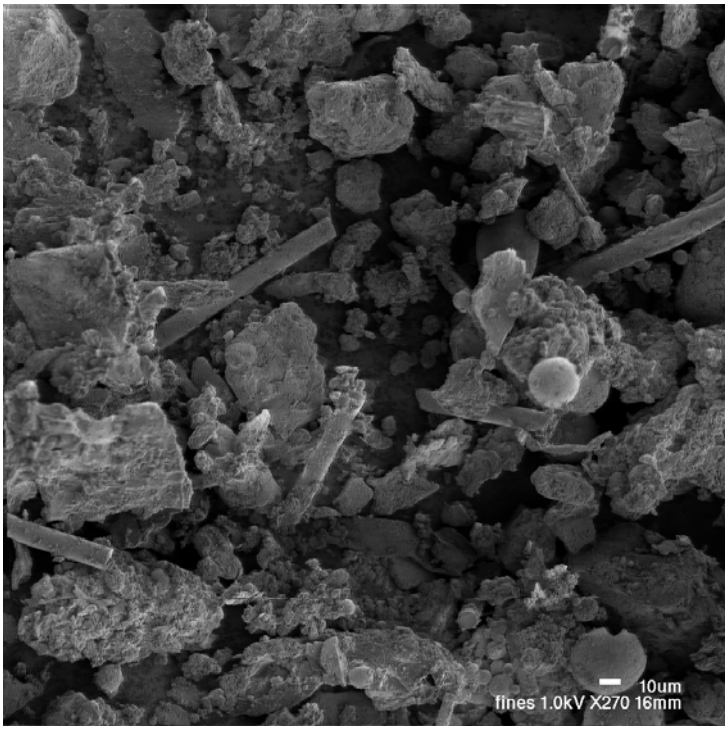

Fig. 37. SEM photo of fines <75 µm from Plant B.

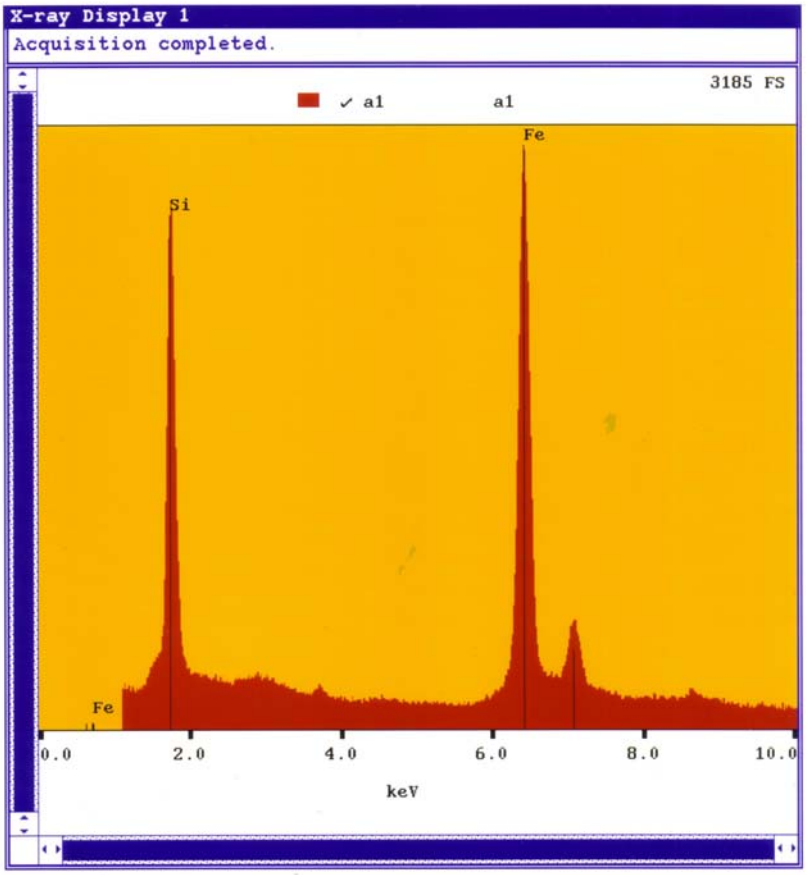

Fig. 38. X-ray analysis of 75- to 500-µm particles from Plant A.

Table 5 summarizes the results of Table 5 and provides an overall summary of the particle-size distribution for all three plants. Note that Plant-C data were not considered in Table 5 because the debris-collection technique at Plant C did not enable the collection of very small particles.

Table 5. Summary of Particle-Size-Distribution Results

Plant	>2 mm	500 µm–2 mm	75 µm–500 µm	<75 µm
A	39.5 %	8.3%	32.5%	19.6%
B	18.4%	23.3%	12.6%	45.7%
D	8.2%	33.2%	37.1%	21.5%
Overall Average	22.0%	21.6%	27.4%	28.9%

As discussed previously, using the results of the analysis of the vacuum filters and the masolin cloth, some insights were gained into the fraction of the <75-µm particles that might actually fall into the <10-µm range. These results are rough approximations and are presented in Table 6. Plant-A results may yield the best approximation because no mass correction was required to compensate for the presence of residual trapped fiber (i.e., ~50% of the <75-µm material is actually <10-µm particles).

Table 6. Analysis of <75-μm Particulate Fraction

Plant	Particulate Weight (g) 10 μm–75 μm	%	Particulate Weight (g) <10 μm	%
A	0.38	51	0.36	49
B	84.12	9.1	839.63	90.9
D15	2.01	12.6	13.9	87.4
Overall Average	–	24	–	76

Fig. 39 presents the particle-size distribution results for Plants A, B, and D. Trends in Fig. 39 are difficult to discern, given the differences between plant collection methods; thus, the overall average size distribution given in Table 5 will be assumed to be representative of all latent debris particulates. The fraction of very small particles (i.e., <75 μm) is highly dependent on the debris-collection method at each plant, which may help to explain the lack of very small particles in the Plant-C debris sample. The results of the masolin-cloth and HEPA-filter analyses show that the fine particulate quantities are large, as shown in Table 6.

3.2.2 Classification of Fibers

Fiber samples that were separated from the debris shipments from Plants A, B, and C were viewed under an optical microscope using a 20X objective lens. Fig. 26, Fig. 27, and Fig. 28 show several selected microscopic images of "fibrous" samples from Plants A, B, and C, respectively. In addition, Fig. 32 and Fig. 33 show SEM images of a fiber sample from Plant A. Because of the large variation in the fiber shapes and dimensions, these images are not necessarily fully representative of the original samples. This variation is not surprising considering the difference in sample collection locations within the plant, the dominant materials present in the plant at the time of sample collection, the methods used to collect the samples, and the manual techniques used to separate the samples. However, several useful observations can be drawn from these images.

As these images depict, the fibers are between ~1 and 20 μm in diameter (or thickness), with the majority being closer to the upper range. The larger fibers (>>5 μm in diameter or thickness) appear to be almost straight cylinders; single, tortuous, and flexible strands; or twisted, flat, ribbon-like strips. Some of these strands appear to be interwoven to form larger clusters of multiple fibers that are attached at different points and have random orientations. The smaller fibers (<<5 μm in diameter or thickness) appear to be interwoven together to form larger clumps. The sizes of these clumps range between a few microns to more than a millimeter (not shown in these images). The images also indicate that these clumps tend to attach (or clamp) to neighboring fibers.

Another important observation from these images is that almost all of the fibers have particles attached to them. This attachment is apparently physiochemical rather than mechanical. The sizes of these particles are comparable to the diameters (or thicknesses) of the hosting fibers in most instances but can be much larger in other instances. However, because of the limited resolution of optical microscopy, it is not obvious whether these attached particles are single particles or clusters of smaller individual particles. These attached particles (or clusters) can have a significant effect on the overall hydraulic behavior of the debris, not only because they induce

additional physical roughness to the fiber surfaces, but also because they can act as seeds that stimulate further attachment of other particles or further clustering of the fibers themselves.

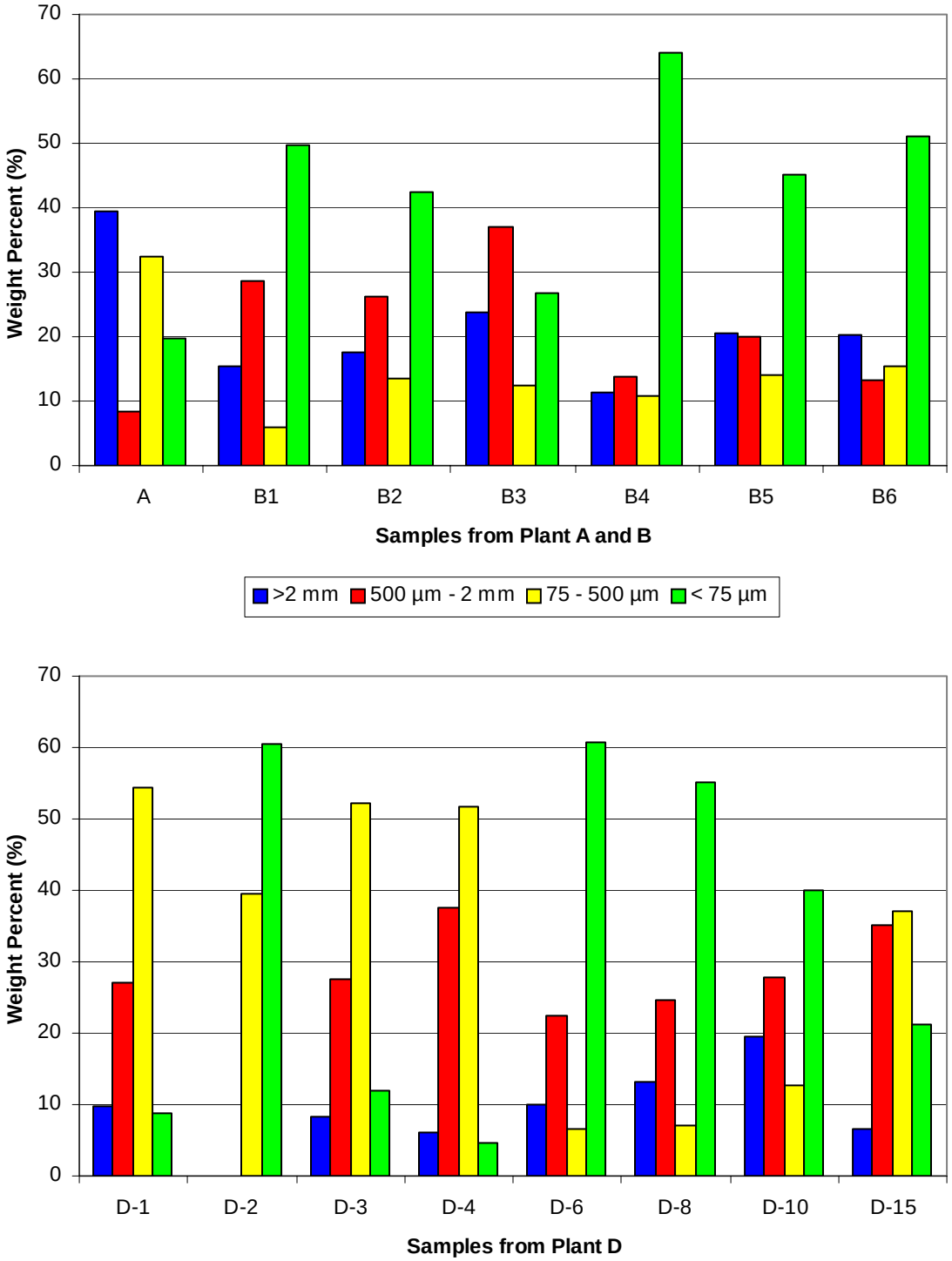

Fig. 39. Particle-size distributions of latent debris of Plants A, B, and D.

Overall, the fiber characteristics qualitatively reflect the fiber-debris classification by shape, as summarized in Table B-3 of NUREG/CR-6224. [2]

3.2.3 Fiber Density and Thickness/Diameter Measurements

Table 7 summarizes the results of the fiber thickness/diameter measurements. The thickness/diameter measurements were determined using the protocol described in Section 3.1.4. From Plants A, B, and C, 630 fibers were evaluated.

Table 7. Results of Fiber Thickness/Diameter Measurements

Plant	A	B	C	Collective
Number of fibers measured	116	231	283	630
Most occurring thickness range (μm)	16.00–18.00	10.00–12.00	12.00–14.00	12.00–14.00
Smallest thickness (μm)	7.71	3.45	1.54	1.54
Largest thickness (μm)	60.32	49.26	53.56	60.32
Mean/median (μm)	16.48/15.21	12.91/11.10	15.16/14.22	14.58/13.57

Fig. 40 shows the distribution of the measured fiber thickness/diameters for each of the three plants considered, whereas Fig. 41 shows the collective thickness distribution for all of the fibers measured. As Fig. 40 depicts, the thickness or diameter of the majority of the fibers from Plant B falls approximately within 10 to 12 μm; Plant C, from 12 to 14 μm; and Plant A, from 16 to 18 μm. If all of the fibers are considered collectively (i.e., regardless of their source), the majority falls between 12 and 14 μm in thickness. As noted previously, the fibers are very long compared with the diameter.

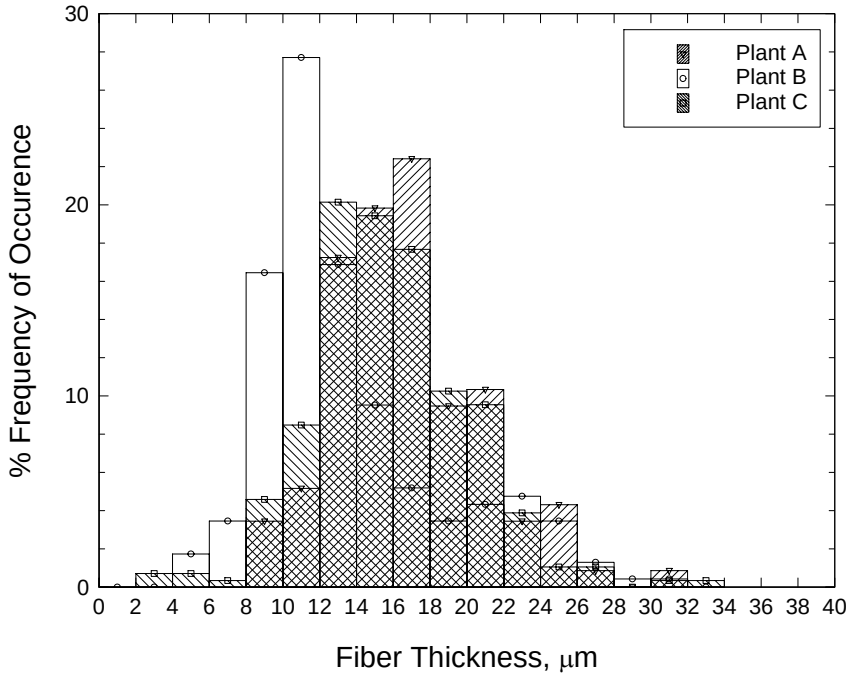

Fig. 40. Distribution of measured fiber thickness/diameter for Plants A, B, and C.

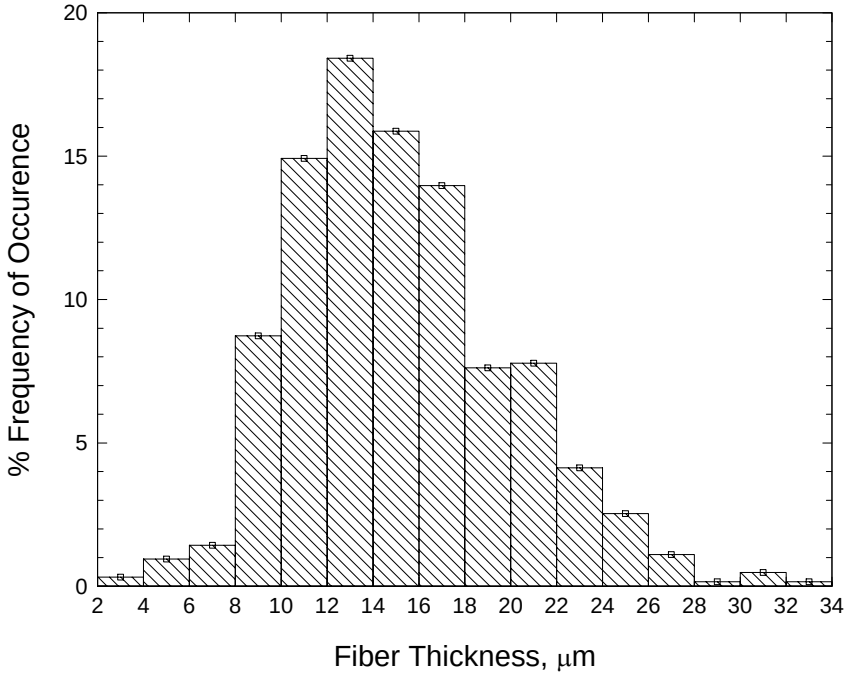

Fig. 41. Collective thickness/diameter distribution.

The material density of a representative sample of fiber from each plant was measured using the experimental protocol discussed in Section 3.1.5. The results of these measurements, as presented in Table 8 suggest an average material density of the fiber mass between 1.3 and 1.9 g/cm^3. An attempt to estimate the uncertainty in these density measurements is summarized qualitatively in Tables 9 and 10 and quantitatively in the column titled "Uncertainty Estimate" in Table 8.

Four major sources of error were identified that could influence the measurement of fiber density. Table 9 lists the possible sources of error and the impact on the density measurement. Table 10 presents a qualitative analysis of the source of error listed in Table 9.

Table 8. Material Fiber Density

Sample ID	Sample Weight (g)	V_w (cm^3)	V_{w+f} (cm^3)	Density of Fiber (g/cm^3)	Uncertainty Estimate[a]
A	0.75	15.0	15.5	1.5	-15%
B1	10.31	50.0	55.5	1.9	-32%
B2	10.95	50.0	56.5	1.7	-24%
B3	6.09	50.0	53.5	1.7	-24%
B4	8.91	50.0	55.5	1.6	-20%
B5	9.02	50.0	55.5	1.6	-20%
B6	8.51	50.0	55.5	1.5	-13%
C2	0.31	5.00	5.30	1.0	+30%
D4	2.20	15.0	16.4	1.6	-20%
D15	7.00	50.0	55.5	1.3	±5%

[a]Collective estimate of uncertainty.

Table 9. Possible Sources of Error in Bulk Fiber Density Measurements

#	Source of Error	Impact on the Density Measurement
1	Precision of cylinder used	±
2	Evaporation	+
3	Attached particles (adhered to fiber)	+
4	Trapped air	–

Table 10. Qualitative Assessment of Error Sources

Sample ID	Error				Total Impact on Density Measurement
	Precision of Cylinder Used	Evaporation	Attached Particles	Trapped Air	
A	0.6%	0.1%	Small	Small	Increase
B1	0.9%	0.2%	Moderate	Small	Increase
B2	0.9%	0.2%	Moderate	Small	Increase
B3	0.9%	0.2%	Moderate	Small	Increase
B4	0.9%	0.2%	Moderate	Small	Increase
B5	0.9%	0.2%	Moderate	Small	Increase
B6	0.9%	0.2%	Moderate	Small	Increase
C2	0.1%	0.05%	Very small	Very small	Decrease
D4	0.6%	0.1%	Small to moderate	Small	Increase
D15	0.9%	0.2%	Small to moderate	Small	Increase or decrease

Filter-bed densities were measured following the procedures described in Section 3.1.5. Results presented in Table 11 suggest that a nominal fiber density of 0.09 g/cm^3 (5.62 lbm/ft^3) might be a reasonable estimate for the dry fiber-bed density. Recall that the NUREG/CR-6224 [2] head-loss correlation uses the dry, as-fabricated density for fibrous insulation debris. However, because latent fibers have no equivalent definition of fabrication density and because the sample fibers were wet washed and manually separated before drying, some degree of conservatism is prudent.

Table 11. Wet and Dry Densities of Fibrous Debris Beds

Sample #	Fiber Mass (g)	Dry Dispersed Fiber-Bed Density (g/cm^3)	Dry Compressed Fiber-Bed Density (g/cm^3)	Wet Compressed Fiber-Bed Density (g/cm^3)
B-2-F	23.17	0.086	0.51	0.37
B-4-F	13.18	0.094	0.44	0.38

To compensate for possible variations in latent fiber and to simplify the treatment of latent fiber properties, it is recommended that the standard density of 2.4 lbm/ft^3 used for fiberglass also be applied for latent fibers when assessing the potential of latent fibers to form, or contribute to, a thin-bed fibrous filter on the sump screen.

3.2.4 BET Surface Area and Density of Particles in Latent Debris

According to the ECCS Strainer Blockage Model, [2] the formation of a debris layer on the strainer surface results in pressure drops across a fibrous bed. The extent of the pressure drop depends largely on the character of the debris, including its SSA and density of the particles. Following the protocol discussed in Section 3.1.6, SSA and density measurements of various-sized particles of latent debris from Plants A, B, and C were made. The average results of these measurements are listed in Table 12. Again, although the BET surface area determined by nitrogen adsorption may be a contributing factor to the hydraulic specific surface area needed for head-loss estimation, the two are not identical. BET surface areas are reported herein as a quantitative measure of comparison between latent-debris samples and surrogate particulate formulas that will be discussed in Section 4.0. In this section, the acronym SSA will be understood to refer to the BET specific surface area.

Table 12. BET SSA and Density of Particles in Debris from Plants A, B, C, and D

Sample ID	<75 µm		75–500 µm		500 µm–2 mm	
	SSA (m^2/g)	Density (g/cm^3)	SSA (m^2/g)	Density (g/cm^3)	SSA (m^2/g)	Density (g/cm^3)
A	0.48	2.25	0.75	2.47	1.96	1.48
B1	0.66	2.80	0.11	2.51	0.05	2.69
B2	0.81	2.67	0.38	2.38	0.18	2.40
B3	0.68	2.88	0.43	2.87	0.99	2.10
B4	0.28	3.27	0.16	3.60	0.10	2.89
B5	0.28	3.28	0.06	3.83	0.69	3.18
B6	0.42	3.31	0.29	2.65	0.89	2.46
C1	-[a]	-	0.29	1.62	2.05	2.49
C4	-	-	1.79	4.12	-	-
C7	-	-	0.41	2.18	0.65	2.21
C8	-	-	5.85	3.16	0.01	3.00
D1	0.31	3.28	0.07	3.02	-	-
D3	0.03	4.14	0.46	3.28	0.22	2.62
D4	0.27	4.99	<0.0001	3.78	0.14	3.19
D8	-	-	0.09	3.47	0.09	2.56
D10	-	-	1.69	2.62	0.12	2.41
D15	<0.0001	1.94	1.48	3.16	<0.0001	2.68
Average 1[b]	0.38	3.16	0.82	2.98	0.54	2.56
Average 2[c]	0.38	3.16	0.46	3.05	0.45	2.56

[a]Denotes insufficient amount of sample to conduct tests.

[b]Average 1: average result, including samples from Plant C.

[c]Average 2: average result, excluding samples from Plant C.

The relationship between particle size, SSA (m^2/g), and density (g/cm^3) for all measurements shown in Table 12 is depicted in Fig. 42 except that the axes ranges have been truncated and Plant-C data have been omitted. The densities of particles in the debris range from 2 to 4 g/cm^3 with only a few exceptions. The densities for most of the samples, regardless of their particle-size and surface-area differences, range between 2.5 and 3.0 g/cm^3. Interestingly, the surface

areas of particles sized between 75 and 500 µm are generally smaller than the surface areas of particles sized <75 µm. Two ranges of surface areas appear for the large particle sizes shown in Fig. 42. One set clusters around a low surface area of ~0.2 m^2/g, whereas the other clusters around a large surface area of ~1 m^2/g. Thus, it seems that the average density of the debris does not depend on its particle size; however, the surface area of the debris does seem to depend on its particle size. In general, the smaller the particle size of the debris, the larger the surface area. Exceptions occur in which larger particles also have larger surface areas, thus reflecting the stochastic variability in the physical and chemical characteristics of the debris. Whereas Fig. 42 summarizes the results of surface-area and particle-density measurements, excluding the data from Plant C, Fig. 43 presents the average SSA and particle density by size for Plants A, B, and D combined.

An experienced practitioner of the NUREG/CR-6224 [2] head-loss correlation may recognize that the product of the BET surface area and the material density reported in Table 12 provides an estimate of the hydraulic SSA when converted to English units. When this exercise is performed for the last row in Table 12, Average 2, and the individual size-bin products are weighted by the average respective mass fractions reported in Table 5 (the mass fractions should be renormalized over the sum of the smaller three size bins for consistency), an estimate for the hydraulic SSA of S_v = 383,560 ft^2/ft^3 is obtained. This estimate is conservatively high for direct application in the head-loss correlation for two reasons. First, the BET technique is sensitive to extremely small pore sizes that water actually may not pass through when the particulate is present as a constituent in a fibrous debris bed; therefore, the measurement of actual surface area is inflated beyond that needed to explain hydraulic friction losses in a composite bed. Second, the actual material density has been used in this estimate rather than the granular packed bed density, which would be lower. Nevertheless, this estimate might be no greater than a factor of 2 higher than hydraulic surface areas inferred from large-scale head-loss measurements. With proper correlation, the BET method may prove to be a very efficient means of obtaining critical material property data.

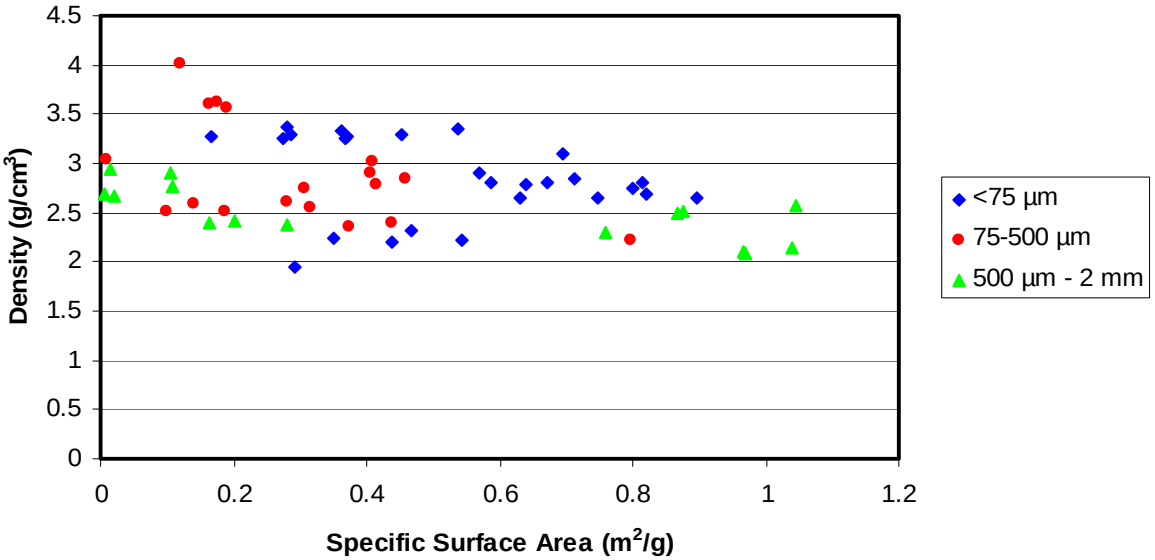

Fig. 42. BET SSA and density of latent debris as a function of its particle size.

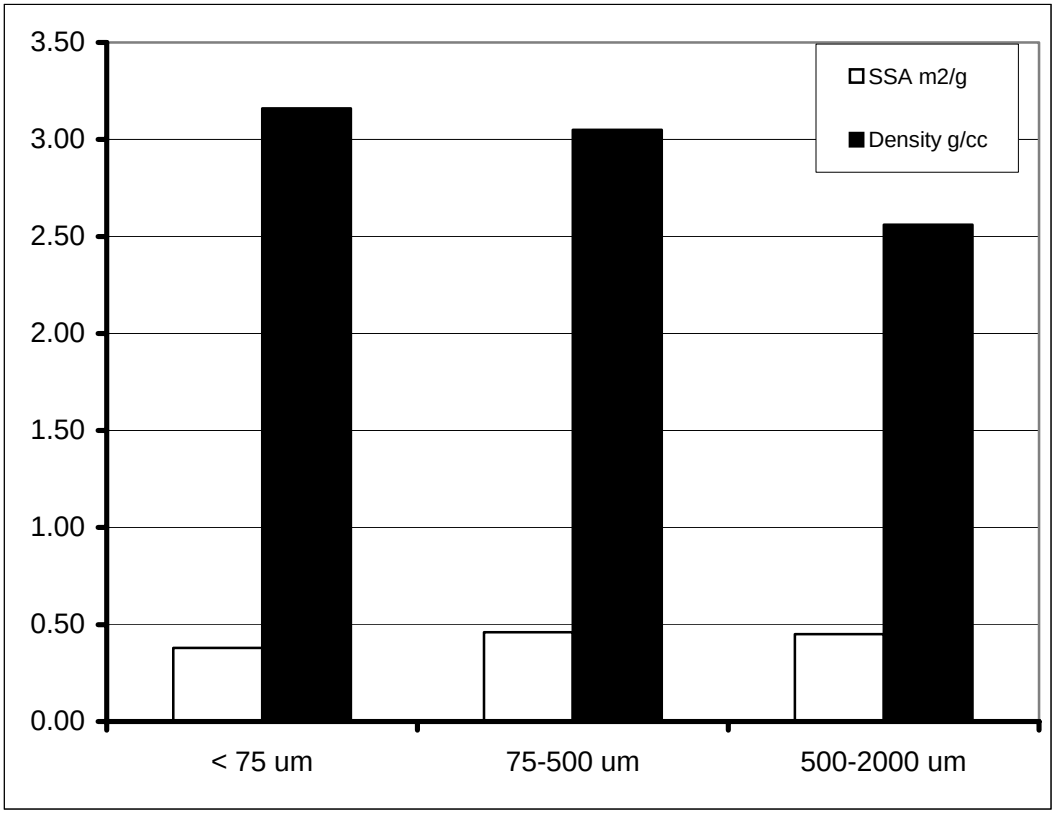

Fig. 43. BET SSA and density of latent debris as a function of particle size.

3.2.5 Characteristics of Pores in Latent Debris

As discussed in Section 3.2.4, the total internal and external surface area of particles depends not only on the particle size but also on the character of the porosity, the pore distributions, and the shape of the pores in the particles. Representative data for latent particle debris with a particle size of 75 to 500 μm were analyzed using software AS1 Autosorb 1, provided by Quantachrone Instruments. The Horvath/Kawazoc (HK) [5] method was applied to the determination of distributions for micropores (<20 Å), whereas the Barrett/Joyner/Halenda (BJH) [6] method was applied to the determination of distributions for mesopores (20 to 500 Å).

Fig. 44 and Fig. 45 present the results of the HK and BJH methods when applied to determine the precise pore distribution of representative particle-debris samples. These results are typical of the particle-debris samples analyzed to date. As shown in Fig. 44 and Fig. 45, the pore diameters range from 10^{-3} μm to 3×10^{2} μm for particles in the range of 75 to 500 μm.

3.3 Guidance for Preparation of Surrogate Debris

Numerous head-loss tests have been designed and conducted at UNM [7],[8] to verify head-loss correlations for particulate debris such as calcium silicate. However, to conduct meaningful head-loss tests with debris that is representative of that found in PWR nuclear power plants, a

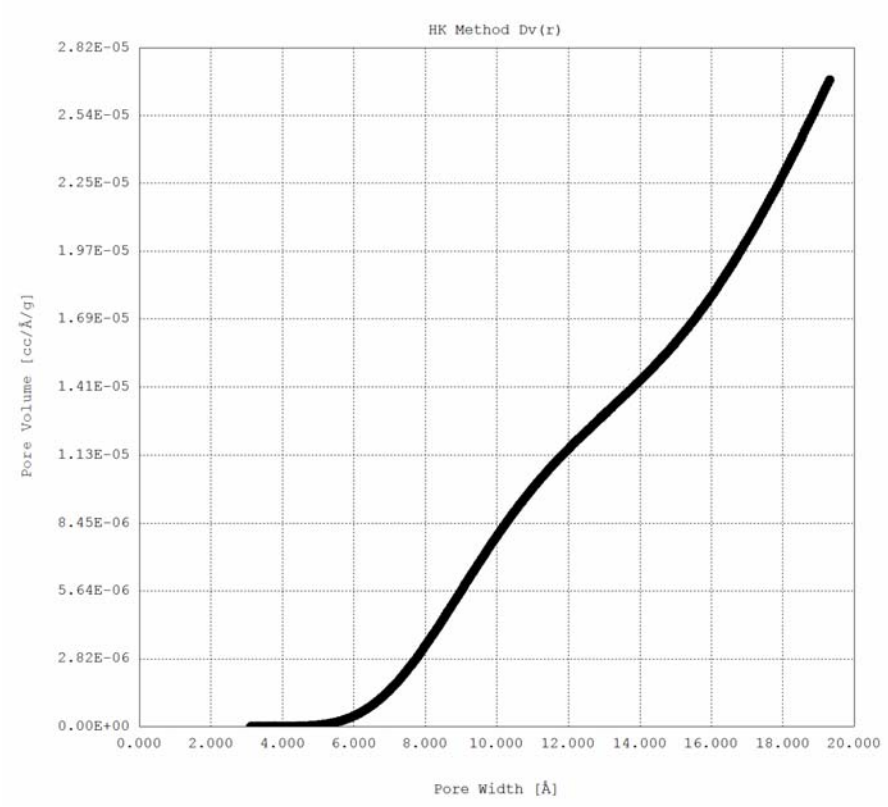

Fig. 44. Micropore distributions in the representative particle debris.

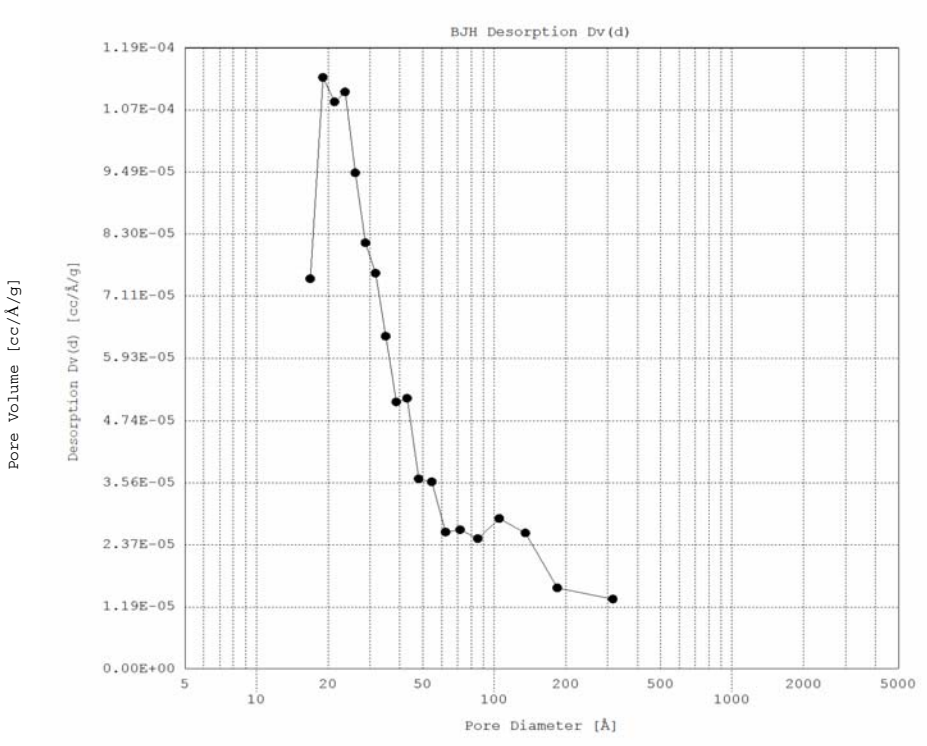

Fig. 45. Mesopore distributions in the representative particle debris.

recipe or formula for preparation of a surrogate was developed based on the characterization data presented in the previous section. A surrogate material is needed because the latent-debris samples are radiologically contaminated and because there is insufficient quantity to execute meaningful tests. This section presents ideal recommendations for most closely matching the measured physical properties of the plant samples.

Based on a review of the experimental data in Section 3.2, it was decided that the surrogate should be developed by considering the latent plant debris as comprising two fractions, one of fibrous matter and the other of particulate matter. The initial characterization of the latent plant debris in this report considers a third fraction, labeled "other," which consisted of larger material, such as bolts, nuts, cable ties, rags, and other material that is not expected to transport to the cooling system screen or to form a uniform debris bed on the screen (see caveats in Section 3.2.1). The fibrous surrogate fraction should be prepared such that the length-to-diameter ratio is large (latent fibers are very long compared with their diameter), and be characterized by the proper density and diameter distribution. If possible, random shapes should be considered consistent with the photomicrographs shown in Fig. 26, Fig. 27, Fig. 28, and Fig. 32 and similar to the fiber patterns shown in NUREG/CR-6224. [2]

The particulate surrogate fraction should be divided into four discrete size fractions, as shown in Table 4 and Table 5, and each fraction should be characterized by representative sizes, densities, and surface areas. Particular efforts should be made to match the fraction of fine particulates (i.e., <10 μm) because these very small particles are important contributors to "thin-bed" head-loss behavior, where a thin mat of fiber is capable of supporting a packed bed of sludge particulates. Note that the characterization tests described in Section 3.2.4 indicated that the latent particulate debris had an average density of 2.5 to 3.0 kg/m^3, which is somewhat higher than the density of common silica-based sands and soils. In addition, if possible, samples of prepared surrogate debris should be tested in a small-scale, packed-bed column to compare the hydraulic characteristics of the surrogate debris with those of the latent debris, as described in Section 4.2. Table 13 summarizes the overall guidance developed based on the characterization measurements in Section 3 and recommended for preparation of a surrogate latent-debris material for head-loss testing.

Table 13. Summary Guidance for Latent-Debris Surrogate

Debris Parameter/Characteristic	Recommended Value
Relative weight fraction fiber/particulate	Range: 5%/95% to 16%/84%
Fiber morphology	Straight cylinders; single, tortuous flexible strands; twisted, flat, ribbon-like strips; interwoven large clusters; large L/D
Fiber diameter	Mean 12–14 μm, range 6–26 μm
Material fiber density	Mean 1.6 g/cm^3, range 1.3–1.9 g/cm^3
Dry bulk-fiber density	Observed 90 kg/m^3, recommended 38.4 kg/m^3 (2.4 lbm/ft^3)
Particle density	Median 2.7 g/cm^3, range 1.5–4.0 g/cm^3
Particle SSA (based on BET measurement)	Average 0.4 m^2/g, range 0.01–2.0 m^2/g
Particle-size distribution—weight fraction (see Tables 5 and 6)	Plant average: 22%, >2 mm; 22%, 500 μm–2mm; 27%, 75 μm–500 μm; 7%, 10 μm–75 μm; 22%, <10 μm

4 HYDRAULIC MEASUREMENT OF SURROGATE DEBRIS

Radiologically contaminated samples from the volunteer plants cannot be tested in the hydraulic circulation loop at UNM. Therefore, a formula was developed for artificially manufacturing a suitable surrogate for latent debris that is found in containment. The following sections describe (1) the basis for the surrogate debris formula, (2) microflow conductivity comparisons of both debris samples and surrogate material, and (3) head-loss measurements of the surrogate to derive hydraulic properties suitable for evaluation of the NUREG/CR-6224 [2] head-loss correlation.

4.1 Surrogate Debris Formula

The following two sections present assumptions related to the three fractions of latent debris that were identified in Section 3.1.2. The latent-debris fractions of "other" and fiber are discussed first, followed by a discussion of the latent particulate treatment. Whereas the previous subsection presented ideal recommendations for most closely matching the physical characteristics of the plant samples, this section relaxes some of the comparative criteria and relies more on the similarity of microflow conductivity measurements to establish equivalent hydraulic behavior. In summary, latent fibers are assumed to have hydraulic properties similar to fiberglass insulation, and latent particulate is simulated with a mixture of common sand and clay/silica-based soil. Quantitative findings for the hydraulic properties of the particulate fraction are found in Sections 4.2 and 4.3.

4.1.1 "Other" and Fiber Surrogate Debris Fractions

Physical characterization of plant samples reported in Section 3.1.2 divided latent debris into the broad categories of fiber, particulate, and other. The category "other" was observed to contain a variety of larger chips, grains, and objects that are considered to be nontransportable under typical recirculation velocities but may pose a screen penetration potential if transported at high water velocity during pool fill. Although bed-formation scenarios may exist where larger pieces are incorporated in the composite, the low SSA of this debris fraction is not likely to contribute significant additional head loss in combination with fiber and small particulates. Therefore, this debris fraction will not be considered further in this analysis.

Fibers observed in the latent-debris samples have a variety of characteristics. In general, latent fibers are thought to be anthropomorphic in origin, arising primarily from the shedding of human hair, clothing fibers, cleaning-rag fibers, and canvas insulation jacket fibers. Latent fibers generally tend to be longer and thicker (15 to 25 μm in diameter) than the strands found in commercial fiberglass insulation (7 to 10 μm in diameter). Although the fiber fraction manually separated from the raw plant samples after wet sieving was observed to be clumped and matted, it is conservatively assumed that latent fibers in the plant are relatively independent and, therefore, are easily suspended and transported under reasonable water velocities associated with spray washdown and recirculation.

In accident scenarios where little or no fiberglass insulation debris is generated, the principal concern is the formation of a latent fiber thin bed that can sustain a layer of latent particulate. This bed configuration would approach the sludge-limit condition where head loss is dominated

by the properties of the particles and not affected greatly by the characteristics of the latent fiber. In scenarios where sufficient fiberglass debris is generated, the latent fiber characteristics are not expected to perturb the behavior of the predominantly fiberglass bed. Given the above comparison of latent fiber and fiberglass-strand diameters and the assumption of similar packing behavior, it is conservative to assume that the latent fiber component has hydraulic properties similar to those of fiberglass. Therefore, the latent fiber fraction was not isolated for hydraulic testing in this study.

4.1.2 Particulate Surrogate Debris Fraction

In aggregate, the particulate fraction of the latent-debris samples appeared to be similar to common "dirt"; therefore, soil was one obvious choice for formulating a suitable surrogate. Particle size and morphology are two of the key parameters controlling hydraulic pressure drops in mixed particulate beds; thus, particle-size distribution and BET SSA of actual latent particulates were compared to alternative compositions of surrogate soil. As a final check of gross similarity, both plant samples and surrogate samples were subjected to microflow conductivity tests as described in Section 4.2. Basic characteristics of the stock soil and the methods used to prepare the surrogate mixture are presented here.

Bulk soil samples collected at the Denver International Airport were available in the UNM Civil Engineering department to use as stock material for the surrogate. This soil is light brown in color with little humus (organic) content and has an average water content of 3.45% as measured by replicate samples weighed before and after drying at an elevated temperature. A density of 2.65 g/cm^3 was measured by water-volume displacement of a known mass of soil after removing air occlusions in a vacuum chamber. Fig. 46 displays the distribution of particle grain size determined by dry mechanical sieving and the distribution of pore sizes determined by hydrometric analysis. These data are presented as inverse cumulative distribution functions where the ordinate reports the cumulative mass fraction of the sample with sizes smaller (finer) than the corresponding value of the abscissa. Note the reversed direction of the particle-size scale.

Basic data for the mechanical sieving process are presented in Table 14 to document the discrete mesh sizes that were used for characterization. The mass fraction of this soil type with sizes <75 μm is <10%, whereas the latent-debris particulate samples had fine fractions on the order of 20% to 30%.

The bulk soil characterized above was mechanically dry sieved into size bins matching those of Table 5, which summarizes the latent particulate-size distributions. Visual inspection of the sieved soil bins suggested that the particles >2 mm would have very limited transport potential and very little impact on the estimated hydraulic SSA, which is dominated by fine particulates. After eliminating 22% of the mass for particles >2 mm, the renormalized particulate mass distribution becomes 27.7% between 500 μm and 2 mm, 35.2% between 75 μm and 500 μm, and 37.1% <75 μm in diameter. Sieved-soil masses of each size category were then combined according to these proportions and thoroughly mixed to form the surrogate particulate debris fraction.

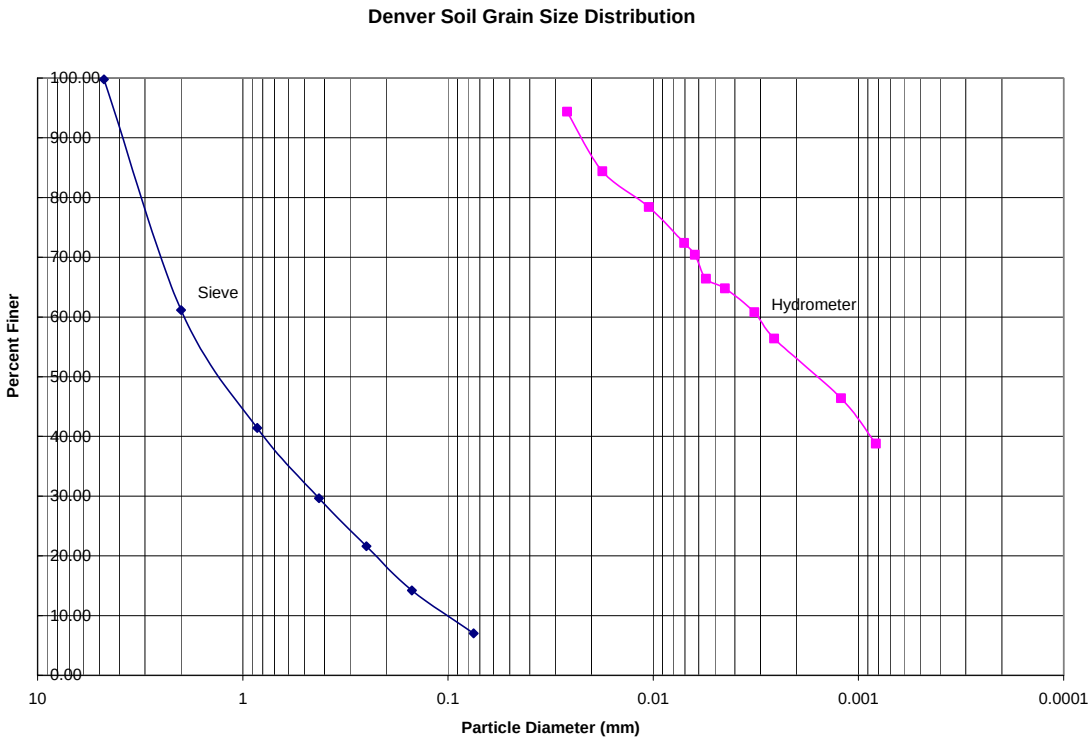

Fig. 46. Original grain-size distributions of bulk soil used to prepare surrogate particulate debris.

Table 14. Mesh Sizes and Mass Fractions Used for Mechanical Sieving of Stock Soil

Sieve #	Diameter (mm)	Mass Retained	% Retained	Cumulative% Retained	% Passing
4	4.75	1	0.20	0.20	99.80
10	2	193	38.64	38.84	61.16
20	0.85	98.6	19.74	58.58	41.42
40	0.425	58.8	11.77	70.35	29.65
60	0.25	40.1	8.03	78.38	21.62
100	0.15	37	7.41	85.79	14.21
200	0.075	35.9	7.19	92.97	7.03
Pan		35.5	7.11	100.00	0.00
		499.9			

Preliminary head-loss tests indicated that the larger soil particles disintegrated into fine clay silt when exposed to water, leading to excessive head loss. If disintegration occurred when wet sieving the latent-debris samples, the constituent particles were accounted for in the <75 µm mass fraction; therefore, degradation of the soil during the test introduced more fines than were actually represented in the plant samples. To address the complication of soil disintegration in water, properly sieved common sand was substituted for soil in the larger two size categories.

Thus, soil was used to represent fines only <75 μm in diameter, which amounts to 28.9% of the total mass composition. Although particle disintegration was still observed during testing, similar behavior may have occurred when wet sieving the latent-debris samples. This effect may account for the large proportion of fines observed in the plant-sample average when compared with the stock-soil distribution.

4.2 Microflow Comparisons

To supplement the comparison of latent particulates and the soil surrogate fabricated on the basis of particle-size distribution, a microflow test apparatus, as shown in Fig. 47, was built. The objective of these tests was to compare the bulk-averaged hydraulic behavior of the samples by passing water through a small packed bed of particulate. Although the pressure drop incurred across such a sample is not directly relevant to debris-induced head loss on a sump screen, the same hydraulic properties of the porous medium act to impede water flow. Thus, if the behavior of the surrogate mixture falls within the variability of the latent-debris samples as measured by the microflow test, credibility is added to the choice of the surrogate formula. Conductivity measurements provide another basis for comparing the degree of similarity between the latent-debris samples and the surrogate.

The cylindrical sample column (shown in Fig. 48) of the microflow test loop is 1 cm in diameter and 5 cm long. Debris and surrogate samples ranging from 1 to 5 g were manually packed into the column over a microporous filter of 2-μm pore size and allowed to saturate in water under vacuum to remove any air occlusions. The packed-debris beds were covered with a layer of 3-mm-diameter glass beads to ensure a stable bed configuration. Relatively large objects like the glass beads do not affect flow through the bed, which is controlled principally by the fine particulate. A reservoir of water above the test column provides approximately constant static head to drive water flow through the bed. By measuring the volume of water passing through the bed in a given time, bulk-flow velocities can be derived. Typical test durations exceeded 2 hours. A microporous filter was required to confine the smallest particulates present in both the latent and surrogate samples. In early attempts with more-porous filter media, the very fine debris migrated through the bed and washed through the filter.

According to Darcy's Law for one-dimensional vertical flow, the saturated hydraulic conductivity of a flow cell (column) can be calculated by measuring a constant hydraulic head difference, which is applied across the sample packed in a flow cell (column), the length of the flow path, and the outflow volume of fluid, which is calculated over measured time intervals by weighing the mass of the outflow. The saturated volumetric water content of the flow cell is calculated from the mass difference of the saturated and dry flow cell. Thus,

$$v = K * A * \frac{\Delta H}{L} \quad , \tag{4}$$

where

v = the volumetric flow rate (cm^3/s),
K = hydraulic conductivity of the system (cm/s),
ΔH = a constant hydraulic head difference between the water surface in the supply reservoir and the outflow of the flow cell (cm),
L = the flow cell length (cm), and
A = the cross sectional area of the flow cell.

The basic experimental procedure comprises the following three steps.

1. Flow Cell (Column) Packing

   The column used for the saturated hydraulic conductivity test is a FLEX-COLUMN (length 5 cm, diameter 1 cm) with a 20-µm pore polyethylene bed support. To obtain a better packing, the dried test material is added to the column slowly while at the same time applying manual vibration to the column. The column is filled up to a reference mark at the top end of the column. The remaining space, i.e., the translucent reservoir top (from the top end of the column to the Luer lock fitting), is filled with 3-mm-diameter glass beads, as illustrated in Fig. 48.

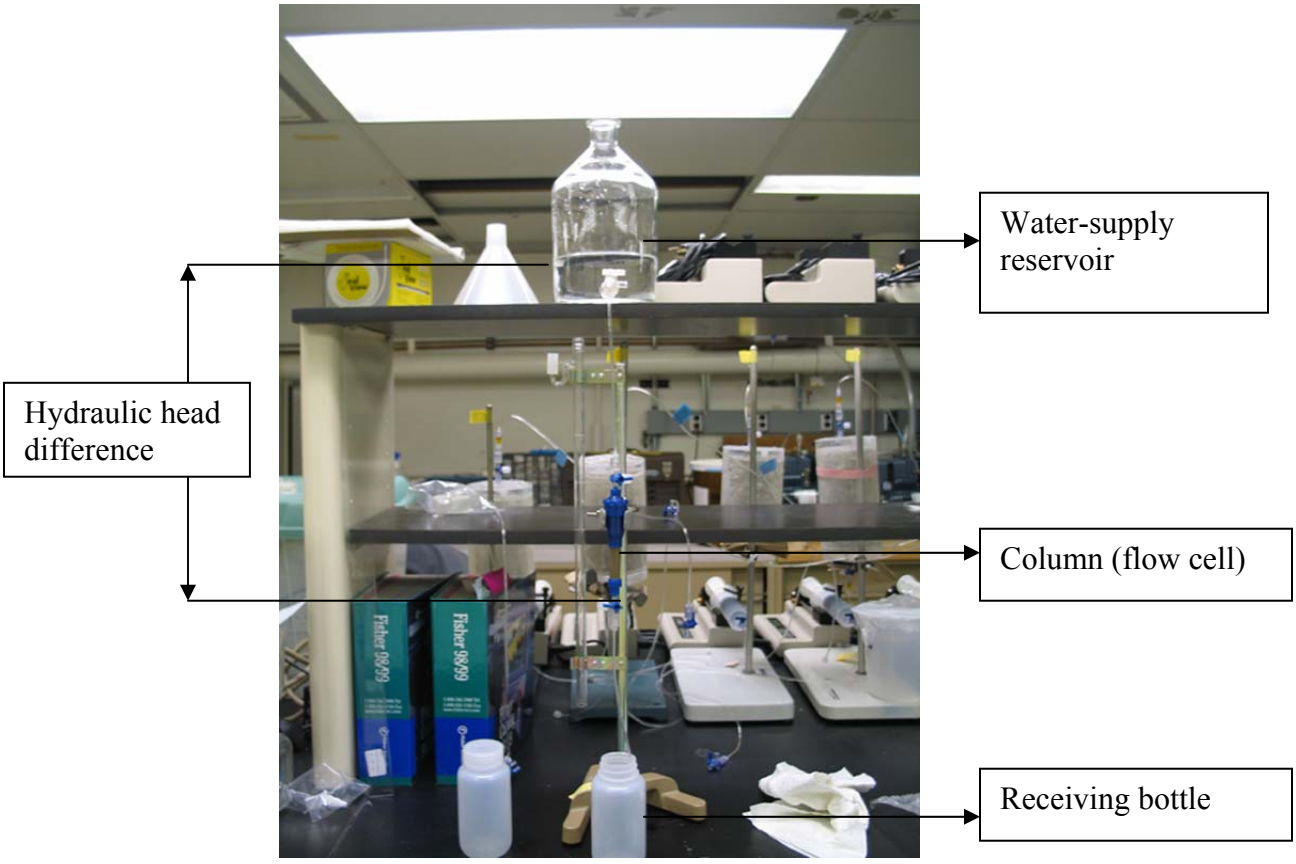

Fig. 47. Microflow test apparatus for debris-conductivity measurements.

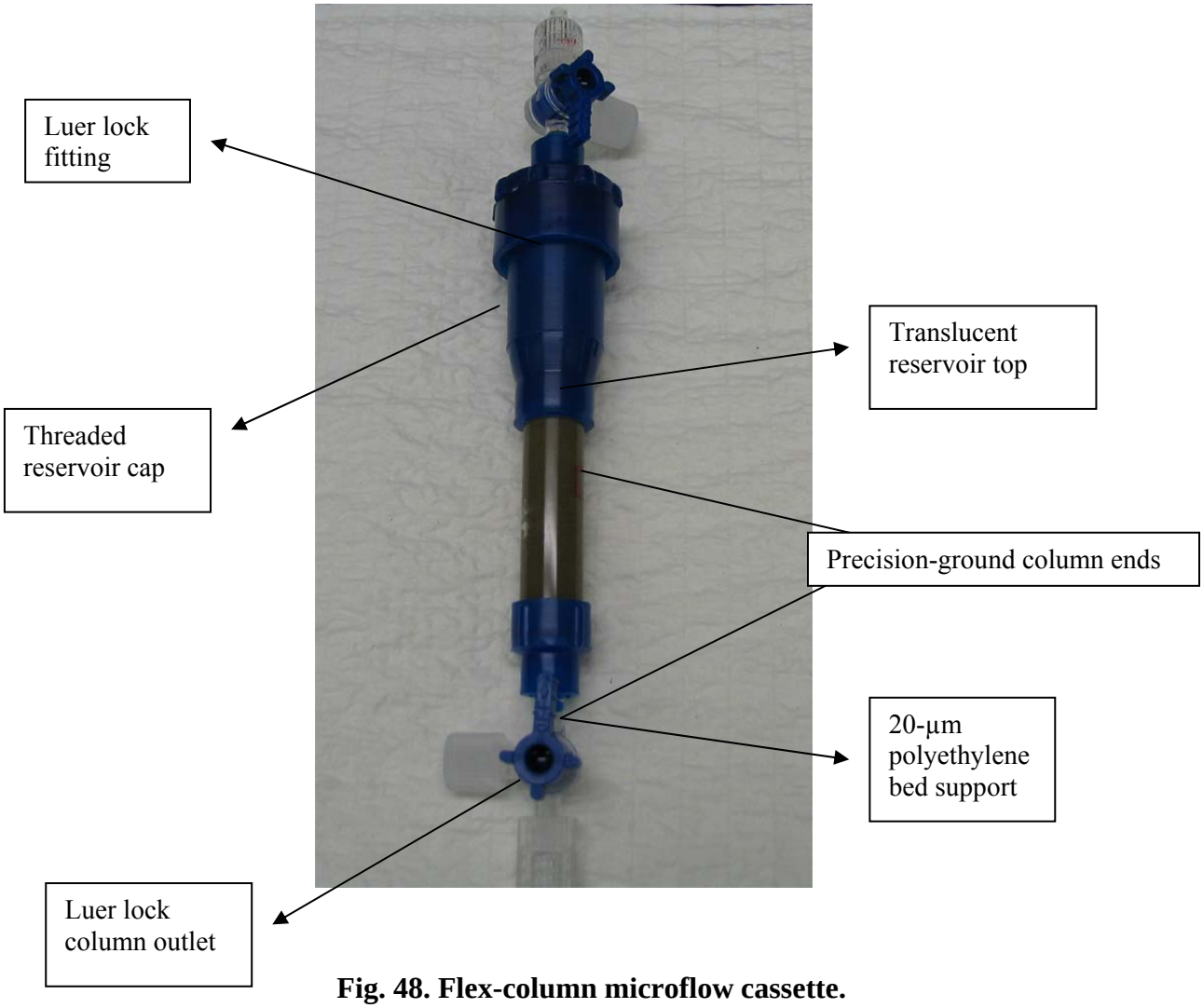

Fig. 48. Flex-column microflow cassette.

2. Column Saturation

   The packed column is placed in a beaker filled with water, followed by placement of the beaker in a vacuum chamber to draw out air bubbles and saturate the sample fully. Depending on the sample material, completing saturation of the column may take from a few hours to a few days. Figure 49 shows a photograph of the saturation system. After saturation, the column is removed from the vacuum chamber and connected to the constant-head supply reservoir. The outlet of the column is connected to the receiving bottle.

3. Saturated Hydraulic Conductivity Test

   The hydraulic head difference between the water surface in the supply reservoir and the outflow of the column is adjusted to obtain a measurable amount of water per hour. The hydraulic head difference is recorded for each test run. To keep the hydraulic head difference approximately constant, the volume of the supply reservoir should be large

enough so that the amount of run off does not decrease the supply water level appreciably. Water is added to the reservoir at the beginning of each test whenever the water level has decreased noticeably.

One deficiency noted in the microflow comparison is that the mass fraction present in the latent debris of fine material smaller than 75 μm may be underrepresented because particles of this size could not be separated from the filter cartridges and cloth wipe. Some attempt was made to renormalize the suggested surrogate mass distribution to account for small-particle retention; thus, the surrogate samples did contain the desired proportion of fine particulates. Thus, one might expect the conductivity of the surrogate to trend slightly lower than those of the debris samples.

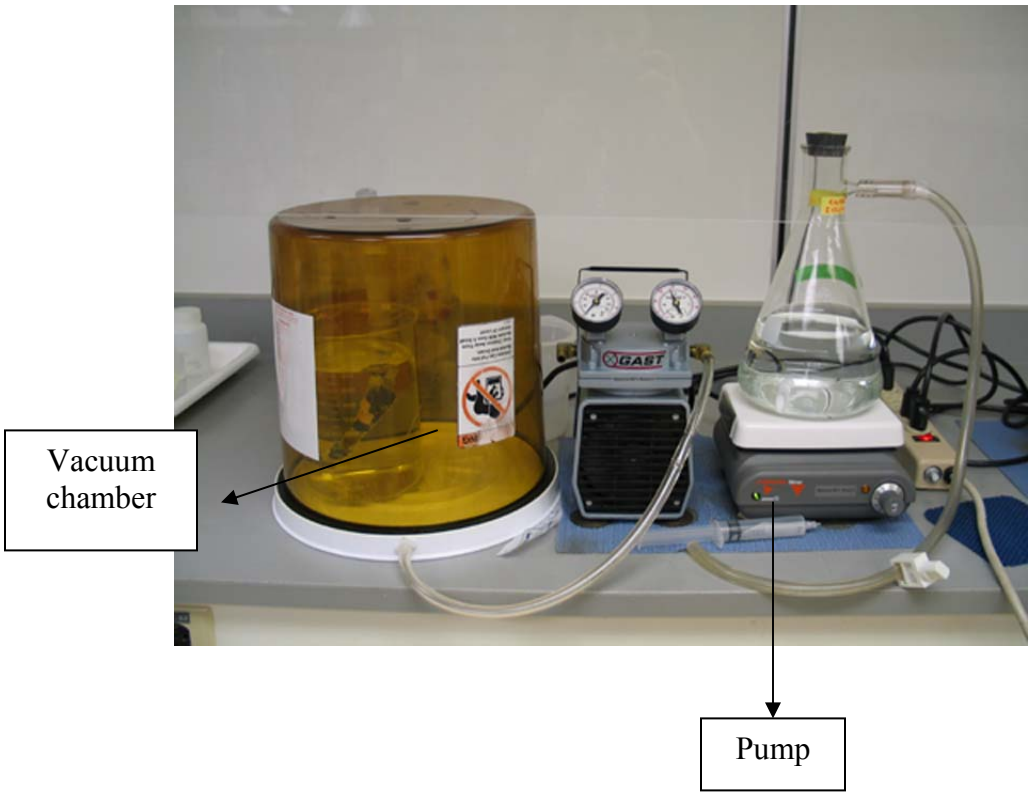

Fig. 49. Saturation vacuum system.

Figure 50 presents the results of microflow hydraulic conductivity measurements for selected latent debris and surrogate soil. As shown in Fig. 50, either four or five separate conductivity measurements were made to ensure that the column performance had stabilized. As indicated in Fig. 50, the hydraulic conductivities of surrogate soil and Plant D latent debris with particle sizes <75 μm are similar. As shown in Table 15, these two samples have similar saturated volumetric water content. However, the hydraulic conductivity of Plant B latent debris with particle sizes <75 μm is significantly larger than the former two samples. This difference most likely is due to the larger volumetric water contained in the Plant B sample. Figure 50 also shows that the

<75-µm particle size columns exhibit significant smaller hydraulic conductivity than the larger particle size columns.

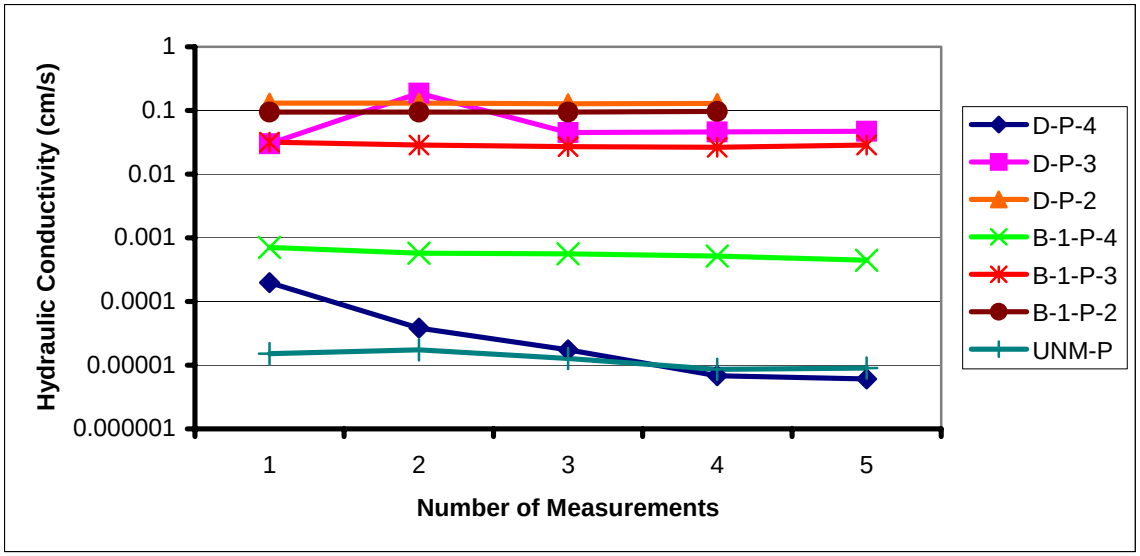

Fig. 50. Hydraulic conductivity of selected latent debris and surrogate soil.

Table 15. Characteristics of Columns for Microflow Comparison Experiments

Column ID	Sample ID	Particle Size (µm)	Column Diameter (cm)	Sample Length in Column (cm)	Saturated Volumetric Water Content (cm^3/cm^3)
1	D-P-4	<75	1.00	1.33	0.27
2	D-P-3	75–500	1.00	5.00	0.47
3	D-P-2	500–2000	1.00	5.00	0.67
4	B-1-P-4	<75	1.00	2.30	0.34
5	B-1-P-3	75–500	1.00	5.00	0.46
6	B-1-P-2	500–2000	1.00	5.00	0.64
8	UNM-P	Surrogate soil	1.00	2.00	0.23

4.3 Surrogate Debris Head-Loss Testing

4.3.1 Overview

The ultimate objective of latent-debris characterization is to make recommendations regarding the hydraulic behavior of this material in composite debris beds that may form on recirculation sump screens during postulated accident scenarios. Typical sump screen head-loss analyses apply the NUREG/CR-6224 [2] correlation for mixed debris beds to predict pressure drops for various accident scenarios. Proper application of this correlation depends on the availability of material-specific parameters that control the behavior of the equations. Important material properties include the SSA (related but not identical to the BET SSA reported in Section 3.1.6), the sludge porosity, and the material density.

In general, the hydraulic properties of the surrogate particulate can be inferred from properly controlled experimental measurements of pressure drop across debris beds of known composition over a range of flow velocities. The basic procedures and apparatus have recently been described in Ref. 8; thus, only the important differences needed to obtain consistent results with the soil surrogate will be described herein. The process of converging on an appropriate set of hydraulic properties involves iterative application of the head-loss correlation with varying values of the parameters until the predictions envelope a number of well-behaved tests that represent a range of possible fiber-to-particulate mass ratios. The fiber beds used in these tests were formed of shredded NUKON™ fiberglass insulation, which has relatively well-characterized properties that reduce the uncertainties in the estimates of appropriate soil properties. As explained in Section 4.1.1 above, latent fiber is assumed to have hydraulic properties similar to fiberglass insulation.

Head-loss tests were conducted at the UNM vertical-flow-loop assembly using mixtures of fiberglass and a soil-based surrogate for latent particulate prepared as described in Section 4.1.2. Each test consists of these generic steps: (1) known masses of fiber and particulate are prepared; (2) a uniform mixed bed is established on the test screen at low flow velocity; (3) velocity is increased in increments, and at each plateau, steady-state pressure drops are recorded; (4) after some practical peak pressure drop is reached, velocities are decreased in increments and steady-state pressure drops are recorded again at each plateau.

Tests conducted with fiberglass and soil-based particulates posed surprising experimental challenges. The principal difficulty lay in adequately filtering the finest suspended debris from the circulating water. Accurate comparisons of the head-loss correlation depend on knowing the mass of fiber and particulate present in the bed; therefore, large fractions of suspended particulate represent large uncertainties in the estimated properties. Two factors may have contributed to this difficulty. First, the soil grains appeared to disintegrate into very fine silt when soaked in water, and second, the fine particulate seemed to migrate through the fiber bed in an almost continuous fashion.

Attempts to calibrate the turbidity of the circulating water with a mass concentration of suspended particulate, which would allow correction of the debris-bed mass, were complicated by uncertainties in the size fraction of the suspended material; thus, three minor changes were made to the experimental protocol. First, the soil surrogate was presoaked in hot water, along with the fiber, to allow more complete decomposition before the test was initiated. Second, the fiber and the particulate were introduced into the test loop at the same time in an effort to pre-saturate the fiber mat with particulate. Third, the particulate-to-fiber mass ratio was increased and data collection was delayed to higher flow velocities to compress the fiber bed and improve filtration efficiencies. As discovered in earlier work, preblending the debris to separate fibers and to slow introduction of the debris in a water suspension greatly improves the uniformity of the debris bed that is formed for testing.

Head-loss tests that were designed to infer hydraulic properties can be very sensitive to the experimental procedures that are employed. It is essential that regular fiber mats be formed to assure uniform filtration of particulate and uniform water velocities. For this reason, the debris was preblended and introduced to the circulation loop very slowly. This procedure may be criticized as being atypical of debris beds formed during an accident sequence, but there is, in

fact, no intent in these tests to represent the morphology of an actual sump-screen debris bed. The focus of these tests is to isolate the hydraulic properties of the constituents so that more robust predictions can be made for a wider range of bed types. To meet this objective, the bed formation must be controlled carefully. A more direct answer to this criticism is to recall that very thin, very uniform fiber beds have been observed on vertical screens in the integrated tank tests conducted at UNM, [9] so the test conditions do, in fact, represent a physical possibility for in situ bed formation. Additionally, thin beds also have been responsible for operational events leading to excess head loss at nuclear plants (e.g., NRC Bulletins 93-02, 95-02, and 96-03).

During all tests, turbidity was measured after each velocity increment to qualitatively track the amount of suspended particulate. After the above improvements were implemented, turbidity was reduced to the range of a few nephelometric turbidity units (NTUs), consistent with levels achieved during the calcium silicate head-loss testing reported in Ref. 8. To the unaided eye, the circulating water was ostensibly clear near the end of the test and the composite debris bed was stable. These improvements permitted reproducible tests that support the following analyses of hydraulic properties for the soil surrogate.

Latent particulate debris transported to the sump screens would contribute to debris-bed head loss and must be included in head-loss calculations. Those calculations need the specification of certain parameters required as input to the head-loss correlation (e.g., the NUREG/CR-6224 [2] correlation). This report addresses the characteristics of containment latent debris as determined by samples collected at volunteer plants and analyzed at LANL in a laboratory equipped to handle the slightly radioactive materials. Surrogate debris was created for head-loss testing in the closed-loop head-loss simulation loop operated by the Civil Engineering Department at UNM. The head-loss testing then generated data to support the selection of head-loss parameters for applying the NUREG/CR-6224 correlation to containment latent particulate.

The head-loss test loop consisted of (1) a vertical test section constructed of nominal 12-in. transparent polyvinyl chloride (PVC) pipe, (2) a circulation pump, (3) a throttle valve, and (4) loop piping. A course supporting steel grating and then the actual 1/8-in. rectangular mesh screen similar to that used as PWR recirculation sump screens were placed on the support ring mounted approximately midheight in the transparent section of the test loop to support the debris being tested. Instrumentation included (1) a flow meter to determine flow velocity through the test screen, (2) a pressure transducer to determine the head loss across the screen, (3) a thermal couple to determine water temperature, and (4) a nephelometric turbidity meter to measure mass concentrations in water samples. The test apparatus and base test procedures are described in detail in the calcium silicate debris test report. [8]

The latent debris characteristics pertinent to the specification of a formula to create a suitable surrogate include the particulate density and the particulate-size distribution. Note that fibrous debris generated from the well-known NUKON™ fibrous insulation was used as the fiber component for these tests because the head-loss parameters for NUKON™ were already available.* Table 5 of this report provides a size distribution for the particulate debris characterized at LANL, and Table 12 provides the particulate density data. The particulate-size

* The head-loss parameters assumed for NUKON™ were (1) a specific surface area of 171,000/ft, (2) a fiberglass density of 175 lbm/ft^3, and an as-manufactured density of 2.4 lbm-ft^3.

distribution used to create the final surrogate formula is shown in Table 16. The latent debris characterized at LANL included particulate larger than 2 mm; however, this size of debris was not included in the surrogate formula on the basis that the larger debris was much less likely to transport to the sump screens. The distribution was normalized to the three size groups included in the formula. The density of the latent debris characterized at LANL varied but is well represented as a density of 2.7 g/cm^3. Note that the initial surrogate formula used in these tests did not match the final formula in Table 16 because the latent debris characterization was still in progress while these tests were undergoing preliminary testing.

Table 16. Surrogate Particulate Size Distribution

Size Range	Fraction
500 μm to 2 mm	0.277
75 μm to 500 μm	0.352
<75 μm	0.371

The surrogate debris tested at UNM was constructed from common sand and soil (referred to as dirt) already available in the laboratory. The common sand was used for the two larger size groups and the dirt for the <75-μm size group.* Both materials were found to have a density near 2.7 g/cm^3. The dirt had a clay component that tended to disintegrate, in part, in water, thereby adding substantial particulate <10 μm to accommodate the LANL finding that substantial very fine debris was collected in the filters.

A total of 20 head-loss tests was conducted during the course of the testing that included variations in the formula before finalization of the formula and the testing of individual formula components. Both thin and mixed debris beds were tested. The tests and the data are reported in Appendix A.

The introduction of debris into the test section focused on the formation of a uniform bed of debris. The NUKON™ debris was processed in the food processor to a fineness that allowed the fibrous debris to settle gently at an initial flow velocity of ~0.1 ft/s, thereby forming a very uniform debris bed. For thicker beds, the particulate was integrated with the fibrous debris before the introduction into the test section to homogenize the debris (i.e., avoid debris stratification). For thin beds, the fibrous debris was introduced initially without the particulate to maximize the uniformity of the fibrous debris bed; then the particulate was added slowly on top of the fibrous debris. The primary objective of the thin-bed tests was to create a granular layer of particulate and, in any case, the particulate tended somewhat to penetrate the thin layer of fibrous debris. Because the dirt component (<75 μm) appeared to consist at least partially of clay that decomposed into finer debris in water, the dirt was presoaked in water before being introduced into the test loop to accommodate the decomposition.

The decomposition of the clay in the dirt particulate resulted in substantial quantities of particles so fine that a significant portion of the dirt particulate did not filter from the flow. The particulate

* Sifting common sand did not result in enough particulate <75 μm to support the testing; therefore, an alternate source of particulate was used, i.e., the laboratory-available dirt.

that remained in solution kept the water from clearing; however, more importantly, this particulate did not contribute to the head loss, and its mass needed to be removed from the head-loss calculations. The nephelometric turbidity measurements were used to estimate the particulate remaining in solution. The filtration of the sand component of the formula was nearly complete.

Two forms of leakage were observed whereby a portion of the flow bypassed the debris bed. Leakage around the gap between the debris and the pipe wall was observed. The gap leakage varied with the thickness of the debris bed and with bed formation. Typically, a relatively tight gap seal was formed initially at low-flow velocity, but then a small breach would occur at higher head losses. The gap leakage, based on observed flow areas, is believed to be limited to a few percent of the total flow; perhaps on the order of ~2%. The gap leakage did not appear to invalidate the data and was considered in the data analysis. The second form of leakage occurred at high head losses, where the debris bed was disrupted in some manner such as the development of holes in the bed. When this leakage occurred, the data beyond the point of disruption was considered compromised and invalid.

4.3.2 Common Sand Tests

The surrogate formula contains two size groupings of common sand particulate: (1) 75 to 500 μm, and (2) 500 μm to 2 mm. The density of the sand is ~2.7 g/cm^3.

500 μm to 2 mm The specific surface area for this size group is small relative to the other particulate. Thus, the contribution of this particulate is expected to be a minor relative to the other particulate. When combined with the other particulate in the formula, this grouping brings down the overall specific surface area. The 500-μm minimum particle size indicates that the maximum specific surface area is ~3650/ft but that the likely area should be in the range of 1500 to 3000/ft. Because of the relatively low importance of this size group to the formula head-loss, tests were not conducted specifically to determine the specific surface area for this particulate. The dry bulk density of this sand was measured at ~104 lbm/ft^3.

75 to 500 μm Analytically, the expected specific surface area for this size grouping of sand (assuming a uniform distribution within the size group) is ~8200/ft and the maximum would be ~24,400/ft. Test 16 was conducted with 15 g of NUKON™ and 600 g of sand in this size range. The NUKON™ was introduced first to form a uniformly thin bed of fibrous debris to support the sand, which was slowly drizzled onto the bed. The resulting bed shown in Fig. 51 consisted primarily of a granular layer of packed sand. The fibrous portion of the bed was ~0.23 in., based on the as-manufactured density (the fiber of course compacted to a much thinner layer under flow pressure), and the packed sand was ~0.23 in. thick. The dry bulk density of this sand was measured at ~99-lbm/ft^3, which corresponds to a porosity of ~41%.

The results of Test 16 are shown in Fig. 52, where the head-loss data are plotted as a function of the approach velocity to the debris bed. The data points associated with increasing velocity are shown as solid circles and those associated with decreasing velocities as solid diamonds. The data are also compared to a prediction using the NUREG/CR-6224 [2] correlation using a specific surface area of 10,800/ft, a solid particle density of 166.6 lbm/ft^3, and a packing density of 99 lbm/ft^3. The test results are well within expected values.

Fig. 51. Test 16 debris bed of common sand.

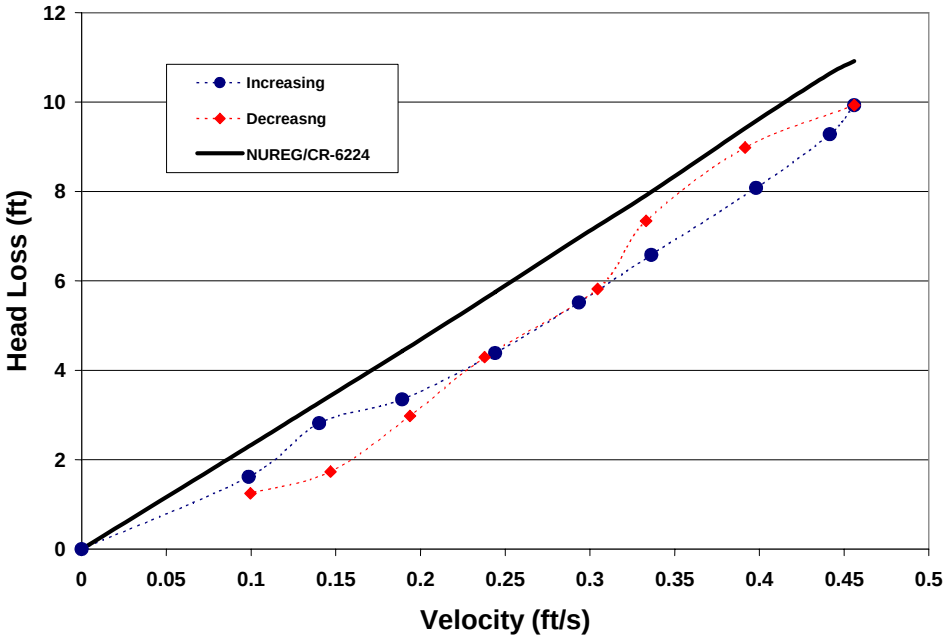

Fig. 52. Test results for Test 16.

Test 20 was another test conducted using only sand in the 75- to 500-µm-size range. This test used 150 g of NUKON™ and 450 g of sand, and the NUKON™ and sand were premixed before being introduced into the test assembly in order to form a relatively homogeneous bed. The resulting bed is shown in Fig. 53, and the analytical results are shown in Fig. 54. In this test, the bed was not pack limited; thus, the packing density did not apply to the application of the correlation to Test 20. Test 20 illustrates a behavior that was observed in many of these head-loss tests to some degree (i.e., a sort of reverse-hysteresis effect, for lack of a better term). The head losses were higher for the increasing velocities than for the decreasing velocities, which is the

opposite of the hysteresis behavior typically observed. A NUREG/CR-6224 [2] correlation prediction is shown that used a specific surface area of 26,000/ft, which is significantly higher than the value indicated by the Test 16 results.

Fig. 53. Test 20 debris bed of NUKON™ mixed with common sand.

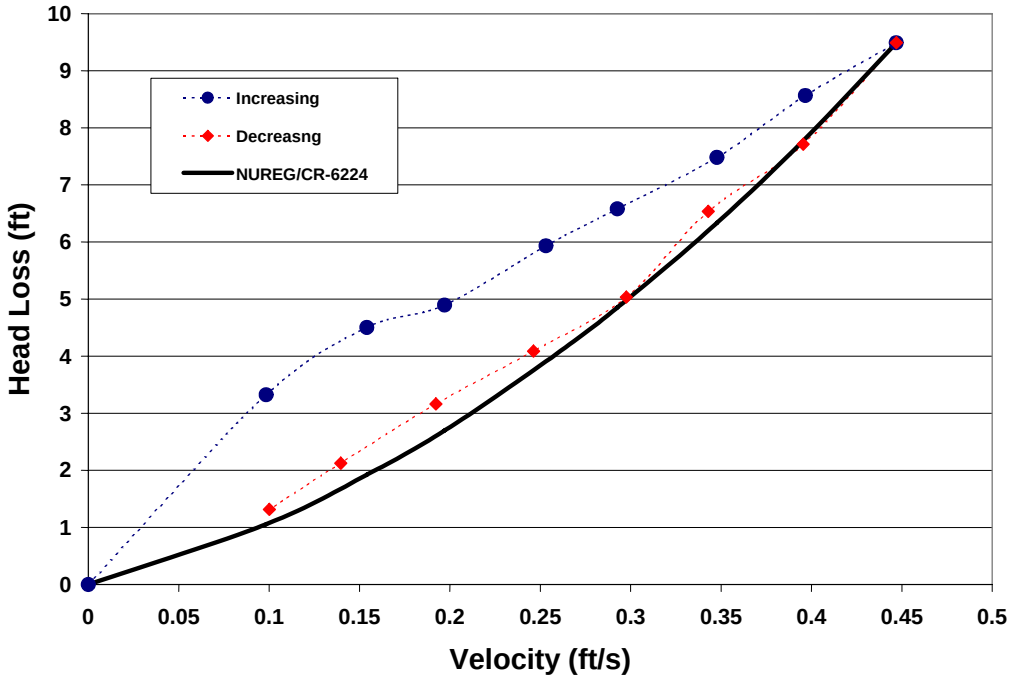

Fig. 54. Test results for Test 20.

Neither the higher indicated specific surface area nor the causes of the reverse hysteresis effect were determined.

4.3.3 Dirt Tests

The less than 75-µm component of the surrogate formula was supplied using dirt that was sifted through a 75 micron screen. This component, which was 37.1% of the total particulate by mass, was the primary contributor to the head loss. Because the particle sizes of the finer portions of this particulate were not known, it was not possible to predict the specific surface area analytically. The material density of this dirt was also near 2.7 g/cm^3, and its dry bulk density was measured at approximately 39 lbm/ft^3 (0.62 g/cm^3).

Test 15 was conducted with 60 g of NUKON™ and 90 g of dirt (<75 µm). The larger sand components were missing from the test so that the dirt by itself could be characterized. The results of Test 15 are shown in Fig. 55. As observed during testing, the loop water remained murky brown, which indicated incomplete filtration of the dirt from the flow; this observation was substantiated by the turbidity measurements that indicated that ~40% of the dirt did not filter from the flow. Significant uncertainty is associated with the turbidity measurements; that uncertainty could not be reasonably quantified. However, it was believed that the dirt remaining in solution was likely between 30% and 45% and that the specific surface area is in the range of 250,000 to 340,000/ft. The specific surface area used in the prediction shown in Fig. 55 was 285,000/ft, corresponding to 40% of the dirt remaining in solution. The reverse-hysteresis effect did not appear to be a factor in the dirt-only tests; thus, it appears to be an artifact of the coarse sand.

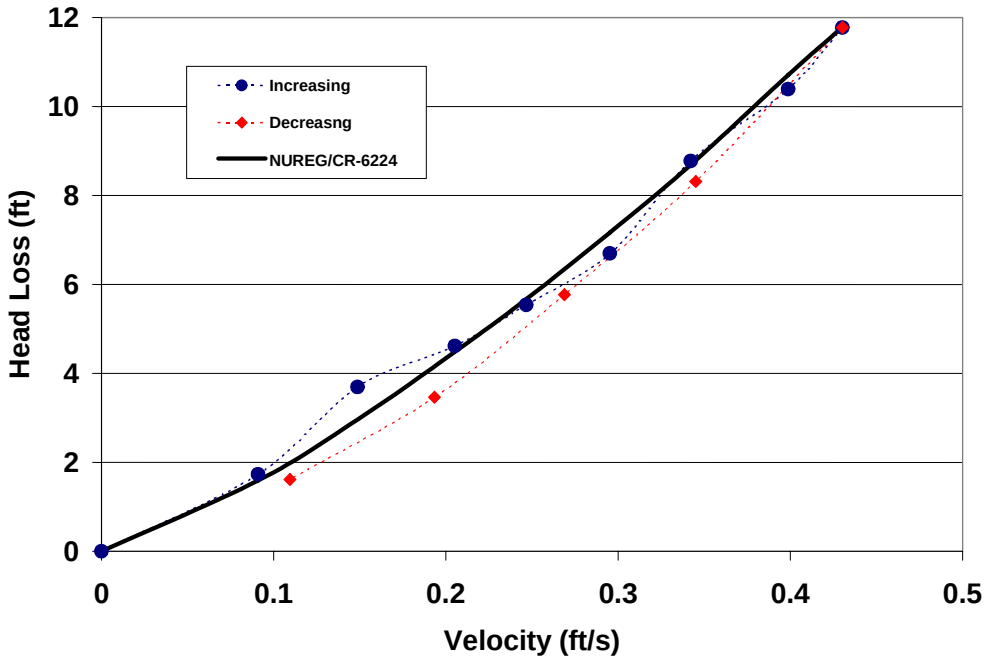

Fig. 55. Test results for Test 15.

A SEM photo from a pretest sample of the dirt after being sifted through the 75-μm screen is shown in Fig. 56. The scale is indicated in the upper left corner as 200 μm for the length of the white bar. The dirt particulate before being exposed to the water in the test loop contains particulate ranging from submicron sizes to particles barely able to pass through the 75-μm screen. SEM photos of higher resolution show that the larger particles appear to consist of conglomerations of fine particulate. When introduced into the test loop along with flow turbulence, this particulate tends to break up further into a finer particulate, some portion of which is apparently too fine to filter from the flow. Thus, turbidity measurements must be used to estimate that fraction that will not filter and subsequent predictions of specific surface areas will have substantial uncertainty associated with the estimates.

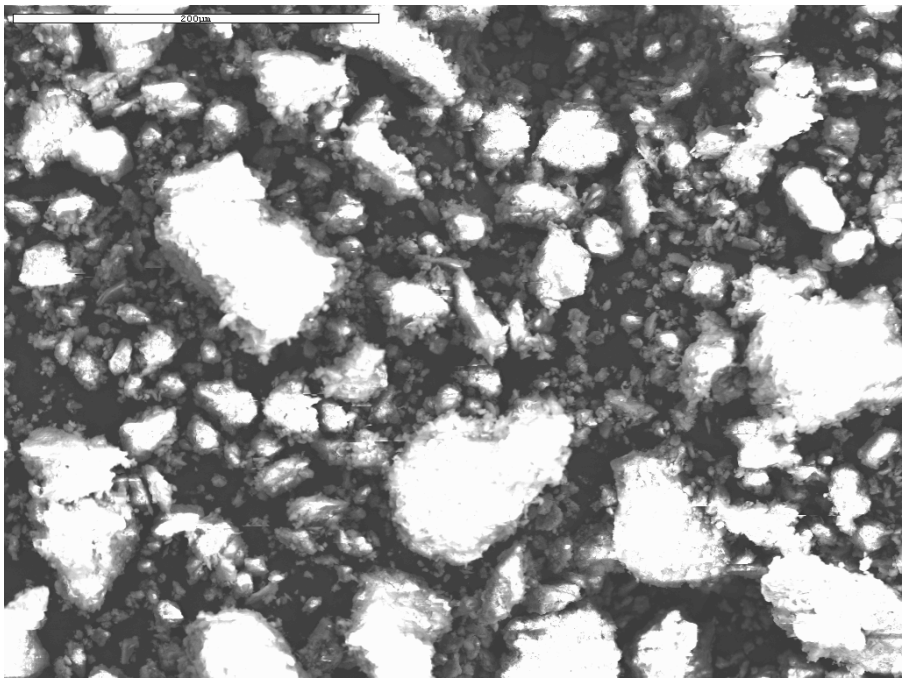

Fig. 56. SEM Photo of dirt sample.

Test 17 was conducted with 15 g of NUKON™ and 120 g of dirt (<75 μm), which formed a thin debris bed. Again, the sand components of the formula were missing from the test. The results of Test 17 are shown in Fig. 57.* Turbidity measurements indicated that ~52% of the dirt remained in solution. A comparison of the turbidity measurements with the thickness of the fibrous debris illustrated higher filtration efficiency for a thicker bed of fibers. The NUREG/CR-6224 [2] correlation calculation shown in Fig. 57 used a specific surface area of 277,000/ft and a dry bulk density of 39 lbm/ft^3 for the thin-bed packing limit. The test results for a thin bed with only dirt particulate agreed well with the results from a mixed bed.

* The debris bed in Test 17 lost integrity after a velocity of 0.25 ft/s was achieved; therefore, subsequent data were invalid.

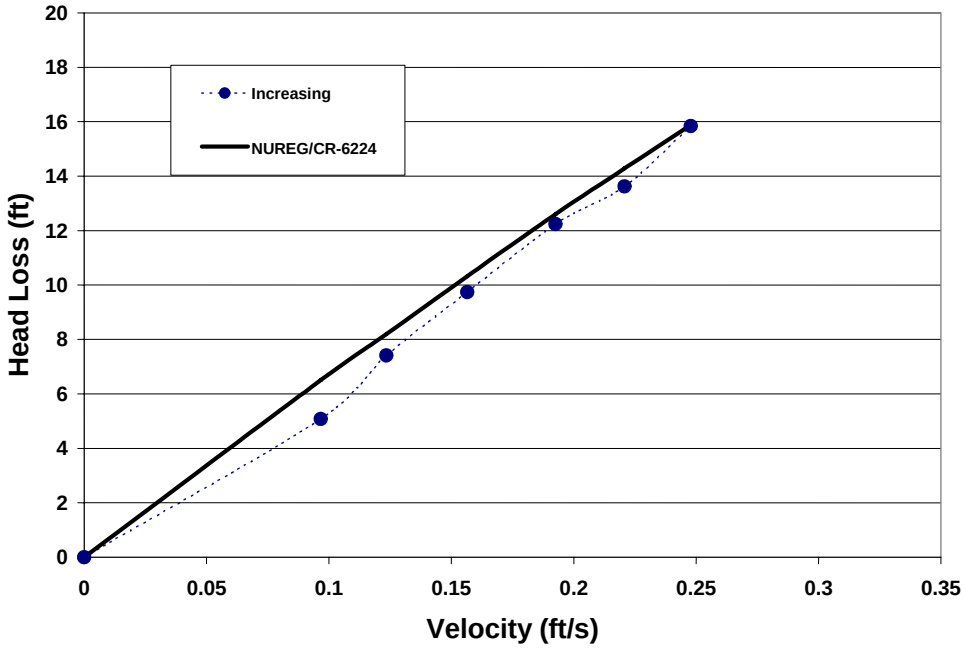

Fig. 57. Test results for Test 17.

4.3.4 Surrogate Formula Tests

Tests were conducted using the surrogate latent debris formula shown in Table 16.

Test 14 was conducted with 60 g of NUKON™ and 113.2 g* of particulate (31.4, 39.8, and 42.0 g of the three size groups of the formula shown in Table 16). The results of Test 14 are shown in Fig. 58. The turbidity measurement has indicated that ~40% of the 42 g of dirt <75 μm was still in solution rather than trapped in the debris bed. All of the coarse sand was assumed to be trapped in the bed. The NUREG/CR-6224 [2] correlation calculation shown in Fig. 58 used 104,000/ft for the specific surface area, and the calculation clearly indicated that the debris was not at the packed-bed limit. Therefore, the density-limiting compaction was not a factor in the calculation.

Test 19 was conducted with 15 g of NUKON™ and 90 g† of particulate (24.9, 31.7, and 33.4 g of the three size groups of the formula). The results of Test 19 are shown in Fig. 59.‡ The turbidity measurement indicated that ~52% of the 33.4 g of dirt <75 μm was still in solution rather than trapped in the debris bed. All of the coarse sand was assumed to be trapped in the bed. The NUREG/CR-6224 [2] correlation calculation shown in Fig. 59 used 106,000/ft for the specific surface area, and the calculation clearly indicated that the debris bed was packed limited. The density-limiting compaction in the calculation was 74.8 lbm/ft^3, which was calculated from the dry bulk densities of the three constituents, the formula, and the estimate of dirt remaining in solution.

---

* Particulate mass determined by the available dirt particulate at the time of the test.

† Test mass determined by the available dirt particulate at the time of the test.

‡ The debris bed in Test 19 lost integrity after a velocity of 0.2 ft/s was achieved; therefore, subsequent data were invalid.

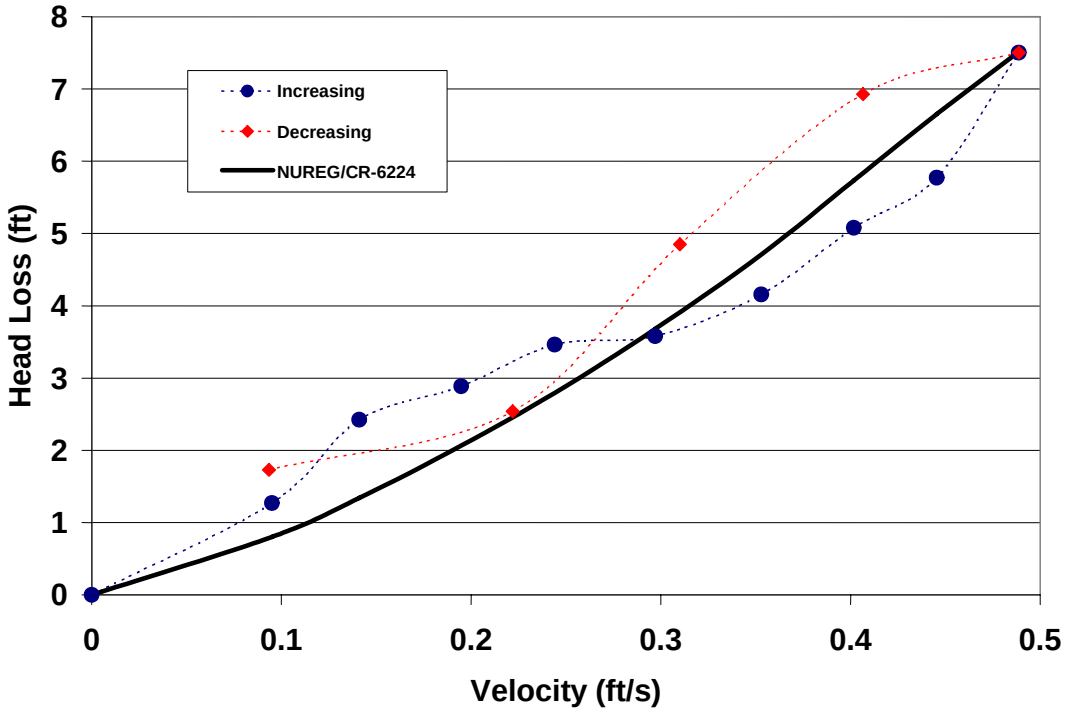

Fig. 58. Test results for Test 14.

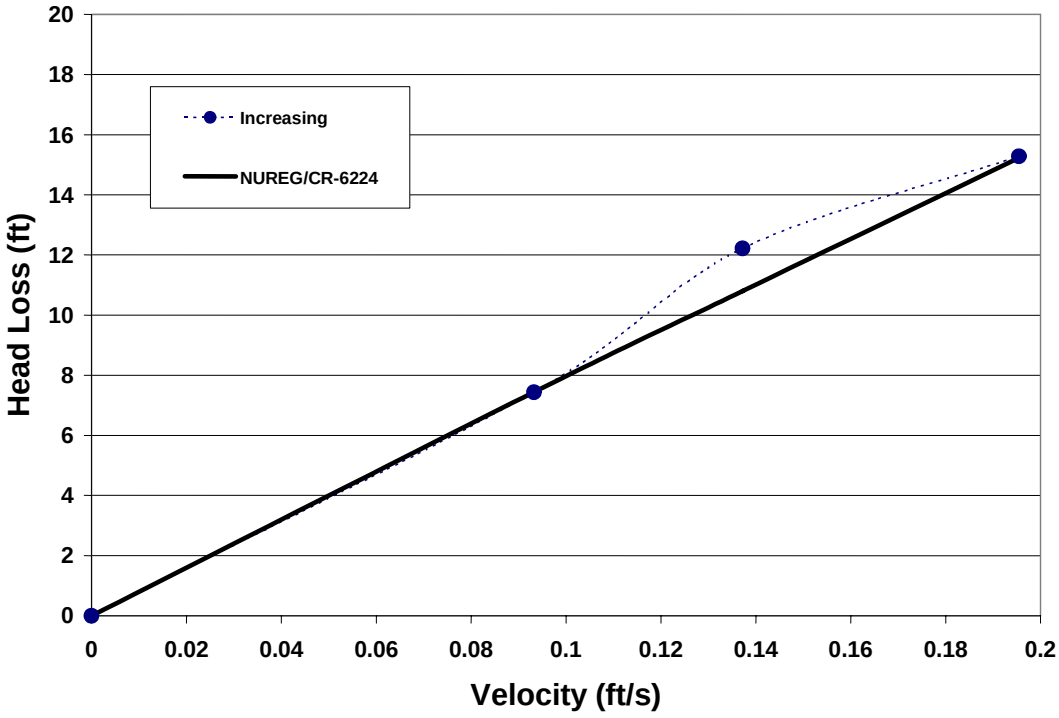

Fig. 59. Test results for Test 19.

4.3.5 Analytical Recombination of Components

Approximate values were determined from the head-loss test data for the specific surface areas for each formula component (except for the coarsest sand, which was estimated analytically) and for the surrogate latent debris formula. The dry bulk density tests, which merely measured the volume of a mass of particulate within a calibrated beaker, appeared to provide a reasonably rough estimate of the particulate packing limit density. It is interesting to note the low bulk density for the fine dirt relative to the sand because both materials had approximately the same density of 2.7 g/cm^3. The difference in the densities definitely is associated with the particle-size distribution, but the reason for this difference was not determined. These data are shown in Table 17.

Table 17. Summary of Test Results

Particulate	Bulk Density (lbm/ft^3)	Specific Surface Area (ft^{-1})
500 μm to 2 mm Sand	104	2000
75 to 500 μm Sand	99	10,800
<75 μm Dirt	39	285,000
Formula	63 to 75*	106,000

Substantial uncertainty is associated with knowing the specific surface areas, especially for the fine dirt. The primary difficulty with determining the specific surface area for the dirt from the head-loss tests was the relatively large fraction of the dirt that would not filter from the flow and the uncertainty associated with the turbidity measurements under these conditions. Further, the particle sizes filtered or not filtered could not be reasonably determined because the dirt particulate decomposed in the test loop apparently into very fine particulate, whereas the sand particles remained intact. Reasonable ranges of uncertainty around the specific surface areas shown in Table 16 are compared in Fig. 60. This comparison illustrates that the specific surface area for the surrogate latent particulate is dominated by the fine dirt in the formula.

The following equation is used to determine the specific surface area of a mixture where the areas are known for the components. If the densities of the components are the same, the equation can be simplified by canceling out the density and then converting the masses to mass fractions as

$$Sv_{Mixture} = \left[\frac{\sum_i \frac{m_i}{\rho_i} Sv_i^n}{\sum_i \frac{m_i}{\rho_i}} \right]^{\frac{1}{n}} ,$$

* The bulk density of the formula particulate depends on debris-bed's filtration efficiency.

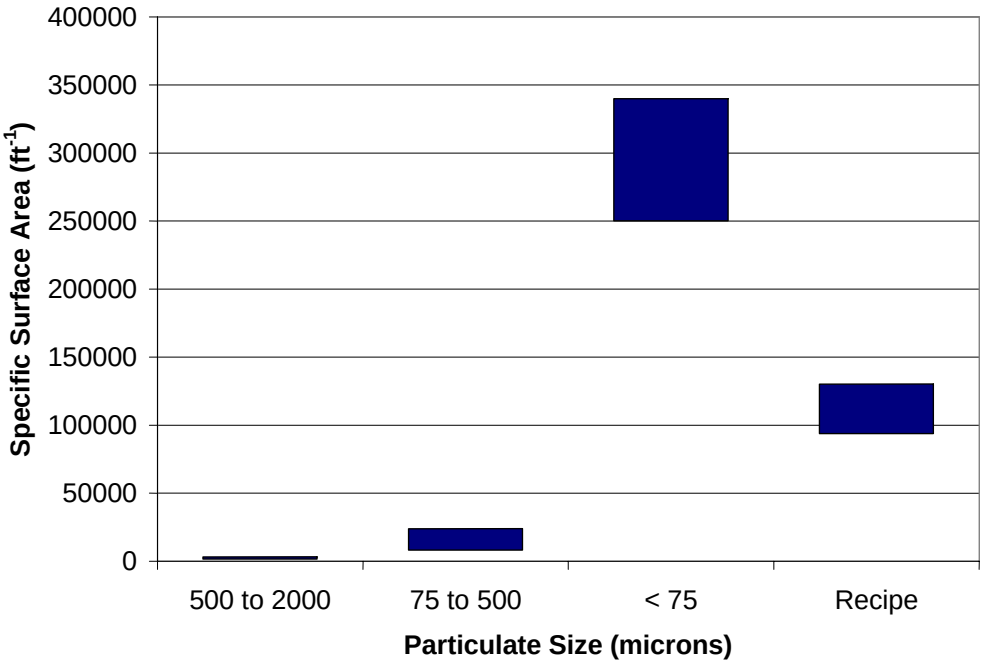

Fig. 60. Comparison of component- and formula-specific surface areas.

where

Sv = the specific surface area for component i or for the mixture,
m_i = the mass of component I,
ρ_i = the solid density of the particles in component I, and
n = the weighting exponent.

The weighting exponent normally would be a one, [10] but some researchers [11] have advocated using the square (i.e., n = 2). To get the test-specific surface area of 106,000/ft in Table 16 from the component areas in that table, the weighting component was adjusted to 4/3.

5 CONCLUSIONS AND RECOMMENDATIONS

This study is limited by the number of volunteer plants that provided the latent debris data and is also complicated by the fact that (1) the latent debris composition varies from plant to plant, (2) the latent debris transported to the sump screen is plant specific because of differences such as flow velocities, and (3) uncertainties are associated with whether the surrogate formula suitably represents actual containment latent debris. Nevertheless, valuable insights were gained from this study. The conclusions and recommendations presented below are intended to provide general guidance for plant-specific assessment of latent-debris contributions to sump-screen head loss. However, because of the reasons mentioned above, these recommendations may not be applicable to some of the operating PWR plants. In these cases, plant-specific debris characterization using methods described in this report may be preferable to the default properties recommended below.

The conclusions and recommendations are organized in the following categories.

Fiber-to-particulate mass ratio

Of the four plant contributions that were characterized fully, all contained measurable quantities of fiber. Approximate fiber-to-sample-mass ratios in the raw samples ranged from 0% to 29%, but on a plant-average basis, the fiber mass fraction ranged from 5% to 16%. For properly collected debris samples, a fiber-to-sample-mass ratio of 15% is recommended. This value is near the maximum of the plant averages for those volunteers that were studied but is only about one half of the maximum that was observed for individual (and perhaps anomalous) samples.

Particulate and fiber size distributions

- The characterization of the plant-collected latent debris has shown a significant fraction of the particulate to be <10 μm. This size of particulate readily would transport to the sump screen, where some portion would filter from the flow with a relatively high impact on the head loss as compared with the larger particulate. These tests clearly indicate that some of the very fine particulate does not seem to be filtered by the NUKON™ fibers; however, the actual size that would not filter could not be determined. If there is a minimum size for effective filtration, it is most certainly significantly <10 μm and likely less than a few microns.

- Latent debris collected from four PWR containment buildings has been characterized. Aggregated debris samples from the four plants show particulate distribution ranging from 84 to 95 wt % and fiber distribution from 5 to 16 wt %. The particle-size distribution appears to be highly dependent on the method used to collect debris samples within the plant; however, the results (excluding Plant C) show the following distribution: >2 mm, 8 to 40 wt %; 500 μm to 2 mm, 8 to 33 wt %; 75 to 500 μm, 12 to 37 wt %; and <75 μm, 20 to 46 wt %. Particle densities were observed to range from 1.5 to 4 g/cm^3, with a median density of ~2.7 g/cm^3. Collection procedures that are based on HEPA filtration or thorough manual wiping are encouraged to enable characterization of very small particulate. The BET SSA of the debris particles ranged from 0.01 to 2.0 m^2/g, with a mean of ~0.4 m^2/g. Smaller-diameter particles exhibited larger BET SSAs.

- Qualitative photomicrograph observations of fibers show fiber diameters ranging from 1 to 20 μm, with shapes including straight cylinders; single tortuous, flexible strands; and twisted, flat, ribbon-like strips. Some fibers appear to be interwoven, forming large clusters similar to the fibrous debris shape classification shown in NUREG/CR-6224. [2] Most of the fibers, regardless of the shape and size, appear to have debris particles attached to them. The attached particle diameters range from ~1 μm to >50 μm. Fiber diameters were measured, and the bulk of the fibers had a diameter between 12 and 14 μm. Material fiber-density estimates ranged from 1.3 to 1.9 g/cm^3, with a mean between 1.5 and 1.6 g/cm^3. An assumed dry latent-fiber bulk density of 0.0384 g/cm^3 (2.4 lbm/ft^3), similar to fiberglass, is appropriate for comparing plant-specific latent-debris inventories and sump-screen areas to the 1/8-in. thickness suggested for evaluation of thin-bed vulnerability.

Surrogate debris and hydraulic properties

- These tests provide useful data to support the determination of head-loss parameters for PWR containment latent debris, and the data clearly show the relative importance of the particulate components. Surrogate particulate debris was formulated from sand and soil constituents to match the average mass fractions observed in the smaller three size categories of the latent debris. After eliminating the mass observed for particles >2mm, the renormalized particulate mass distribution becomes 27.7% between 500 μm and 2 mm, 35.2% between 75 μm and 500 μm, and 37.1% <75 μm in diameter. Because the hydraulic properties of the latent fiber are not thought to dominate head loss for important evaluation scenarios, it is suggested that the properties of fiberglass insulation be applied as an acceptable approximation.

- Head-loss testing of the surrogate particulate supports the following recommendations for hydraulic properties suitable for use in the NUREG/CR-6224 [2] head-loss correlation. A hydraulic SSA, Sv, of 106,000 ft^2/ft^3, adequately predicts pressure drops measured across fibrous debris beds over a velocity range of 0.1 to 0.5 ft/s and particulate-to-fiber mass ratios of 1 to 3.

- Microflow conductivity measurements confirmed that the UNM sand/soil mixture provided a reasonable surrogate for latent-debris particulates. The surrogate contained dry-sieved mass fractions of 28% common sand (density = 2.6 g/cm^3) between 500 μm and 2 mm in diameter, 35% common sand between 75 μm and 500 μm in diameter, and 37% soil <75 μm.

- Estimation of hydraulic parameters for the surrogate particulate was complicated by extremely fine, clay-based silt that was present in the soil constituent; it was difficult to filter this material completely from the circulation loop and to obtain accurate measurements of particulate mass in the bed. NUKON™ fiberglass was used as a fiber substrate for all tests. Over a set of well-conditioned tests where most particulate sizes were captured, the SSA of the surrogate was estimated to be 106,000ft^2/ft^3.

- The hydraulic parameters of latent fiber are assumed to be in the same as those previously reported for NUKON™ fiberglass insulation. Fiber surrogates were not investigated in detail because the head-loss contribution of latent fiber either will be dominated by particulates in a thin-bed configuration or will represent a small increase to a fiberglass-dominated debris composition. Although the average diameter of latent fibers was observed to be slightly larger than for typical fiberglass, which would lead to a slightly lower specific surface area, the wet-bed packing behaviors were not compared rigorously. Thus, the small conservatism of applying fiberglass hydraulic properties as a substitute for latent fibers is reasonable.

- Latent fibers are assumed to be relatively independent when compared with fibrous insulation flocks and therefore are assumed to be completely transportable to the sump screen. A dry-bed bulk fiber density of 2.4 lbm/ft^3 (38.4 kg/m^3), the same as NUKON™ fiberglass, is recommended for the evaluation of potential thin-bed formation from latent fiber. Although higher dry densities were observed for matted fibrous debris, there is no equivalent definition of as-fabricated density for latent fibers to guide handling and preparation methods for the samples. The assumption of equivalent dry density introduces reasonable conservatism and simplifies the treatment of latent fiber.

- To assist with development of a surrogate debris formula for head-loss testing, the "other" debris category was deemed not applicable. The "other" debris consists of larger material, such as bolts, nuts, cable ties, and rags, that is not expected to transport to the cooling system screen under recirculation flow velocities or to contribute to the formation of a uniform debris bed on the screen. Because of the lack of transport expected based on previous testing, this "other" material should not be considered in the surrogate debris preparation. However, the full range of sizes of latent debris, including foreign (or "other" debris category) material should be considered if it is subject to high-velocity water transport toward the ECCS screen. If significant quantities of this material were present, such as large amounts of degraded containment coatings, and the sump-screen geometry were unfavorable, such as a horizontal screen at floor level with no curbing, material in this category may pose a potential to block significant portions of the screen area.

- Latent debris was observed over the full range of sizes, from centimeter-sized paint chips and miscellaneous objects to micron-sized particulates. The full range of sizes should be considered for debris that may be subjected to high-velocity water transport toward the ECCS screen, such as the latent-debris inventory at the sump-pool level. The latent-debris fraction with a nominal dimension >2 mm is not likely to transport at pool velocities <0.5 ft/s that may exist near the screen under recirculation conditions. This size fraction represents ~22% of the particulate mass on average that can be discounted from the inventory available for transport under long-term recirculation.

- With an uncompressed bed thickness of up to 1 in., although the fiber bed remains uncompressed (flow velocities <0.2 ft/s), a significant fraction of the fine material penetrates the bed and continues to circulate. If low flow velocity can be substantiated adequately throughout the duration of the recirculation phase and potential particulate-to-

fiber ratios cannot exceed 3, the estimated particulate loading on a postulated bed can be reduced by 7.5% (one-quarter of the <75-μm mass fraction) to accommodate realistic debris-bed penetration of latent fine particulate. This recommendation does not imply any adjustment to the particulate SSA reported above. Also, it should be recognized that debris penetration of the sump screen may pose concerns for adverse downstream effects.

- If the entire mass of the latent debris is assumed to be deposited onto the sump screen, then a lower specific surface area, such as the formula in these tests, can be applied. However, if transport analyses are used to limit the transport of latent particulate to only the fine particulate, then the appropriate specific surface area would be more like that of the fine dirt in these tests. The same consideration also applies to the limiting packing density.

Plant-specific debris collection and tests

- Manual wiping with lint-free cloth and high-efficiency particulate air (HEPA) vacuuming of surfaces provide the most complete description of particulate-size distribution. Careful filtration of water effluent from washing methods also may be effective but was not represented in the volunteer-plant collection methods. Sweeping with bristled brushes or brooms does not capture accurately the full range of fine particulates.

- It is recommended that plant latent debris estimates be decomposed into as many particle-size groupings as is reasonably possible and that subsequent transport analysis be applied to each group to determine the particulate makeup on the sump screen unless total transport is assumed. Specific surface areas should be determined for each size group based on test data where possible. When the areas must be estimated from the particle diameters, the appropriate diameter is clearly *not* the mean or average diameter of the size group but rather a diameter closer to the minimum diameter of the group. The minimum diameter normally should result in a conservative specific surface area.

Latent-debris inventory

- One key aspect of any plant vulnerability assessment will be an estimate of total latent-debris inventory. Although this report does not provide any direct guidance regarding the amount of debris, practical recommendations can be made regarding the various proportions of debris that may be used for evaluation purposes. As is always the case with generic guidelines, plant-specific information should be used to support appropriate refinements. First, estimates of the bulk mass in containment should include material of all sizes. Generally, it is not convenient or radiologically prudent to sieve debris, but if this sieving is possible, debris >0.132-in. nominal size other than fiber may be removed from the bulk-mass estimate. A fiber-mass proportion of 15% should be applied to the total inventory estimate in the absence of site-specific supporting evidence.

APPENDIX A
SURROGATE LATENT-PARTICULATE HEAD-LOSS TESTS

A.1 INTRODUCTION

This appendix documents the head-loss test data for the surrogate latent particulate debris, which was discussed in Section 4.4. Surrogate debris was created for head-loss testing in the closed-loop head-loss simulation loop operated by the Civil Engineering Department at UNM. The head-loss test loop consisted of (1) a vertical test section constructed of nominal 12-in.-diam transparent PVC pipe, (2) a circulation pump, (3) a throttle valve, and (4) loop piping. A coarse supporting steel grating and then the actual 1/8-in. rectangular mesh screen similar to those used as PWR recirculation sump screens were placed on the support ring mounted approximately midheight in the transparent section of the test loop to support the debris being tested. Instrumentation included (1) a flow meter to determine flow velocity through the test screen, (2) a pressure transducer to determine the head loss across the screen, (3) a thermal couple to determine water temperature, and (4) a nephelometric turbidity meter to measure mass concentrations in water samples. The test apparatus and base-test procedures are described in detail in the calcium silicate debris head-loss test report. [8] This data report builds onto the information in the calcium silicate report as needed to explain these tests, such as deviations from those test procedures.

Data for the surrogate latent debris head-loss tests were collected in log books and in a data acquisition system. The data acquisition system, as configured for these tests, recorded time-dependent differential pressures across the debris bed and the loop flow rate (presented in figures). The other data, which included the water temperature and turbidity measurements, were recorded in a logbook (presented in tables), along with the pressure differential and flow rate when a test data point was declared. Certain deviations were made from previous head-loss testing to accommodate test behavior observed in these tests. Because the LANL latent debris characterization was ongoing during the preliminary head-loss testing, the particulate formula testing was altered somewhat during the course of the tests.

A.2 SURROGATE PARTICULATE

A formulation, or "recipe," for surrogate debris was developed based on the analysis of latent debris at LANL, and surrogate debris sources were identified and characterized. Analysis of latent debris at LANL determined that it consisted of fibrous debris and particulate debris. The particulate debris was characterized principally by the density and particle-size distribution. Suitable surrogate debris was selected by finding a source of material with the correct density and sieving it to the correct particle-size distribution.

The density of the latent debris was determined to range from 2550 to 2750 kg/m^3 (159 to 171 lb/ft^3), with an average of ~2700 kg/m^3 (168 lb/ft^3). This density was noted to be similar to the density of common silica-based or aluminosilicate-based material such as sand or clay. The sources of material for the surrogate were common sand and a soil (referred to as dirt) that were readily available in the UNM geotechnical laboratory. The density of both the common sand and the dirt was measured to be ~2700 kg/m^3 (168 lb/ft^3), and both subsequently were sieved to size

fractions identified by LANL and then mixed in proportions to match the latent debris formula. Because of the limitations of available equipment, the sieve size of one fraction varied from the specified size fraction determined by LANL. A sieve size of 0.590 mm was used instead of the specified 0.500 mm.

Dry bulk densities of the different size distributions were measured using the dry settling method. Twenty g of each distribution was placed into a 50-ml graduated cylinder. The dirt was allowed to settle and noticeable void spaces removed. These data are shown in Tables A-1 and A-2.

Table A-1. Bulk Size Distribution

Bulk Size Distribution and Theoretical Densities	
Size Distribution	**Density (g/L)**
>2 mm	-
2 mm–0.59 mm	1670
0.59 mm–0.075 mm	1600
<0.075 mm	1250

Table A-2. Surrogate Debris Size Distribution

Surrogate Debris Size Distributions				
Size Fraction	**Draft 1 Size Distribution (Percentage)**	**Draft 2 Size Distribution (Percentage)**	**Draft 3 Size Distribution (Percentage)**	**Final Size Distribution (Percentage)**
>2 mm	30	14	0	0
2 mm–0.59 mm	44	30	34	27.8
0.59 mm–0.075 mm	18	25	30	35.2
<0.075 mm	8	31	36	37

An overall representation of the formulas used is represented in Table A-3.

A.3 EXPERIMENTAL PROCEDURE

The test procedures were similar to those developed for the calcium silicate head-loss tests. After the particulate samples were weighted according to size grouping, the dirt particulate debris was presoaked to facilitate dirt (clay) particle decomposition before testing. Because the sand particles would not decompose, the sand did not require presoaking. The NUKON™ was pretreated in the same manner that it was in the calcium silicate tests. For mixed-bed tests, the particulate and NUKON™ were mixed together before introduction into the test chamber to facilitate the creation of a uniform and homogenized bed of debris. For thin-bed tests, where the objective was to create a granular bed of particulate debris, the NUKON™ was introduced first without particulate to enhance the uniformity of the thin fiber bed. Then the particulate was introduced slowly and allowed to settle on top of the fiber. During the course of testing, particulate penetrated into the thin fiber bed. The debris was introduced into the test chamber at the relatively low flow of 0.1 ft/s, which accommodated uniform bed formation. Once the bed was formed, the flow was increased incrementally and then decreased in the same manner described for the calcium silicate tests.

Table A-3. Experimental Matrix for Surrogate Latent Particulate Head-Loss Tests

Experimental Matrix for Surrogate Particulate Tests								
Test	Sand	Clay	NUKON™	Dirt	mm			
					>2	2–0.59	0.59–0.075	<0.075
			g		g			
1		x	100	101	30	44	19	8
2		x	100	101	30	44	19	8
3	x	x	100	101	30	44	19	8
4	x	x	100	100	14	30	25	31
5	x	x	15	10	1.4	3.0	2.5	3.1
6	x	x	25	25	3.50	7.5	6.3	7.8
7	x	x	100	100	-	34	30	36
8	x	x	100	100	-	34	30	36
9	x	x	60	120	-	33.3	42.2	44.5
10	x	x	60	240	-	66.6	84.4	89
11	x	x	60	240	-	66.6	84.4	89
12	x	x	15	90	-	25.0	31.7	33.3
13	x	x	80	240	-	84.5	66.7	88.8
14		x	60	113.2	-	31.4	39.8	42.0
15		x	60	90	-	-	-	90
16	x		15	600	-	-	600	-
17		x	15	120	-	-	-	120
18	x		150	450	-	-	450	-
19	x	x	15	90	-	24.9	31.7	33.4
20	x		150	450	-	-	450	-

A.4 EXPERIMENTAL RESULTS

A.4.1 Test 1: 100 g NUKON™: 101 g Dirt

The data from this test are not useful. This test was used to verify electronics and test debris and preparation.

A.4.2 Test 2: 100 g NUKON™: 101 g Dirt

Very high head losses were obtained during testing. The use of the clay as surrogate debris came into question. Because of the cloudiness of the water, debris tested will be changed to quartz sand for the larger particulate-size groupings.

Table A-4. Log Book Record Test Data, Test 2

Test 2 Log Book Information				
Data Point	**Temperature (°F)**	**Turbidity (NTU)**	**Head Loss (ft-water)**	**Flow (gal./min)**
1	84.6	51.0	11.8	31.1
2	86.6	51.0	14.5	38.4
3	87.7	46.0	17.9	45.8
4	88.6	47.0	20.6	54.2
5	90.0	47.0	23.0	62.1
6	90.9	46.0	19.6	54.9
7	91.2	46.0	16.3	46.1
8	92.6	45.0	14.2	38.2
9	94.2	45.0	11.2	30.8

Fig. A-1. Time-dependent head-loss measurements.

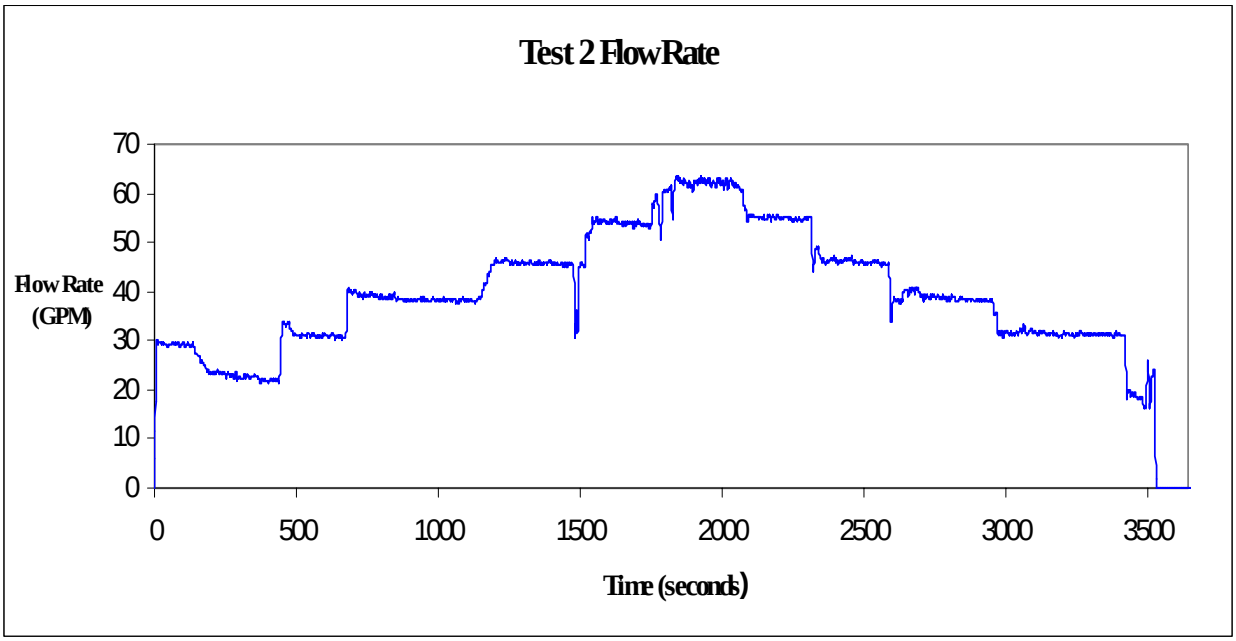

Fig. A-2. Time-dependent flow-rate measurements.

A.4.3 Test 3: 100 g NUKON™: 101 g Dirt

Sand was used in all size distribution, with the exception of the <75-µm particles. The clay dirt was used to represent the smallest particle size because of a lack of availability of sand in this size category. Clay will be used only in the smallest size category for future testing. This test was not completed because of high head loss and changing from the 2-in.-diameter flow meter to the 6-in.-diameter flow meter. When the change occurred, holes were blown into the bed. The flow rate increased only 15 gal./min with the valve fully opened using the 6-in. line. It was decided that no further changeovers from the 2-in.-diameter flow meter to the 6-in.-diameter flow meter would be done. Too much damage has been done to the bed for an insignificant gain of flow to have occurred.

A.4.4 Test 4: 100 g NUKON™: 100 g Dirt

The formula for the dirt was changed to the formula that LANL determined. The water was much clearer than in the previous test. Head losses were similar to those in Test 3.

A.4.5 Test 5: 15 g NUKON™: 10 g Dirt

This was the first attempt at a thin bed for the dirt test. The formation of the fiber bed took longer than expected. Gaps on the screen were seen, so the fiber/dirt mix did not cover the entire screen which leads to lower pressures during the experiment.

Table A-5. Log Book Record Test Data, Test 3

Test 3 Log Book Information				
Data Point	**Temperature (°F)**	**Turbidity (NTU)**	**Head Loss (ft-water)**	**Flow (gal./min)**
1	74.0	13.0	4.5	30.1
2	76.0	12.3	5.8	39.8
3	78.0	9.0	6.8	47.8
4	79.4	10.0	8.2	62.2
5	80.9	8.9	11.0	79.7
6	82.2	8.5	11.4	93.8
7	83.4	8.6	15.0	121.1
8	85.2	11.0	23.1	141

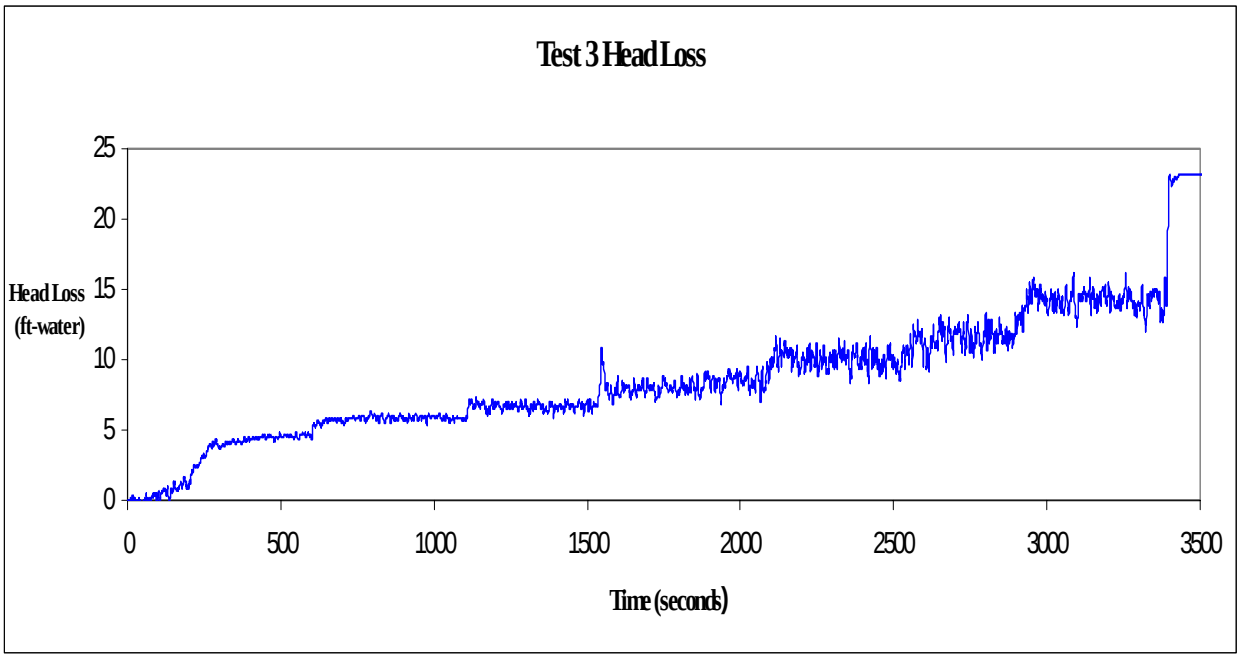

Fig. A-3. Time-dependent head-loss measurements.

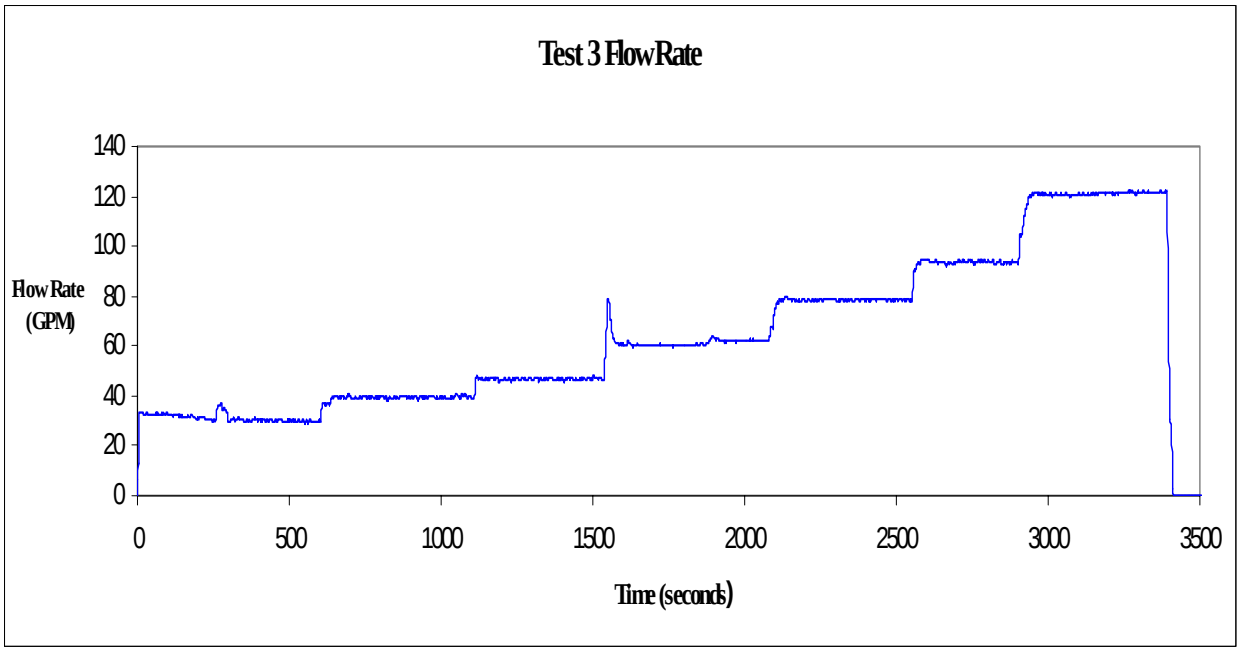

Fig. A-4. Time-dependent flow-rate measurements.

Table A-6. Log Book Record Test Data, Test 4

Test 4 Log Book Information				
Data Point	**Temperature (°F)**	**Turbidity (NTU)**	**Head Loss (ft-water)**	**Flow (gal./min)**
1	79.6	10.2	4.5	31.3
2	80.9	18.4	6.4	47.2
3	82.1	18.1	8.0	62.6
4	83.3	6.9	10.4	78.1
5	84.9	5.7	12.3	97.6
6	86.5	4.4	15.5	116.5
7	87.9	3.0	11.2	93.2
8	89.2	4.4	8.8	78.2
9	90.1	4.1	6.4	60.4
10	91.5	4.3	4.4	45.7
11	92.3	3.7	3.2	31.1

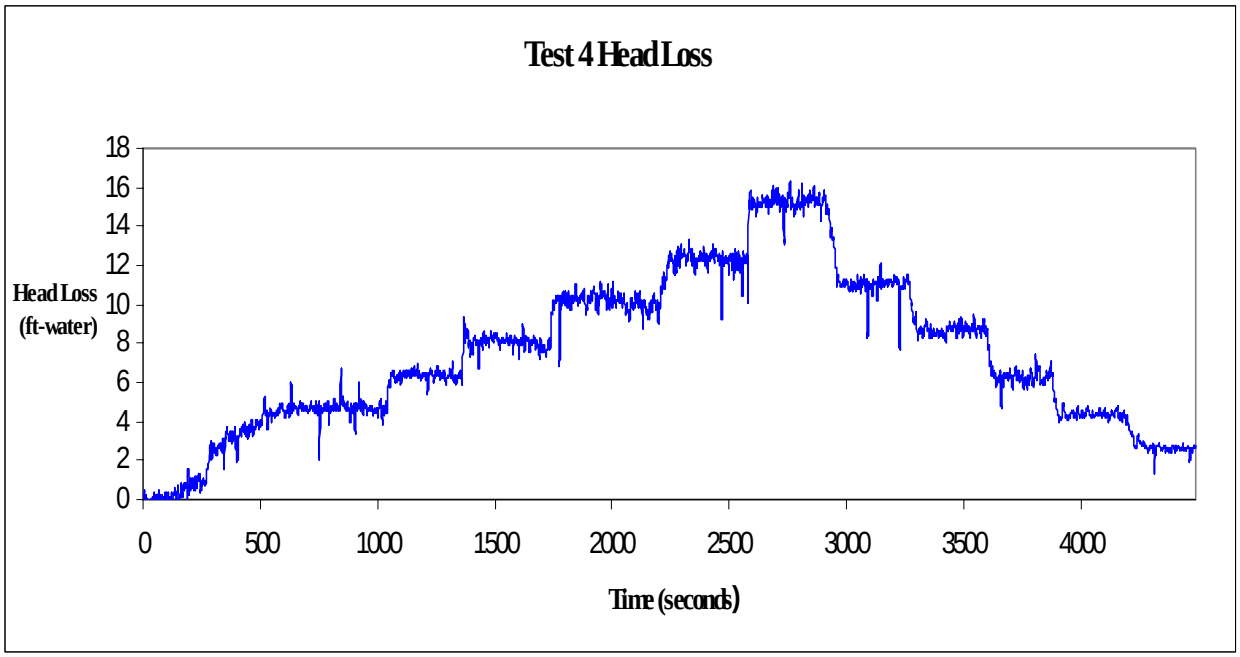

Fig. A-5. Time-dependent head-loss measurements.

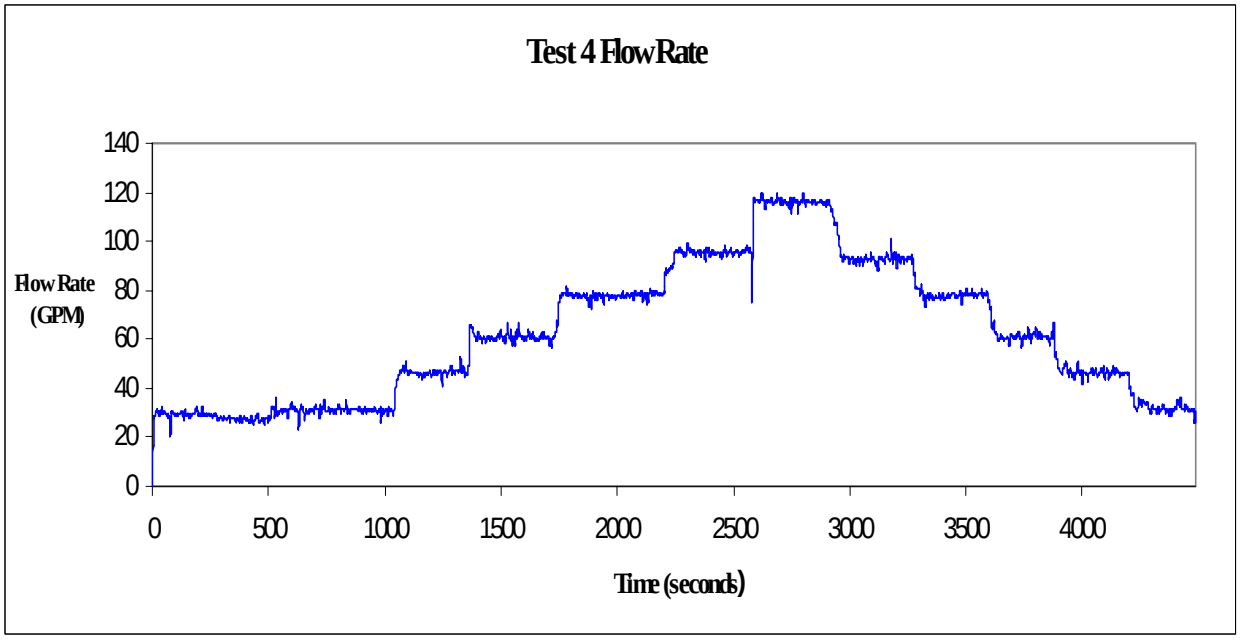

Fig. A-6. Time-dependent flow-rate measurements.

Table A-7. Log Book Record Test Data, Test 5

Test 5 Log Book Information				
Data Point	**Temperature (°F)**	**Turbidity (NTU)**	**Head Loss (ft-water)**	**Flow (gal./min)**
1	77.0	5.2	0.5	31.3
2	77.7	5.0	0.5	45.6
3	79.0	6.0	0.7	78.3
4	79.1	6.0	0.9	110.3
5	79.6	5.9	1.2	141.2
6	80.5	5.9	1.6	174.4
7	81.6	5.7	1.3	140.1
8	82.2	5.6	1.1	109.8
9	83.5	5.0	0.9	74.9
10	84.0	5.0	0.5	47.4

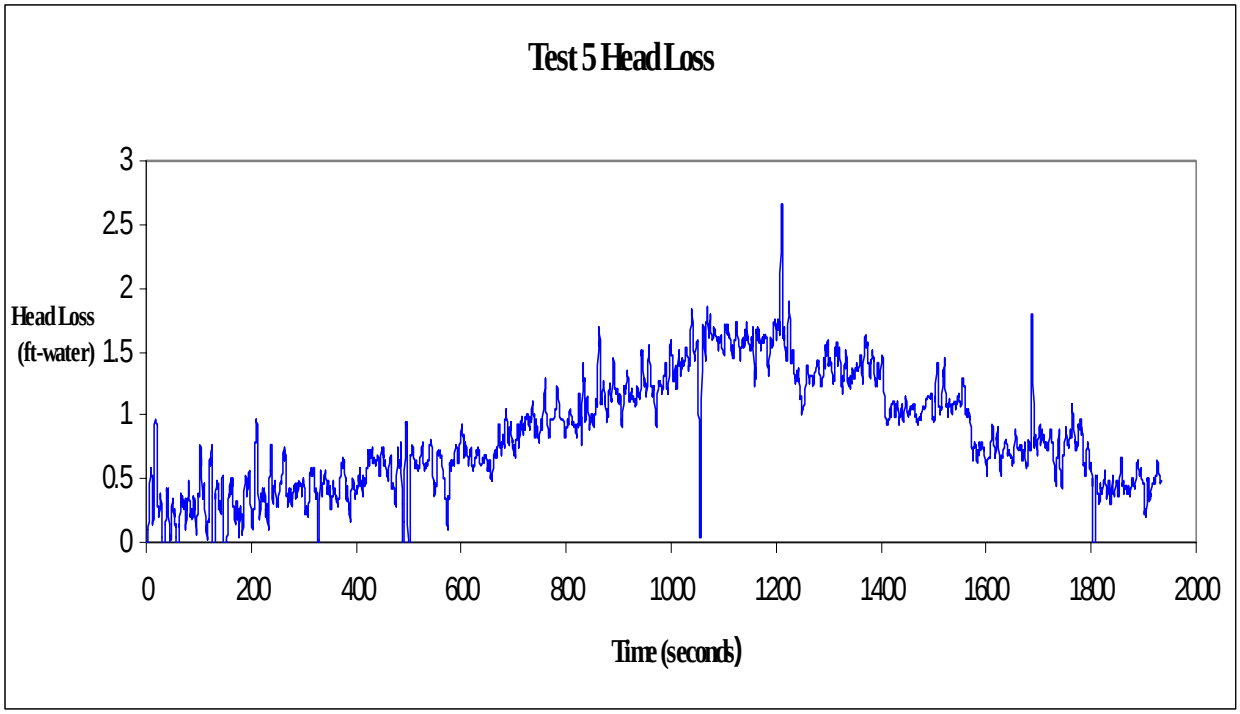

Fig. A-7. Time-dependent head-loss measurements.

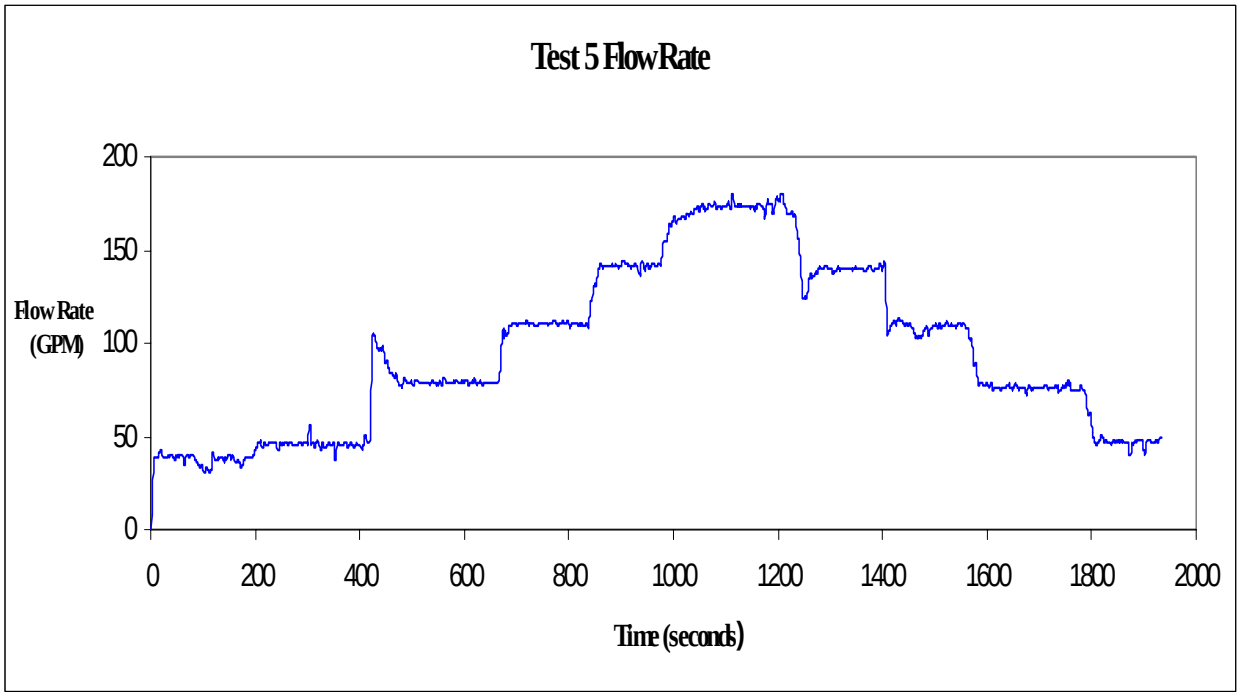

Fig. A-8. Time-dependent flow-rate measurements.

A.4.6 Test 6:25 g NUKON™: 25 g Dirt

Table A-8. Log Book Record Test Data, Test 6

Test 6 Log Book Information				
Data Point	**Temperature (°F)**	**Turbidity (NTU)**	**Head Loss (ft-water)**	**Flow (gal./min)**
1	80.3	5.0	0.5	33.4
2	81.6	4.2	0.8	47.4
3	83.0	5.4	1.2	63.0
4	84.4	6.5	1.5	79.3
5	86.0	5.7	2.3	109.0
6	88.3	4.2	2.7	141.8
7	90.4	4.7	3.3	168.2
8	92.3	4.4	2.8	140.6
9	94.4	4.9	2.1	107.6
10	96.3	4.8	0.6	79.0
11	98.1	2.8	0.4	60.6
12	98.8	3.0	0.1	28.0

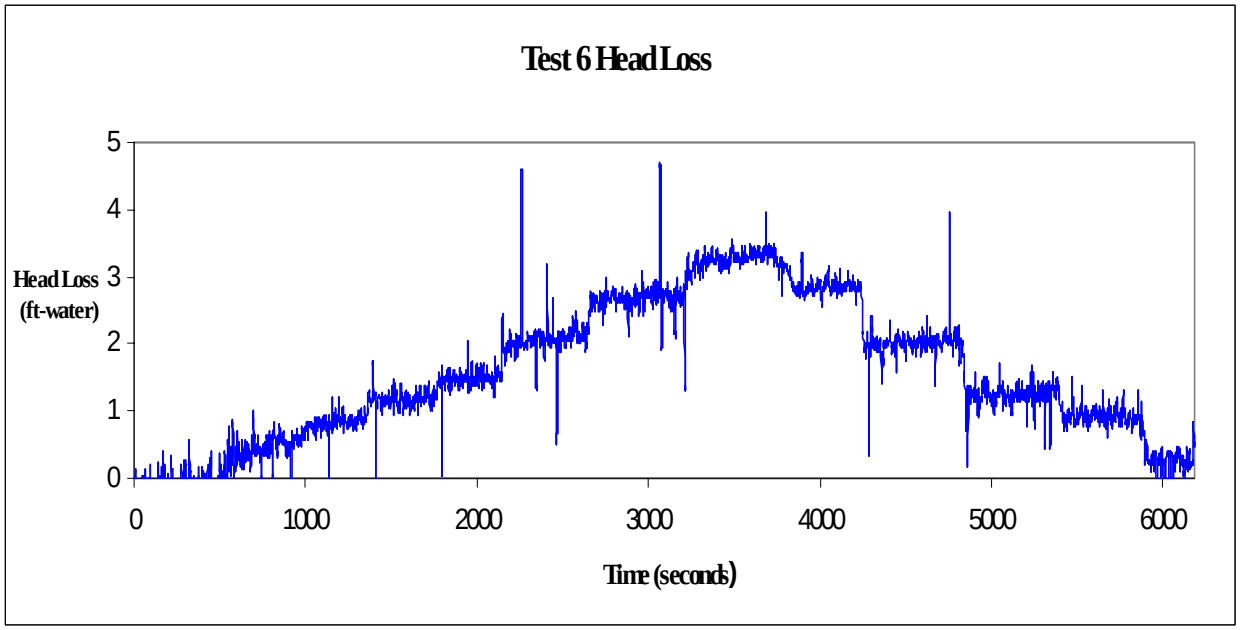

Fig. A-9. Time-dependent head-loss measurements.

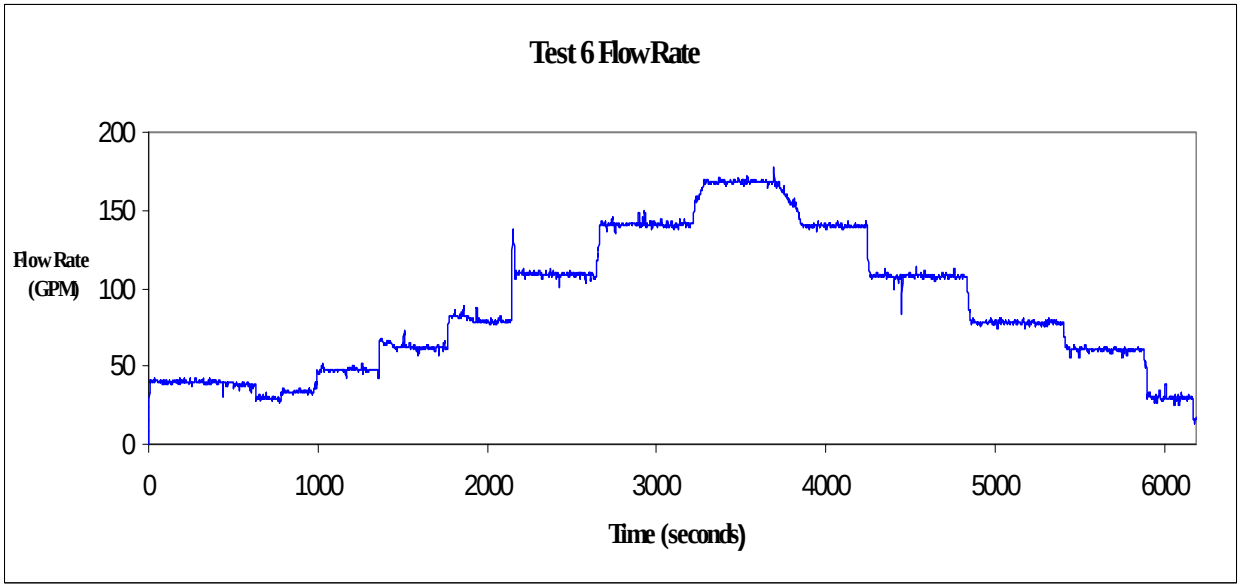

Fig. A-10. Time-dependent flow-rate measurements.

A.4.7 Test 7: 100 g NUKON™: 100 g Dirt

The dirt formula again was changed. The >2-mm particles were omitted.

Table A-9. Log Book Record Test Data, Test 7

Test 7 Log Book Information				
Data Point	**Temperature (°F)**	**Turbidity (NTU)**	**Head Loss (ft-water)**	**Flow (gal./min)**
1	78.4	20.0	2.1	30.0
2	79.9	14.5	3.5	47.0
3	81.0	16.3	4.2	61.3
4	82.3	14.3	4.9	79.9
5	83.8	12.3	5.3	94.3
6	85.0	10.6	5.8	109.2
7	86.2	8.7	6.8	125.3
8	87.8	7.4	7.5	141.7
9	90.0	6.3	8.3	149.4
10	91.2	6.2	7.6	141.9
11	93.4	5.3	6.1	125.6
12	95.1	4.3	4.9	110.3
13	96.7	3.8	4.1	94.5
14	98.0	3.1	3.2	78.9
15	99.1	3.3	2.5	63.4
16	105.0	2.7	1.8	48.5
17	101.7	2.4	0.9	29.7

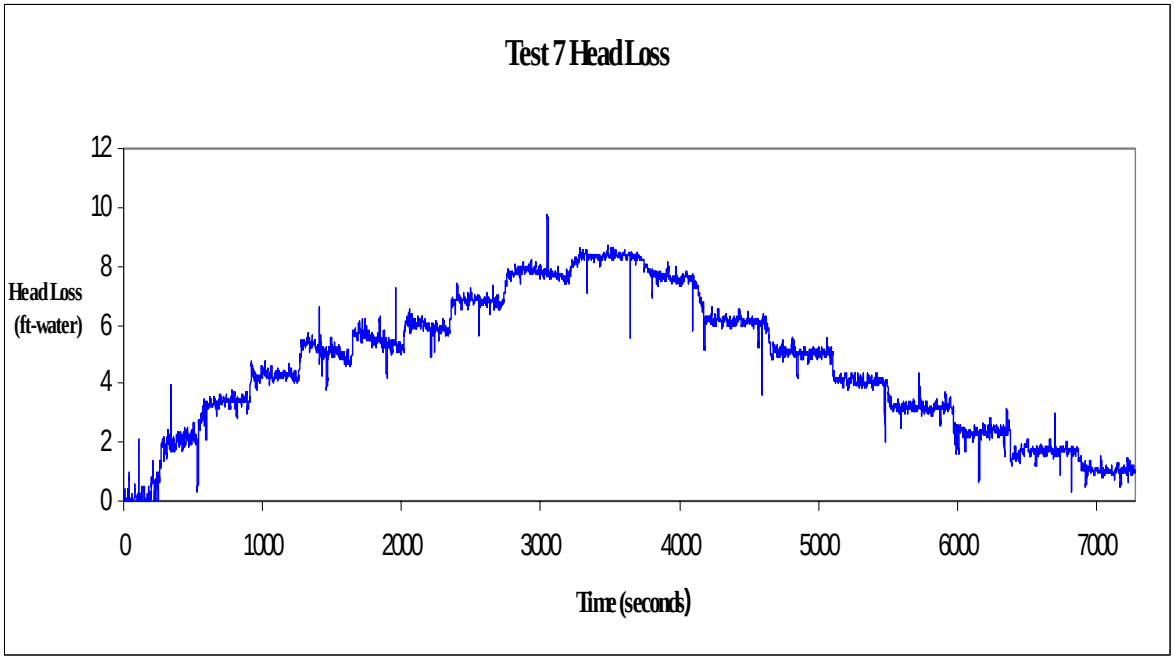

Fig. A-11. Time-dependent head-loss measurements.

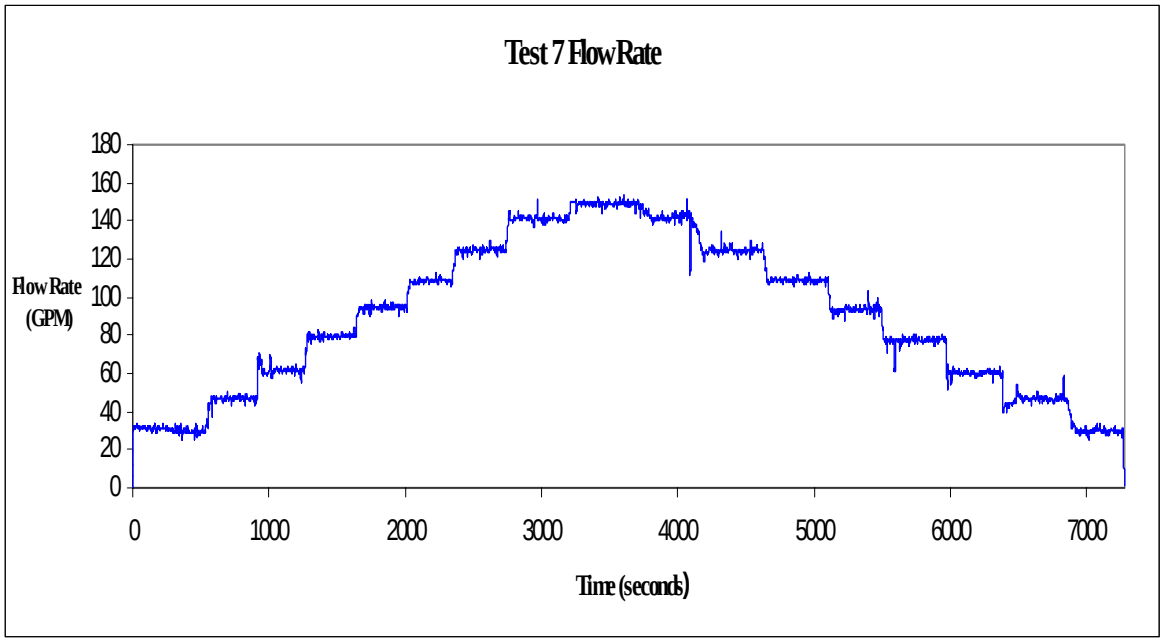

Fig. A-12. Time-dependent flow-rate measurements.

A.4.8 Test 8: 100 g NUKON™: 100 g Dirt

This test was essentially a repetition of Test 7, with a final revision to the formula.

Table A-10. Log Book Record Test Data, Test 8

Test 8 Log Book Information				
Data Point	**Temperature (°F)**	**Turbidity (NTU)**	**Head Loss (ft-water)**	**Flow (gal./min)**
1.0	82.9	8.0	1.8	31.1
2.0	84.5	17.7	2.5	46.1
3.0	88.0	23.0	3.1	61.5
4.0	89.6	22.0	3.5	78.4
5.0	91.2	21.0	3.9	93.5
6.0	92.1	21.0	4.4	109.8
7.0	93.8	22.0	5.1	126.9
8.0	95.9	21.0	6.2	140.2
9.0	97.1	21.0	6.9	154.8
10.0	98.1	19.5	6.0	140.2
11.0	99.8	19.8	4.9	124.1
12.0	101.0	18.1	4.1	109.3
13.0	101.8	15.9	3.0	91.6
14.0	102.8	15.4	2.6	78.0
15.0	103.7	13.8	1.8	61.9
16.0	105.0	12.3	1.5	47.1
17.0	105.7	11.8	0.9	29.3

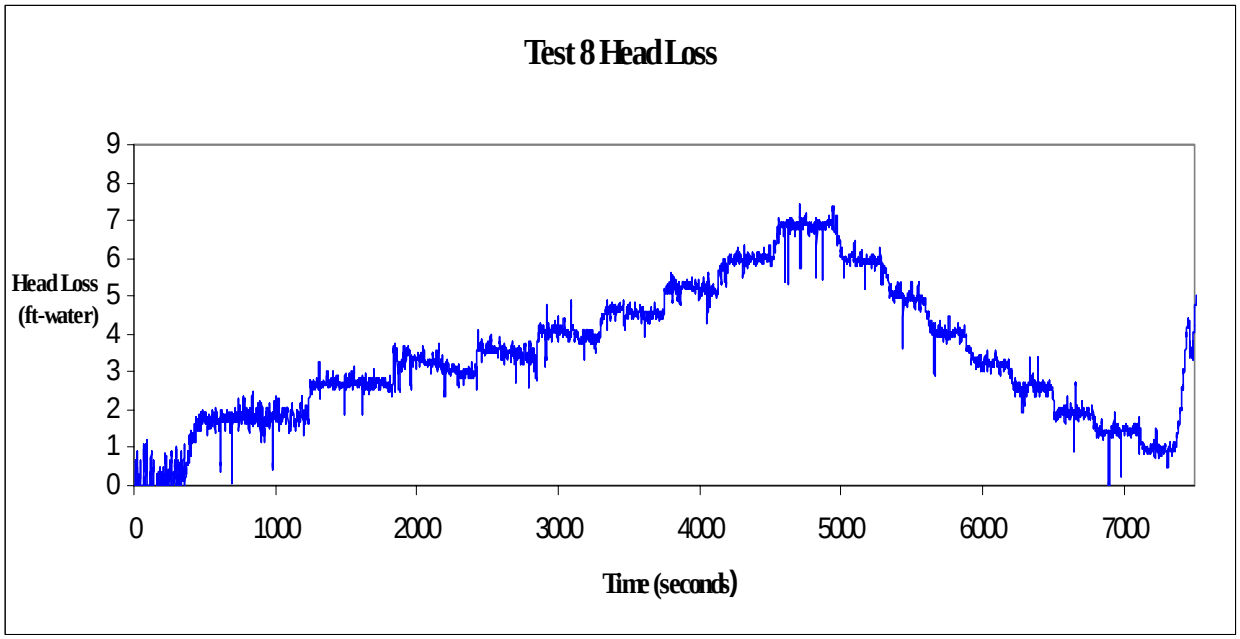

Fig. A-13. Time-dependent head-loss measurements.

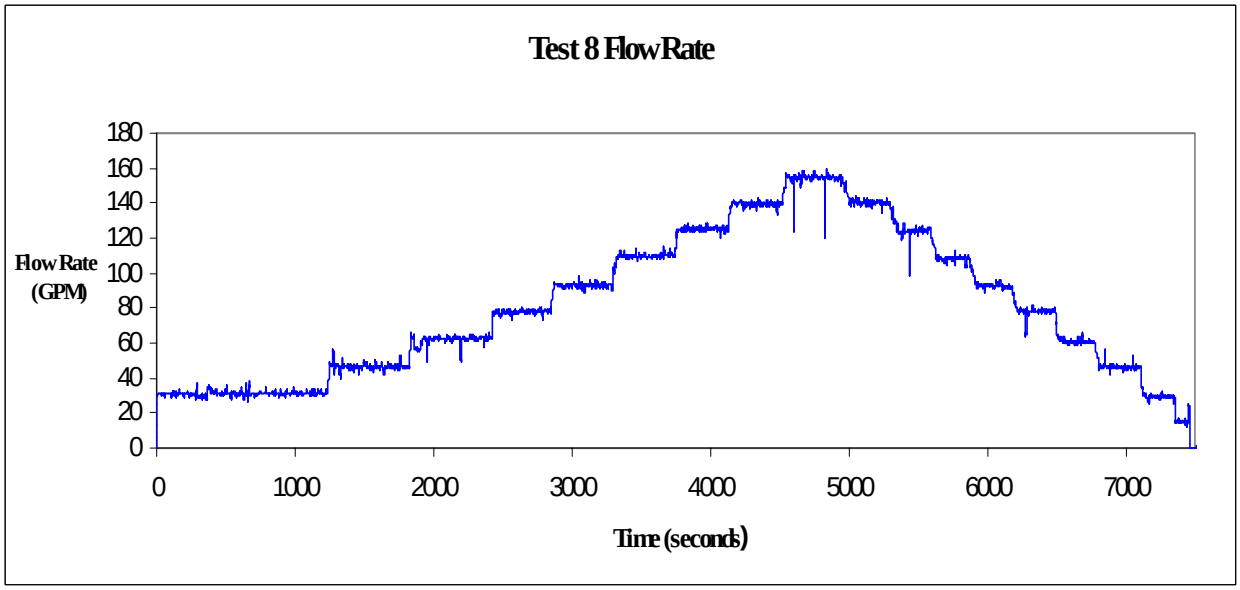

Fig. A-14. Time-dependent flow-rate measurements.

A.4.9 Test 9: 60 g NUKON™: 120 g Dirt

Table A-11. Log Book Record Test Data, Test 9

Test 9 Log Book Information				
Data Point	**Temperature (°F)**	**Turbidity (NTU)**	**Head Loss (ft-water)**	**Flow (gal./min)**
1	81.6	18	1.2	30.7
2	8301	46	1.9	46.7
3	85.1	38	2.4	61.2
4	86.6	37	2.9	78.3
5	88.5	34	3.3	93.2
6	90.3	46	3.7	109.1
7	91.5	41	4.2	124.3
8	93	43	4.8	140.9
9	95	45	5.5	156.7
10	96	39	5.7	160.1
11	97.7	39	4.8	140.2
12	98	38	3.2	109.1
13	100	36	1.9	79.2
14	99.2	39	1.1	45.3

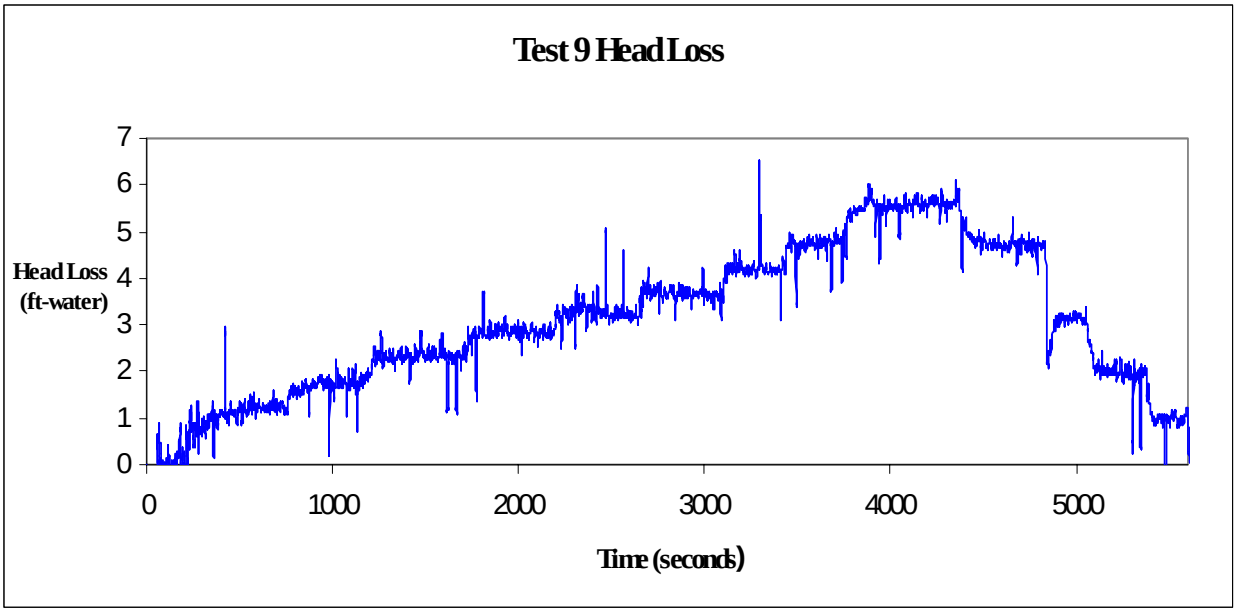

Fig. A-15. Time-dependent head-loss measurements.

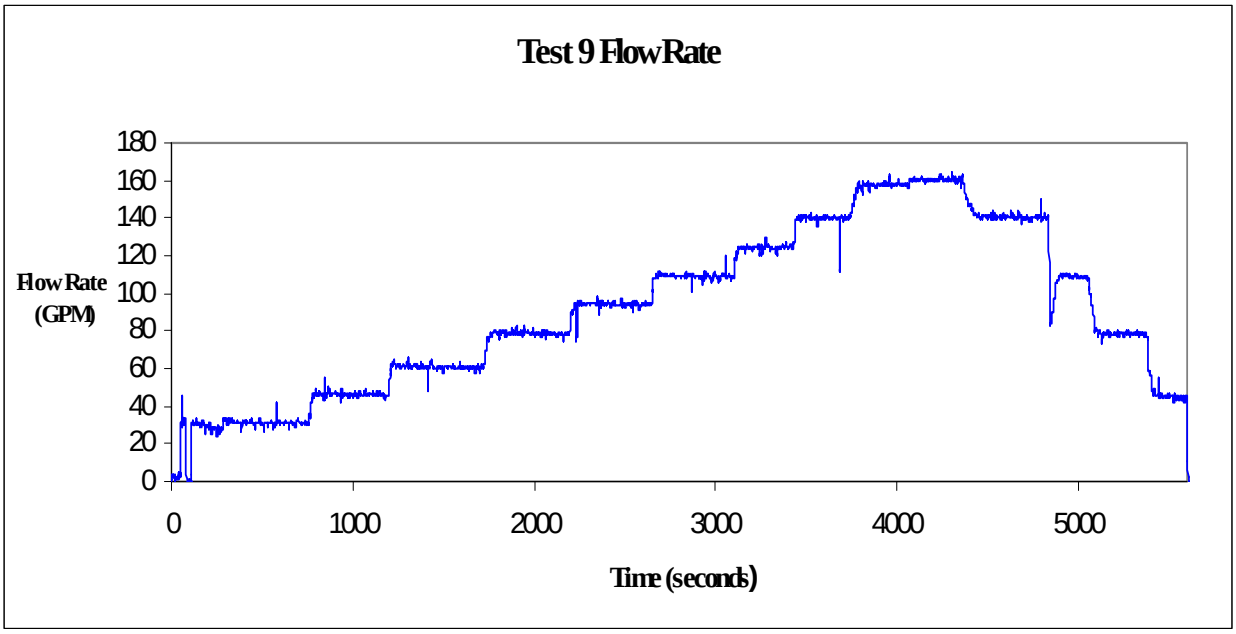

Fig. A-16. Time-dependent flow-rate measurements.

A.4.10 Test 10: 60 g NUKON™: 240 g Dirt

This test was invalid because the debris was poorly formed.

A.4.11 Test 11: 60 g NUKON™: 240 g Dirt

This test was a replacement for Test 10.

Table A-12. Log Book Record Test Data, Test 11

Test 11 Log Book Information				
Data Point	**Temperature (°F)**	**Turbidity (NTU)**	**Head Loss (ft-water)**	**Flow (gal./min)**
1	85.2	64.0	6.3	31.3
2	86.9	102.0	10.3	62.1
3	88.9	56.0	14.4	91.4
4	91.1	82.0	17.5	104.4
5	92.5	74.0	14.2	93.5
6	94.2	83.0	8.1	59.8
7	94.9	76.0	3.3	31.9

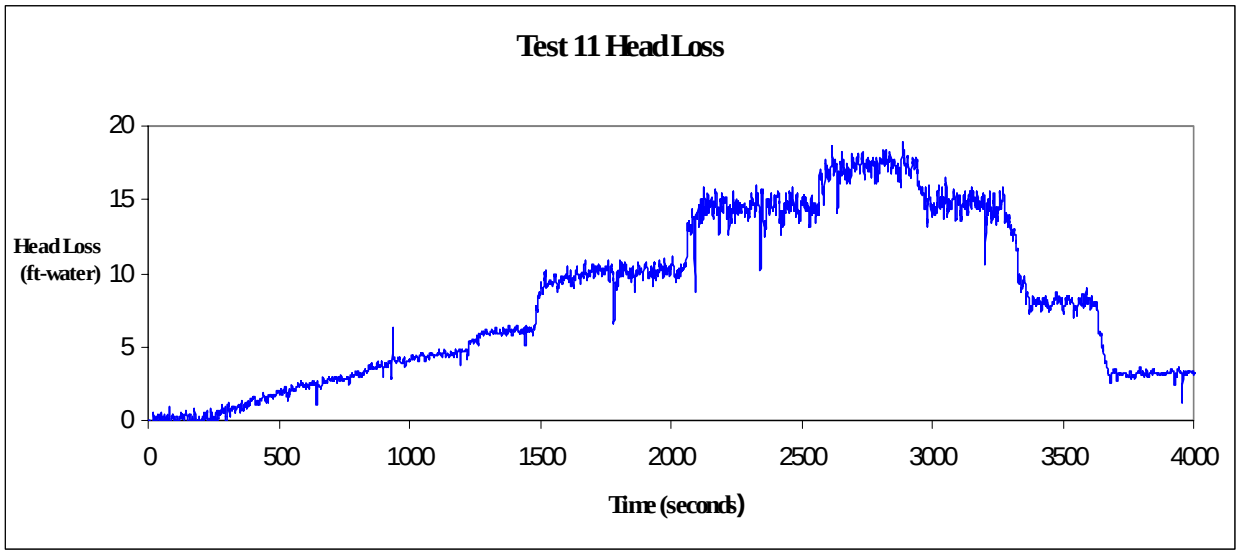

Fig. A-17. Time-dependent head-loss measurements.

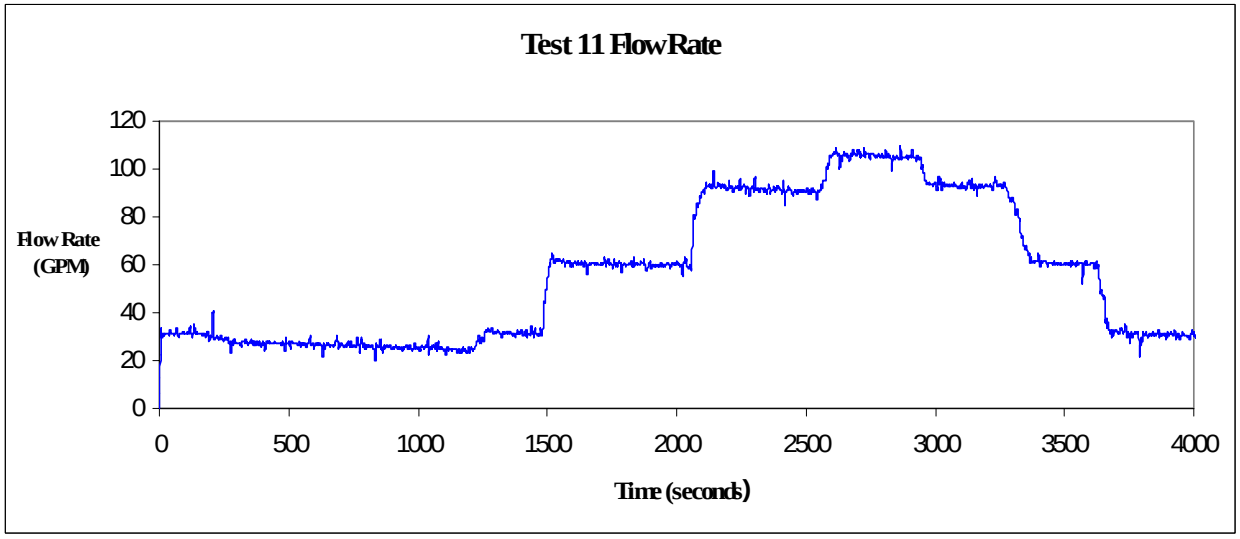

Fig. A-18. Time-dependent flow-rate measurements.

A.4.12 Test 12: 15 g NUKON™: 90 g Dirt

Table A-13. Log Book Record Test Data, Test 12

Test 12 Log Book Information				
Data Point	**Temperature (°F)**	**Turbidity (NTU)**	**Head Loss (ft-water)**	**Flow (gal./min)**
1	83.8	16.5	2.3	30.9
2	89.7	17.9	4.6	45.2
3	91.0	15.2	5.5	60.7
4	93.5	15.8	6.5	76.5
5	94.6	23.0	7.6	93.4
6	96.8	17.6	8.7	109.5
7	99.5	21.0	9.6	124.8
8	101.2	22.0	10.0	138.9
9	103.6	16.0	9.3	124.9
10	104.7	19.0	8.0	109.2
11	105.7	18.0	6.1	93.0
12	106.5	16.1	4.5	77.2
13	107.7	16.1	3.5	60.3
14	108.5	15.0	2.3	45.5
15	109.4	14.5	1.5	31.2

Fig. A-19. Time-dependent head-loss measurements.

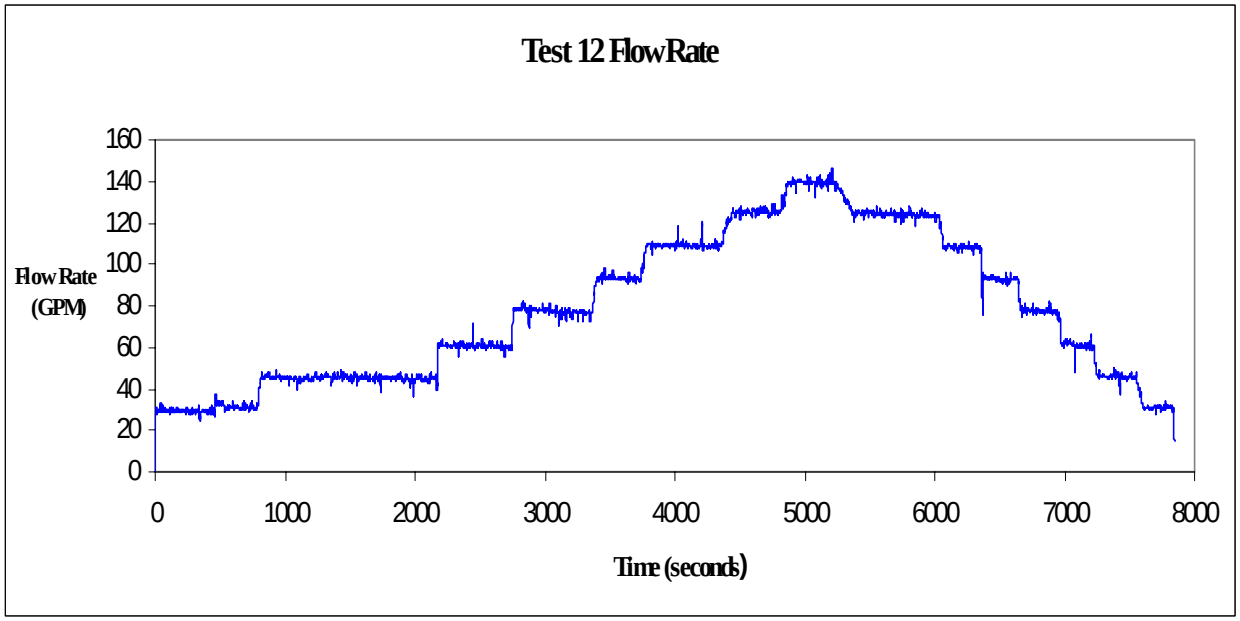

Fig. A-20. Time-dependent flow-rate measurements.

A.4.13 Test 13: 80 g NUKON™: 240 g Dirt

Table A-14. Log Book Record Test Data, Test 13

Test 13 Log Book Information				
Data Point	**Temperature (°F)**	**Turbidity (NTU)**	**Head Loss (ft-water)**	**Flow (gal./min)**
1	82.5	45.0	5.2	28.9
2	84.6	52.0	6.0	46.2
3	86.0	43.0	7.9	63.8
4	88.0	45.0	8.9	78.9
5	89.1	41.0	10.8	93.6
6	90.8	44.0	13.3	106.0
7	92.3	41.0	14.8	118.2
8	94.1	44.0	13.5	107.9
9	95.4	41.0	11.1	93.2
10	96.3	39.0	8.0	76.1
11	97.7	33.0	5.8	60.9
12	98.4	29.0	3.7	44.2
13	99.6	35.0	2.1	32.2

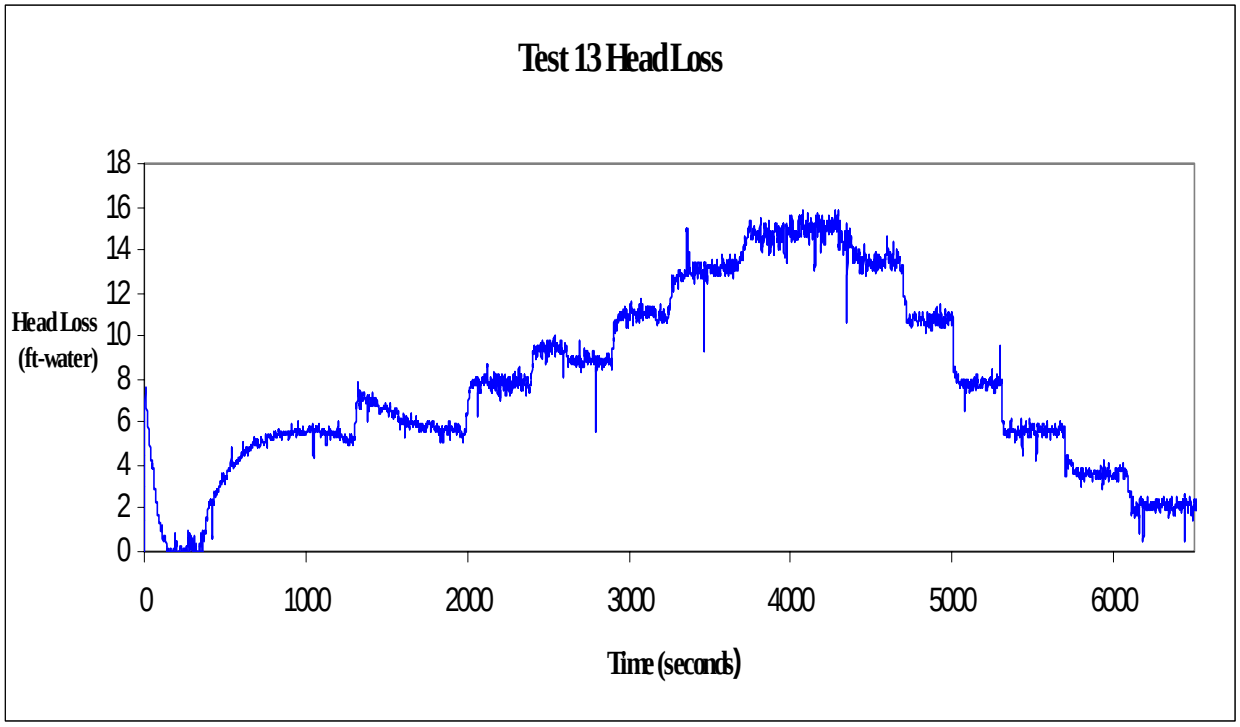

Fig. A-21. Time-dependent head-loss measurements.

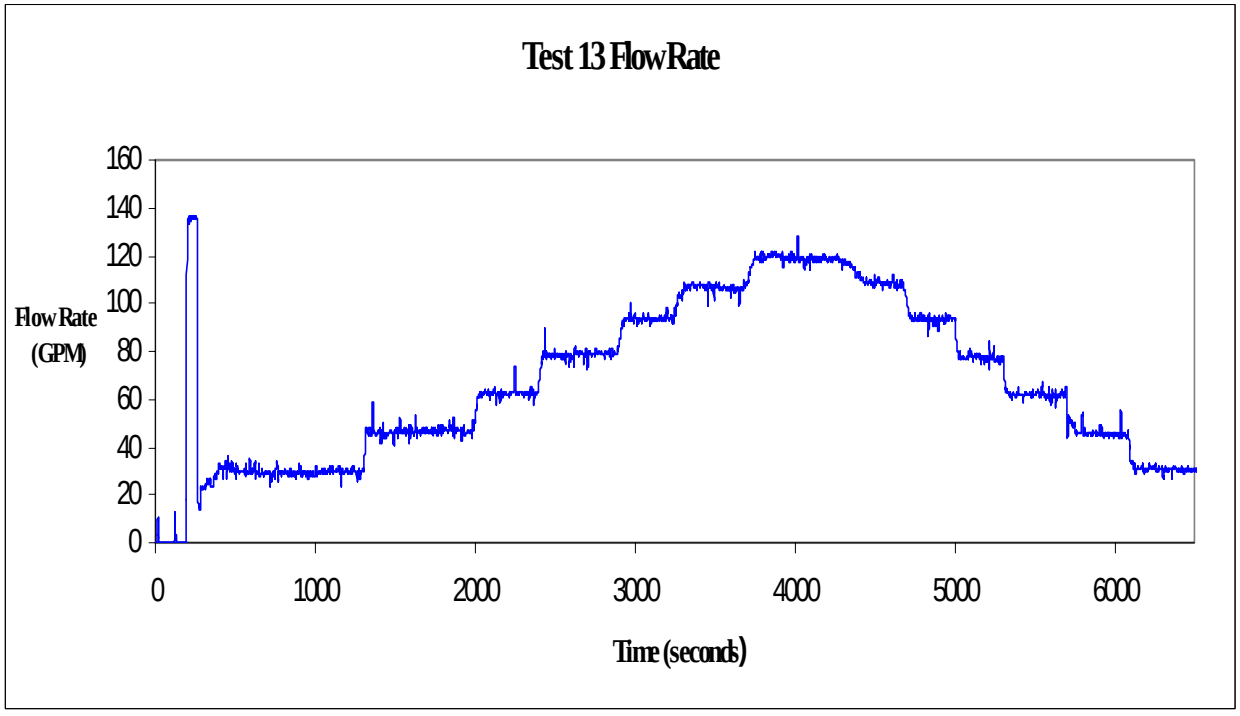

Fig. A-22. Time-dependent flow-rate measurements.

A.4.14 Test 14: 60 g NUKON™: 113.2 g Dirt

Table A-15. Log Book Record Test Data, Test 14

Test 14 Log Book Information				
Data Point	**Temperature (°F)**	**Turbidity (NTU)**	**Head Loss (ft-water)**	**Flow (gal./min)**
1	105.0	43.0	1.3	30.1
2	106.8	31.0	2.4	44.7
3	108.2	7.0	2.9	61.7
4	110.0	24.0	3.5	77.3
5	111.3	24.0	3.6	94.1
6	112.5	22.0	4.2	111.8
7	112.7	19.9	5.1	122.3
8	114.2	20.0	5.8	141.1
9	117.1	37.0	7.5	154.8
10	118.4	30.0	6.9	128.8
11	119.0	25.0	4.8	98.2
12	119.8	22.0	2.5	70.3
13	120.9	21.0	1.7	29.6

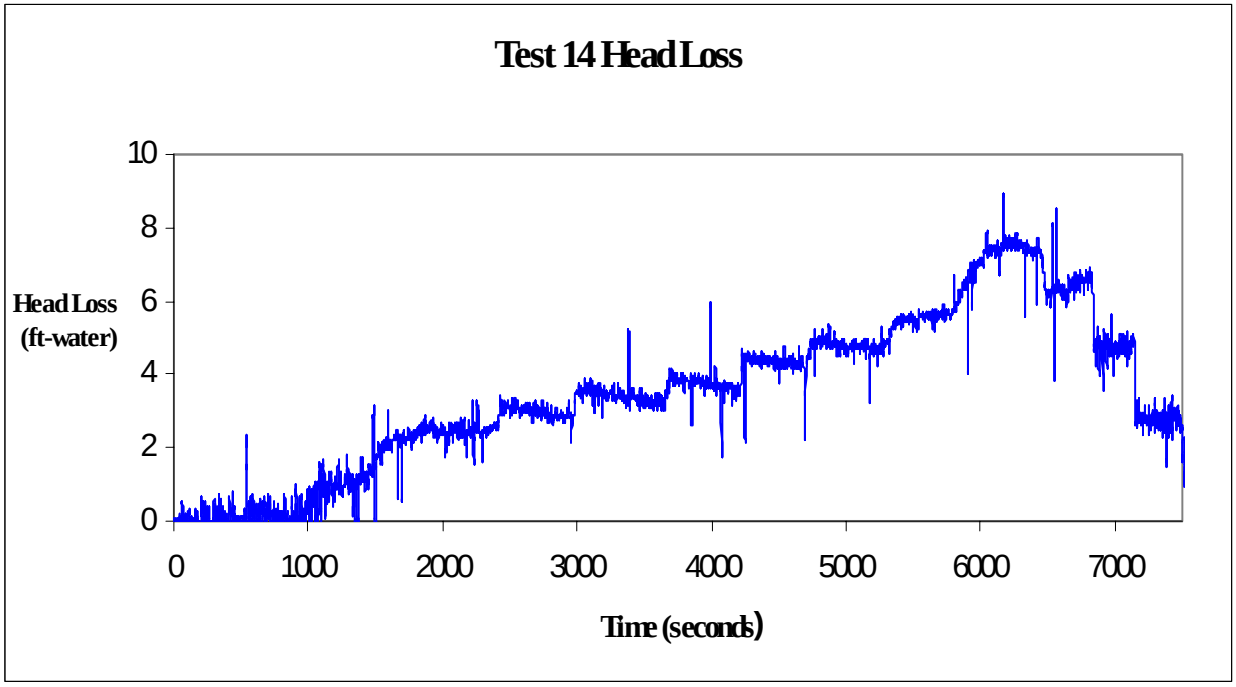

Fig. A-23. Time-dependent head-loss measurements.

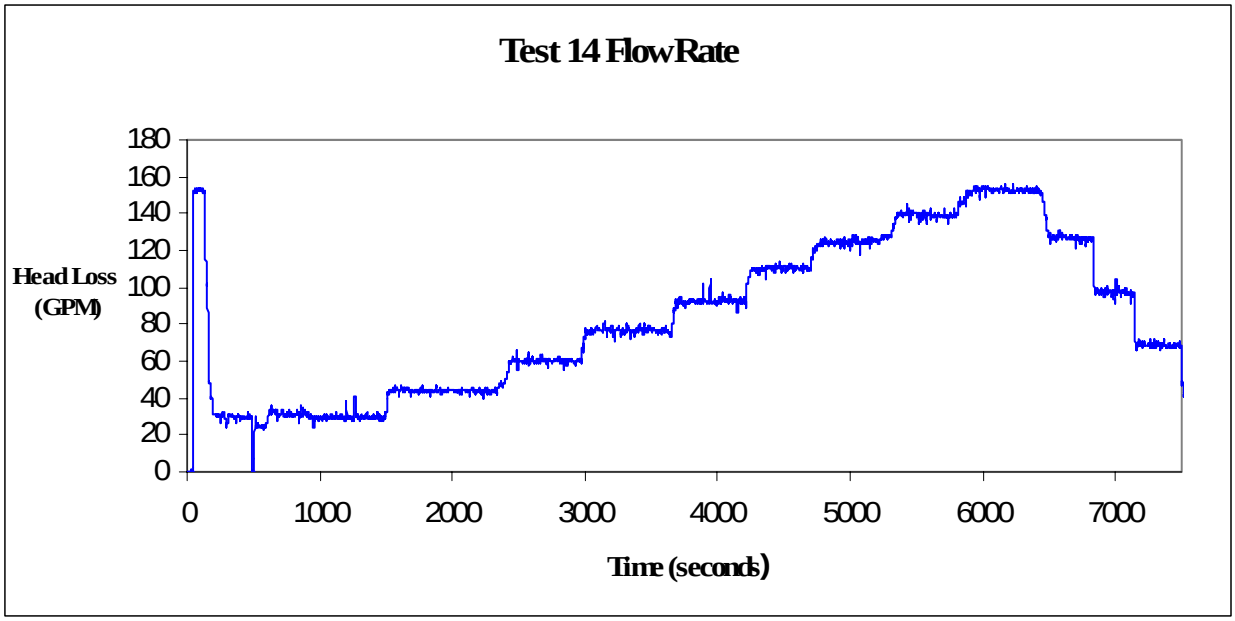

Fig. A-24. Time-dependent flow-rate measurements.

A.4.15 Test 15: 60 g NUKON™: 90 g Dirt

Table A-16. Log Book Record Test Data, Test 15

Test 15 Log Book Information				
Data Point	**Temperature (°F)**	**Turbidity (NTU)**	**Head Loss (ft-water)**	**Flow (gal./min)**
1	106.2	55.0	1.7	28.8
2	108.1	60.0	3.7	47.1
3	109.4	62.0	4.6	65.0
4	110.9	50.0	5.5	78.1
5	122.2	50.0	6.7	93.5
6	113.7	50.0	8.8	108.4
7	114.7	46.0	10.4	126.3
8	116.2	58.0	11.8	136.3
9	117..5	47.0	8.3	109.3
10	118.2	39.0	5.8	85.2
11	119.3	36.0	3.5	61.3
12	119.9	37.0	1.6	34.7

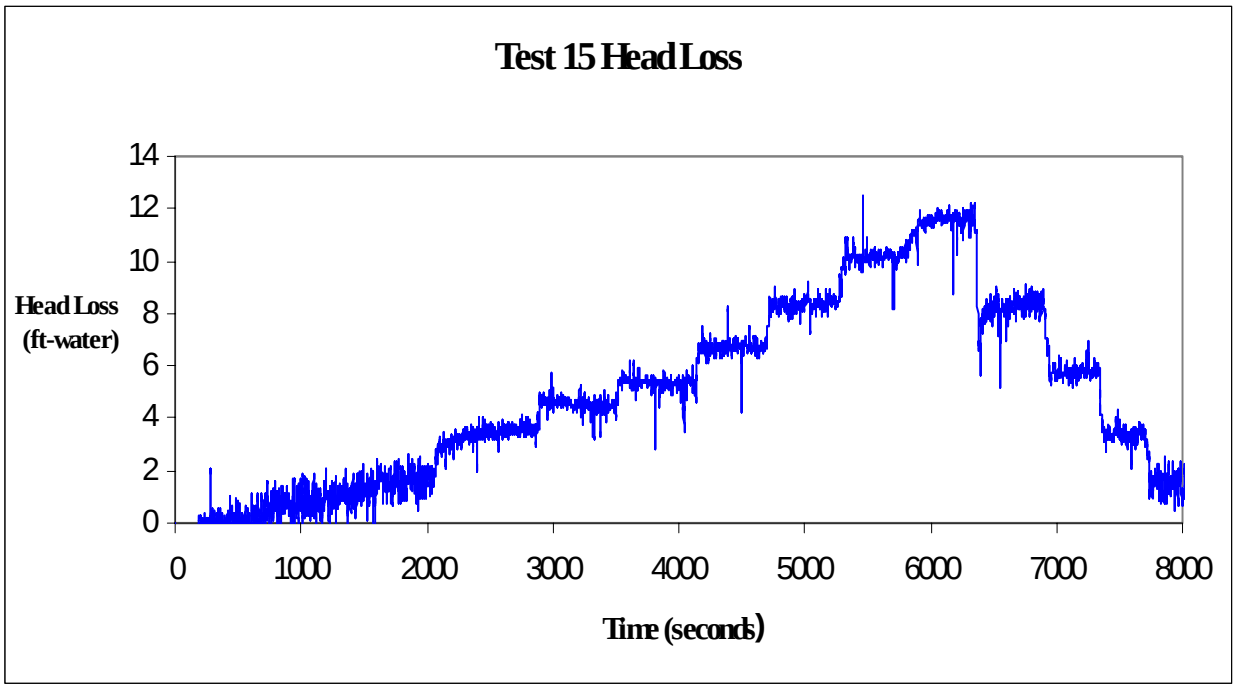

Fig. A-25. Time-dependent head-loss measurements.

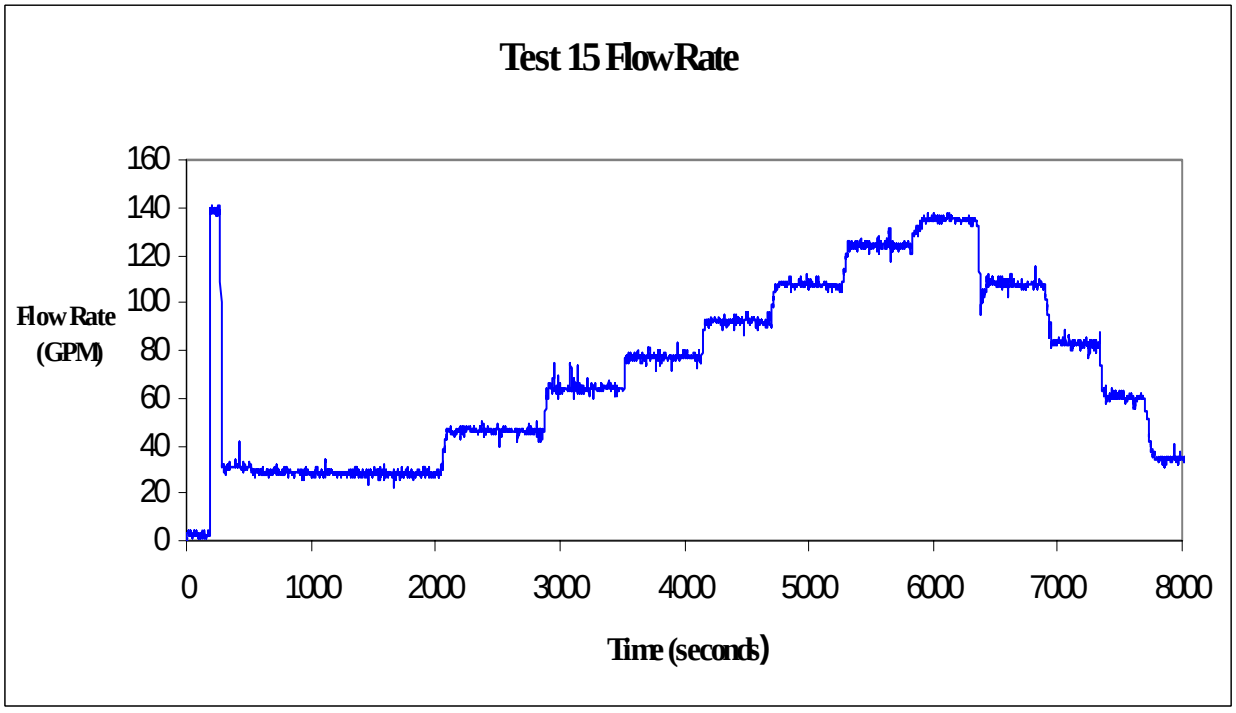

Fig. A-26. Time-dependent flow-rate measurements.

A.4.16 Test 16: 15 g NUKON™: 600 g Dirt

Table A-17. Log Book Record Test Data, Test 16

Test 16 Log Book Information				
Data Point	**Temperature (°F)**	**Turbidity (NTU)**	**Head Loss (ft-water)**	**Flow (gal./min)**
1.0	86.6	8.1	1.6	31.2
2.0	87.7	6.0	3.1	44.4
3.0	89.2	4.7	3.3	59.9
4.0	90.4	4.1	4.4	77.3
5.0	91.4	4.5	5.5	93.0
6.0	92.8	5.8	6.6	106.5
7.0	93.8	5.1	8.1	126.1
8.0	95.3	5.3	9.3	139.9
9.0	96.5	4.5	9.9	144.4
10.0	96.5	5.9	9.0	124.0
11.0	98.7	4.7	7.3	105.5
12.0	99.6	5.0	5.8	96.4
13.0	100.5	4.2	4.3	75.3
14.0	101.5	3.5	3.0	61.4
15.0	102.6	3.2	1.7	46.5
16.0	103.2	2.9	1.2	31.6

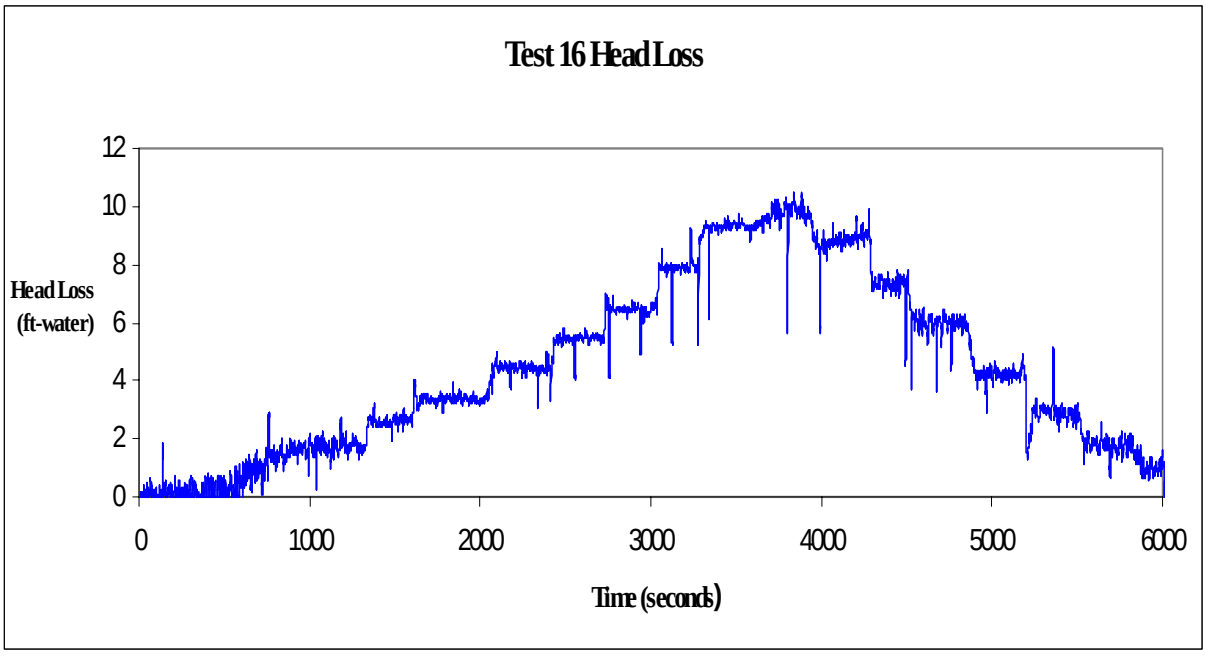

Fig. A-27. Time-dependent head-loss measurements.

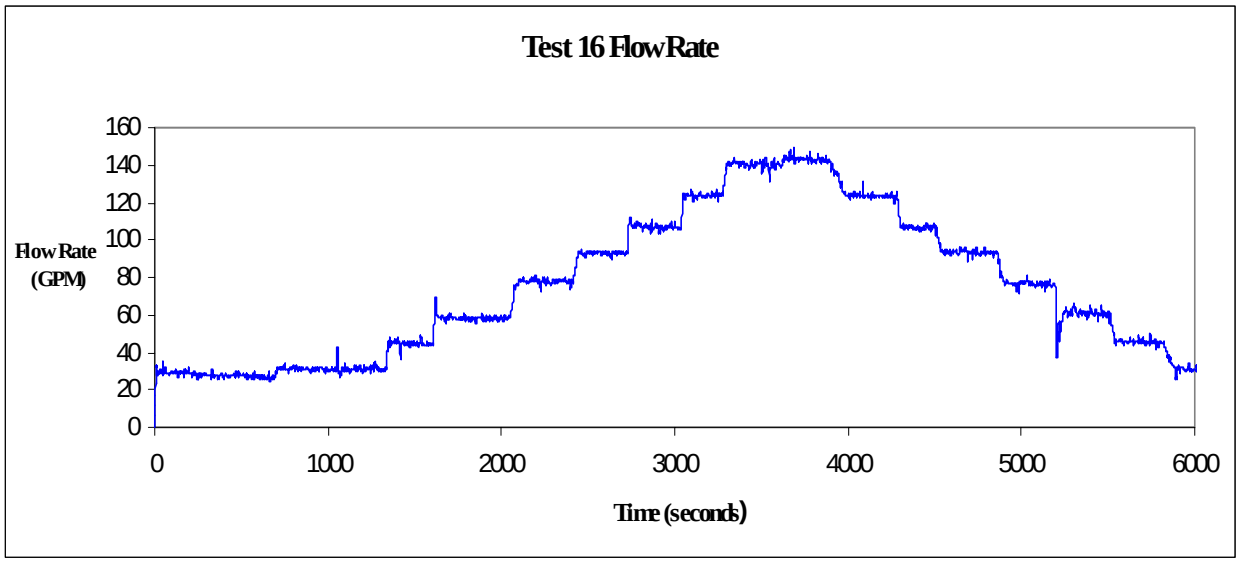

Fig. A-28. Time-dependent flow-rate measurements.

A.4.17 Test 17: 15 g NUKON™: 120 g Dirt

Table A-18. Log Book Record Test Data, Test 17

Test 17 Log Book Information				
Data Point	**Temperature (°F)**	**Turbidity (NTU)**	**Head Loss (ft-water)**	**Flow (gal./min)**
1	88.0	30.0	5.1	30.6
2	89.5	141.0	7.4	39.1
3	90.5	166.0	9.7	49.6
4	91.7	179.0	12.2	61.0
5	93.1	200.0	13.6	69.9
6	94.4	260.0	15.8	78.5
7	95.7	230.0	16.7	90.2
8	96.7	220.0	17.7	103.6
9	98.1	244.0	17.3	109.1
10	99.0	170.0	15.0	99.0
11	99.9	156.0	12.8	89.4
12	100.7	147.0	10.0	81.2
13	101.6	162.0	8.5	70.2
14	102.8	162.0	6.9	61.1
15	103.6	176.0	5.1	49.5
16	104.4	200.0	4.0	40.6
17	105.7	187.0	3.1	32.4

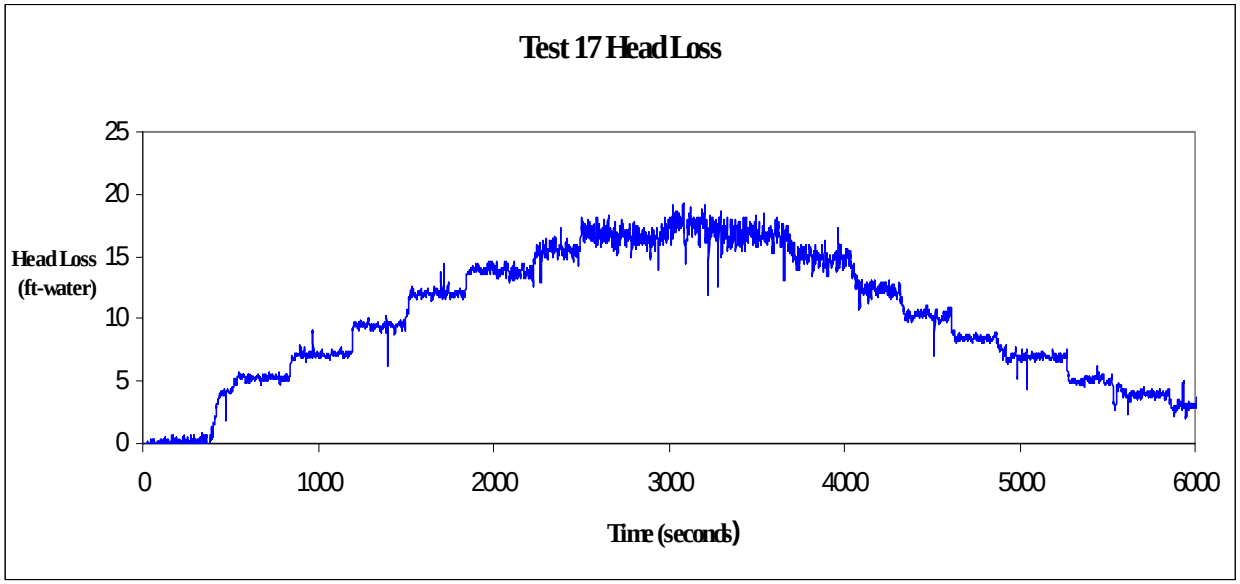

Fig. A-29. Time-dependent head-loss measurements.

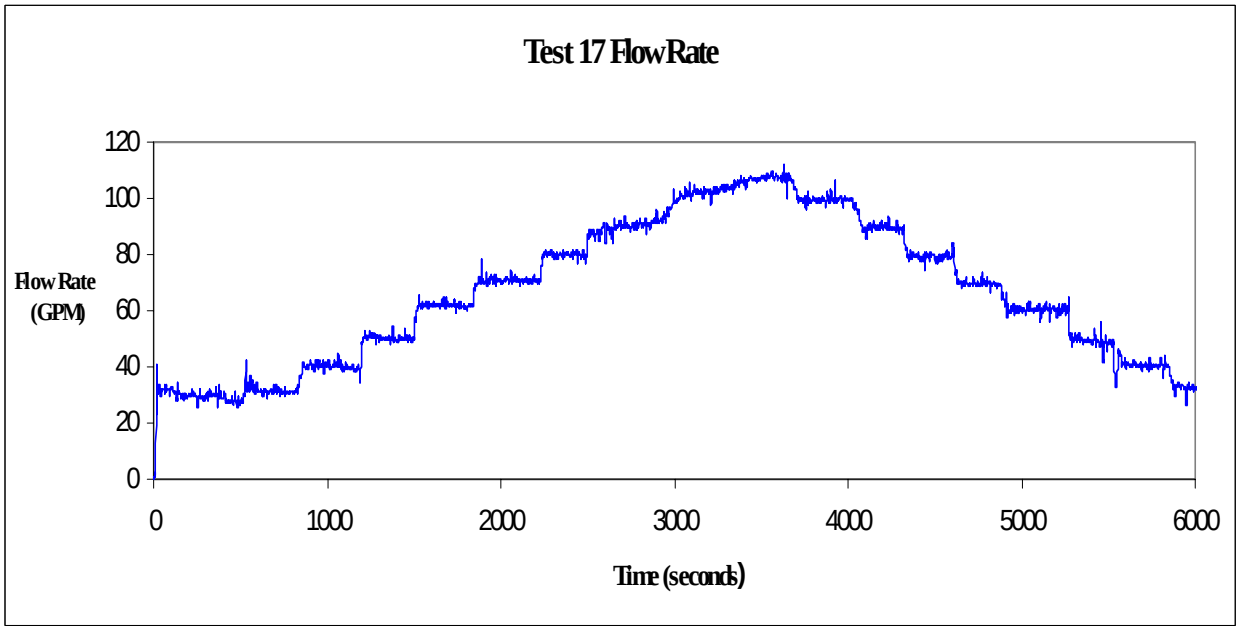

Fig. A-30. Time-dependent flow-rate measurements.

A.4.18 Test 18: 150 g NUKON™: 450 g Dirt

Table A-19. Log Book Record Test Data, Test 18

Test 18 Log Book Information				
Data Point	**Temperature (°F)**	**Turbidity (NTU)**	**Head Loss (ft-water)**	**Flow (gal./min)**
1	85.6	3.4	4.0	30.2
2	87.0	2.7	5.6	46.1
3	88.6	2.5	7.6	62.2
4	89.8	10.1	10.3	78.1
5	91.4	6.0	12.5	93.1
6	92.8	4.6	14.8	109.0
7	94.2	3.2	15.7	115.0
8	95.5	3.1	14.5	107.6
9	97.2	2.1	11.3	91.9
10	98.7	1.8	9.4	78.7
11	99.5	1.7	6.4	58.8
12	100.6	1.1	4.5	46.0
13	101.5	0.9	3.3	31.5

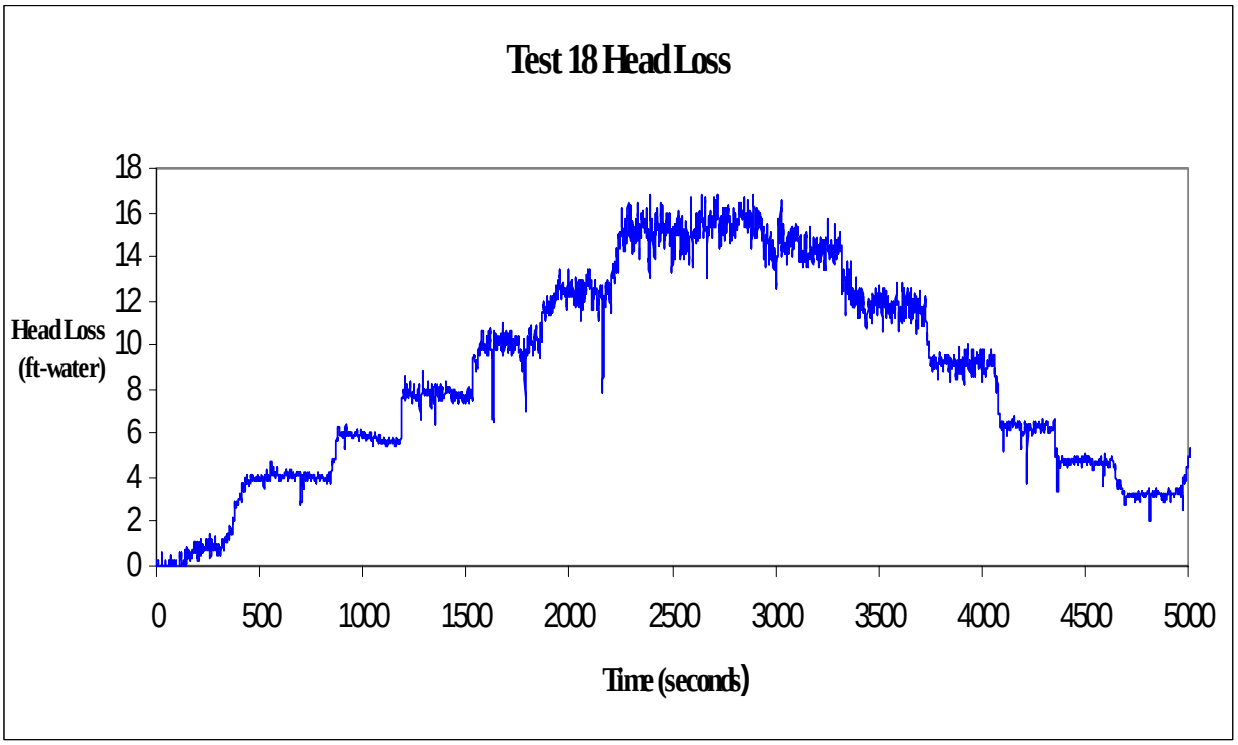

Fig. A-31. Time-dependent head-loss measurements.

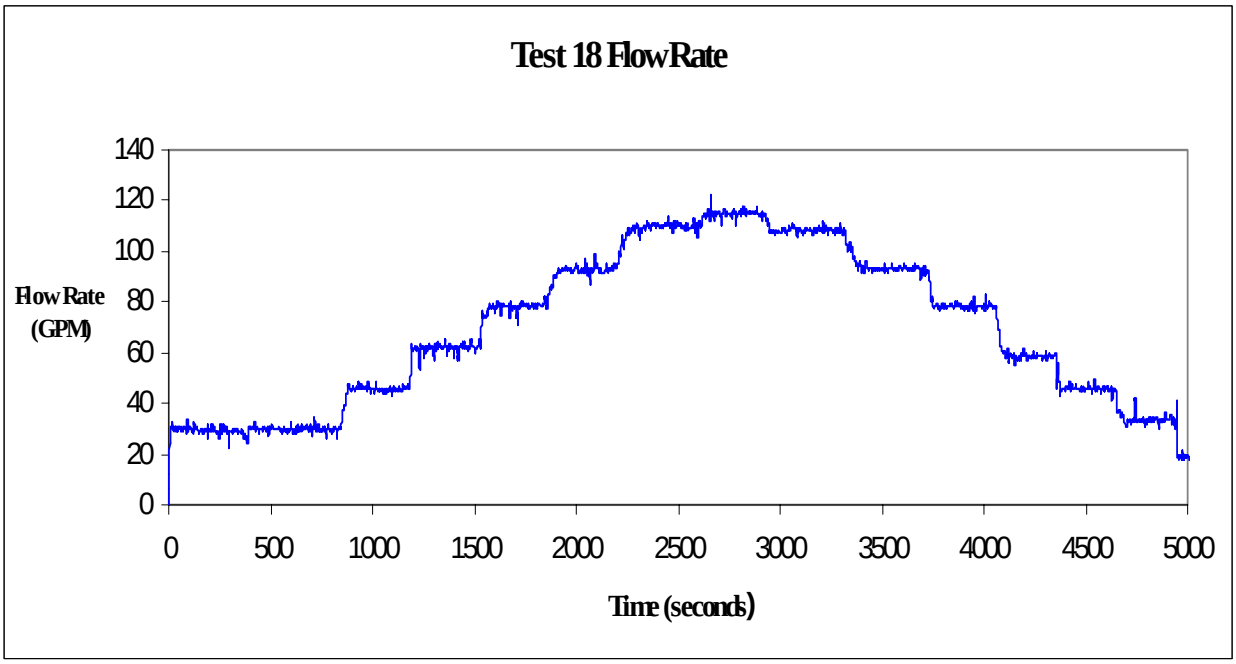

Fig. A-32. Time-dependent flow-rate measurements.

A.4.19 Test 19: 15 g NUKON™: 90 g Dirt

Table A-20. Log Book Record Test Data, Test 19

Test 19 Log Book Information				
Data Point	**Temperature (°F)**	**Turbidity (NTU)**	**Head Loss (ft-water)**	**Flow (gal./min)**
1	88.2	10.6	7.4	29.5
2	92.3	25.0	12.2	43.5
3	93.7	30.0	15.3	62.0
4	97.7	26.0	13.3	77.8
5	98.8	28.0	14.9	98.2
6	100.0	35.0	15.2	113.2
7	101.6	34.0	15.3	118.0
8	102.5	28.0	10.6	93.2
9	103.5	28.0	7.5	75.7
10	104.6	30.0	5.8	61.7
11	105.5	28.0	3.4	48.4
12	106.1	29.0	1.7	28.2

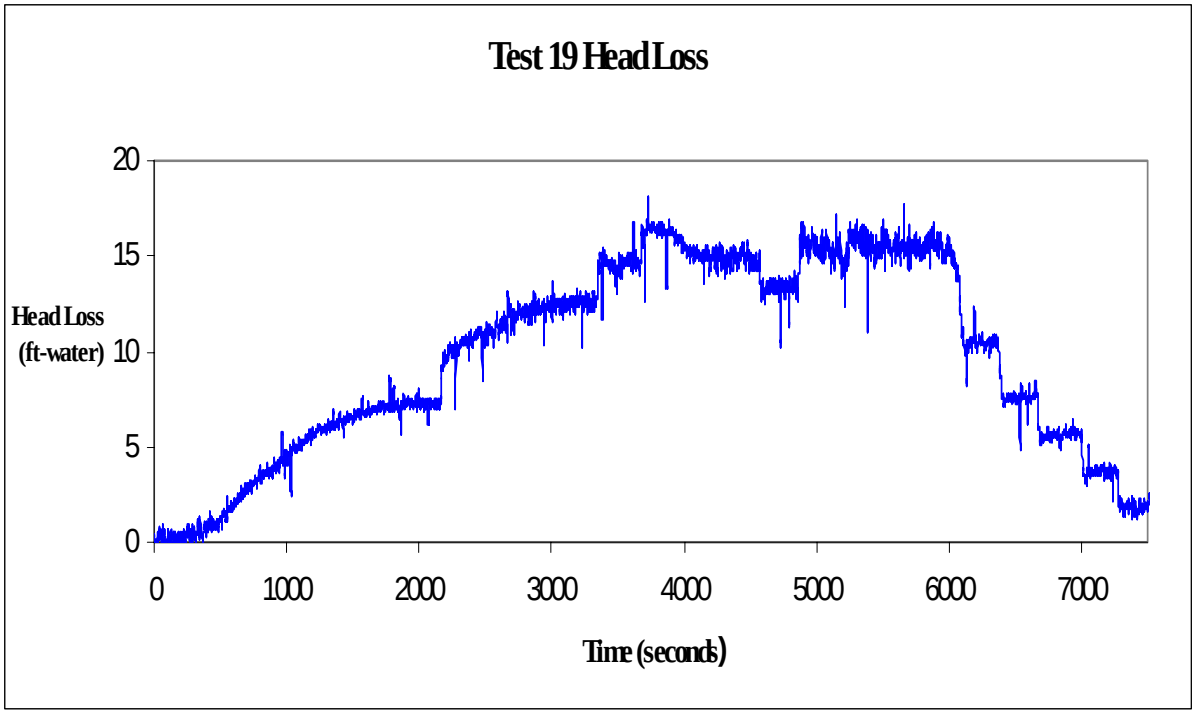

Fig. A-33. Time-dependent head-loss measurements.

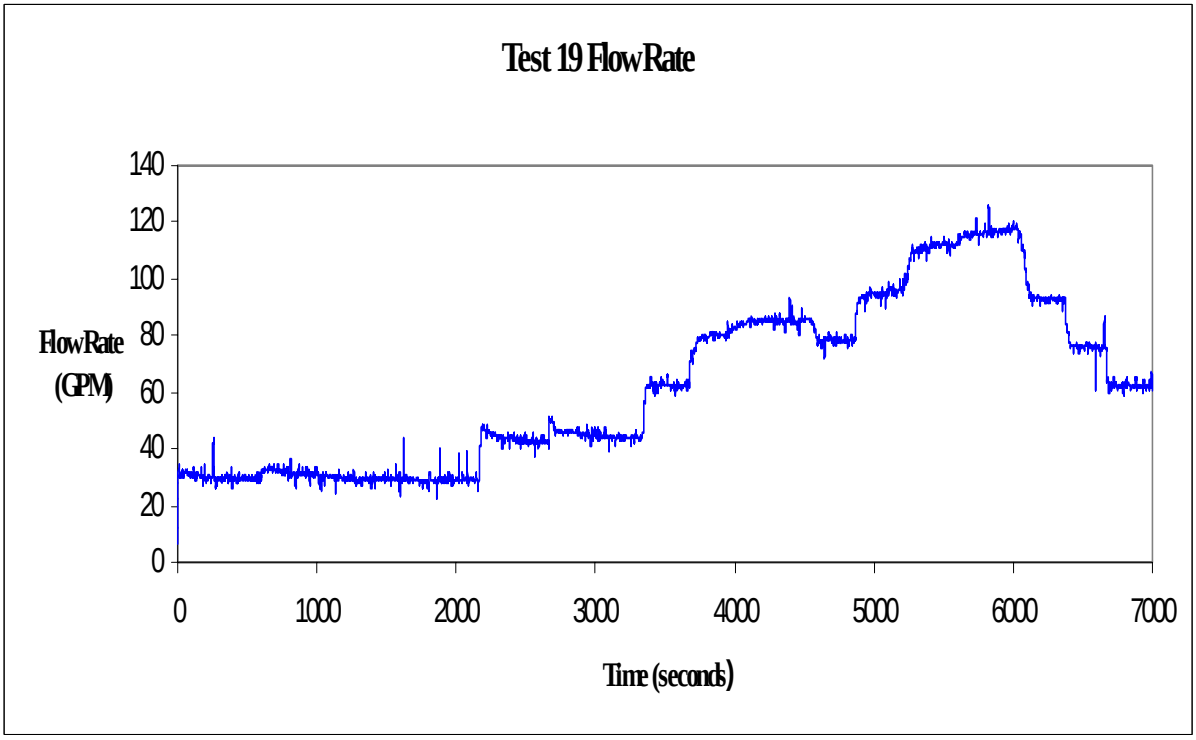

Fig. A-34. Time-dependent flow-rate measurements.

A.4.20 Test 20: 150 g NUKON™: 450 g Dirt

Table A-21. Log Book Record Test Data, Test 20

Test 20 Log Book Information				
Data Point	**Temperature (°F)**	**Turbidity (NTU)**	**Head Loss (ft-water)**	**Flow (gal./min)**
1	86.1	5.2	3.3	31.2
2	87.0	4.6	4.5	48.8
3	88.6	4.1	4.9	62.4
4	89.4	3.5	5.9	80.2
5	90.3	3.4	6.6	92.7
6	91.2	2.2	7.5	110.2
7	91.9	2.3	8.6	125.7
8	92.7	1.8	9.5	141.6
9	94.0	2.1	7.7	125.3
10	95.1	2.1	6.5	108.6
11	96.3	1.7	5.0	94.3
12	97.2	1.5	4.1	78.0
13	98.3	1.0	3.0	60.9
14	99.2	0.8	0.2	44.2
15	100.3	0.7	1.3	31.7

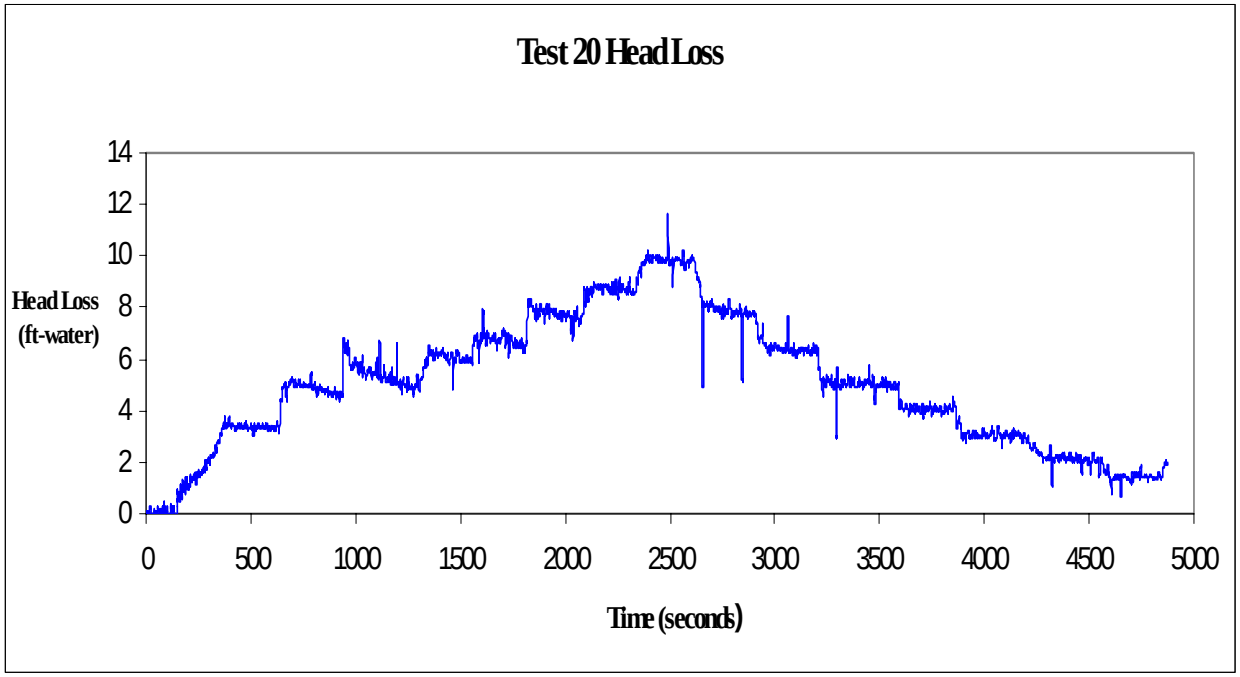

Fig. A-35. Time-dependent head-loss measurements.

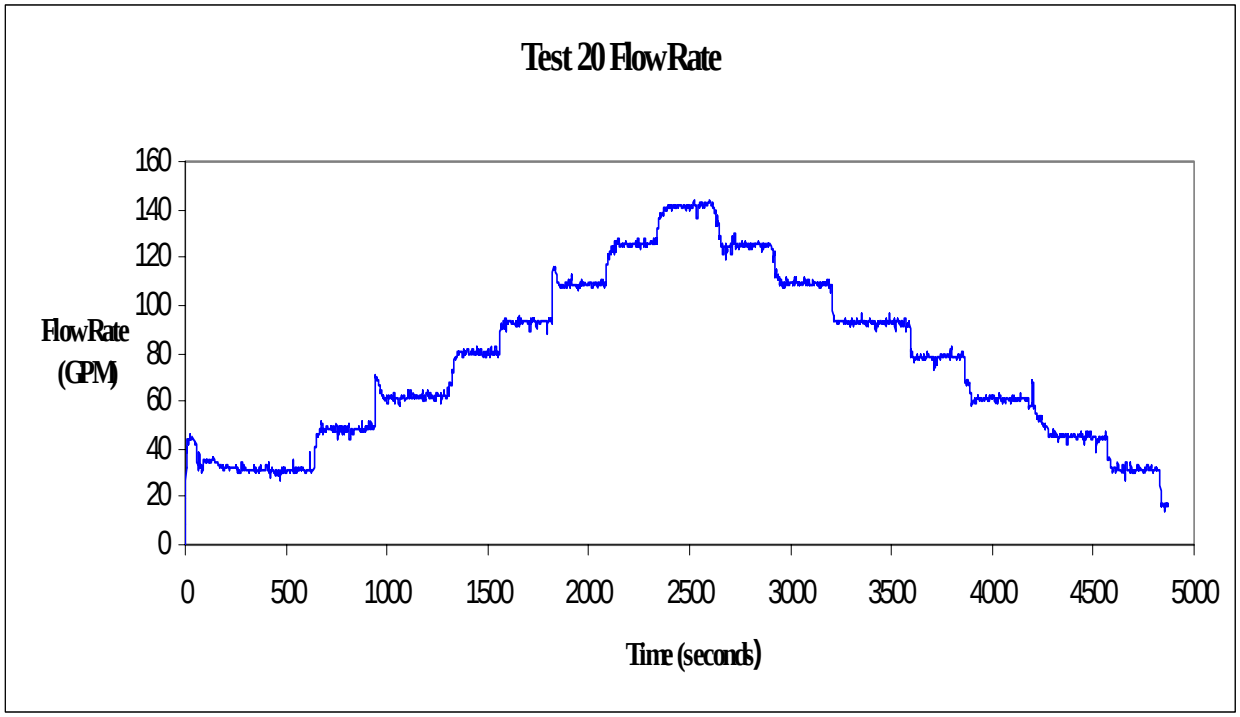

Fig. A-36. Time-dependent flow-rate measurements.

REFERENCES

1. "PWR Containment Sump Evaluation Methodology," Los Alamos National Laboratory draft report (May 2004).

2. G. Zigler, J. Brideau, D. V. Rao, C. Shaffer, F. Souto, and W. Thomas, "Parametric Study of the Potential for BWR ECCS Strainer Blockage Due to LOCA Generated Debris," United States Nuclear Regulatory Commission final report NUREG/CR-6224, Science and Engineering Associates, Inc., report SEA-93-554-06-A:1 (October 1995).

3. Regulatory Guide 1.82, "Water Sources for Long-Term Recirculation Following a Loss-of-Coolant Accident," United States Nuclear Regulatory Commission, Office of Regulatory Research, Rev. 3 (August 2003).

4. Gordon H. Hart, "A Short History of the Sump Clogging Issue and Analysis of the Problem," *Nuclear News* **47**:3, 24–34, (2004).

5. G. Horvath and K. Kawazoe, "Method for the Calculation of Effective Pore Size Distribution in Molecular Sieve Carbon," *Journal of Chemical Engineering Japan* **16**:5, pp. 470–475 (1983).

6. E. P. Barrett, L. G. Joyner, and P. P. Halenda, *Journal of the American Chemical Society* **73**:373 (1951).

7. C. J. Shaffer et al., "Debris Accumulation and Head-Loss Data for Evaluating the Performance of Vertical Pressurized-Water Reactor Recirculation Sump Screens," presented at the NRC/NEA/OECE Debris Conference, February 2004.

8. C. J. Shaffer, M. T. Leonard, B. C. Letellier, D. V. Rao, W. A. Roesch, J. D. Madrid, A. K. Maji, K. Howe, A. Ghosh, and J. Garcia, "GSI-191: Experimental Studies of Loss-of-Coolant-Accident-Generated Debris Accumulation and Head Loss with Emphasis on the Effects of Calcium Silicate Insulation," Los Alamos National Laboratory report LA-UR-04-1227 (April 2004).

9. D. V. Rao et al., "GSI-191: Integrated Debris-Transport Tests in Water Using Simulated Containment Floor Geometries," United States Nuclear Regulatory Commission report NUREG/CR-6773 (December 2002).

10. C. J. Shaffer, W. Bernahl, J. Brideau, and D. V. Rao, "BLOCKAGE 2.5 Reference Manual," United States Nuclear Regulatory Commission report NUREG/CR-6371, SEA96-3104-A:4 (December 1996).

11. "Pressurized Water Reactor Sump Performance Evaluation Methodology," Draft NEI Guidance (May 28, 2004).